3.2.1 Number of papers published per teacher in the Journals notified on UGC website during the year

Title of paper	Name of the author/s	Department of the teacher	Name of journal	Year of publication	ISSN number	Link to the recognition in UGC enlistment of the Journal	DOI/Link
Study of heterosis and inbreeding depression for seed yield or bud fly infestation and its attributes in linseed (Linum usitatissimum L.) in central U.P.	Dr. Rishi Pal	Agriculture	Vegetos	2024	2229-4473	https://link.springer.com/journal/42535	https://doi.org/10.1007/s42535-024-00970-9
Effect of different in-organic additives on growth of spawn and production of Pleurotus species (P. djamor and P. sajor-caju)	Dr. JP Kannaujia,	Agriculture	Internat ional Journal of Advanced Biochemistry Research 2024; 8(4): 11-15	2024	2617-4693	www.biochemjournal.com	https://doi.org/10.33545/26174693.2024.v8.i4a.889
Climate change Impect of Insect Population in Vegetable crops-A Reivew	Dr. JP Kannaujia,	Agriculture	Uttar Pradesh Journal of Zoology	2024	0256-971X (P)	https://mbimph.com/index.php/index/abstracting-indexing	10.56557/UPJOZ/2024/v45i94019
Genome-wide identification of Mate and ALMT gene and their expression profiling in mungbean (Vigna radiata L.) under aluminium stress	Dr. Varsha Rani	Agriculture	Ecotoxicology and Environmental Safety	2024	0149-6513	https://www.sciencedirect.com/journal/ecotoxicology-and-environmental-safety	doi.org/10.1016/j.ecoenv.2024.116558
Assessment of physio-biochemical assesment and gene expression analysis of sugarcane genotyp[es under water stress	Dr. Varsha Rani	Agriculture	Molecular Biology Reports	2024	0301-4851	https://link.springer.com/journal/11033	https://doi.org/10.1007/s11033-024-009251-9
Optimizing Solar Energy Harvesting: Supervised Machine Learning-Driven Peak Power Point Tracking for Diverse Weather Conditions	Dr. Zaiba Ishrat	Electronics & Communication Engineering	International Journal of Robotics and control system	2023	2775-2658	https://pubs2.ascee.org/index.php/IJRCS/index	https://doi.org/10.31763/ijrcs.v3i4.1176
design and simulation of hybrid Tee and 180 degree Ring Hybrid Coupler for S Band	Mr. Ashish Tripathi	Electronics & Communication Engineering	international journal of current engineering and technology	2023	2277-4106	https://inpressco.com/	https://doi.org/10.14741/ijcet/v.13.4.3
Contemporary research in solid mechanics	Mr. Gaurav Kumar	Mechanical Engineering	Journal of fluid mechanics and mechanical Design	2024	2582-9165	https://matjournals.com/Journal-of-Fluid-Mechanics-and-	https://matjournals.co.in/index.php/JFMMD/article/view/4748
The consequence of stress on the microstructure of low carbon sheets	Mr. Gaurav Kumar	Mechanical Engineering	Journal of modern thermodynamics in mechanical system	2024	2582-5771	https://matjournals.com/Journal-of-Modern-Thermodynamics-in-	https://matjournals.co.in/index.php/JMTMS/article/view/4751
Academic Publishing: Shifting Paradigm from Print to Digital Publication	Neeraj Kant Sharma	Pharmacy	Azerbaijan Pharmaceutical and Pharmacotherapy Journal	2023	2959-1929	https://www.azpharmjournal.com/en/	https://doi.org/10.61336/appj/22-2-01

Hepatoprotective Activity of Lagenaria siceraria Leaf Extract against Carbon Tetrachloride-Induced Damage in Rats	Neeraj Kant Shrama, Priyanka, Nitin Kumar, Hasan Ali	Pharmacy	European Chemical Bulletin	2023	2063-5346	https://www.eurchembull.com/	10.31838/ecb/2023.12.si6.131
Formulation and Evaluation of Transdermal Patches Containing Glibenclamide of Enhamced Diabetese Management	Simran	Pharmacy	International Journal of All Research Education & Scientific Methods	2023	24556211	https://www.ijaresm.com/indexing	https://www.ijaresm.com/formulation-and-evaluation-of-transdermal-patches-containing-
Cytotoxicity and bioavailability assessment from thiamin-phospholipid complexation loaded Ajwain oil based self nanoemulsifying system	Amulya Jindal, Piyush Kumar Singh Arya	Pharmacy	Journal of Dispersion Science and Technology Volume 45, 2024 - Issue 13	2023	0193-2691	https://www.tandfonline.com/journals/ldis20	https://doi.org/10.1080/01932691.2023.2266010
Rubia cordifolia L. Attenuates Diabetic Neuropathy by Inhibiting Apoptosis and Oxidative Stress in Rats	Nitin Kumar, Hasan Ali	Pharmacy	Pharmaceuticals	2023	1424-8247	https://www.mdpi.com/journal/pharmaceuticals/indexing	https://doi.org/10.3390/ph16111586
Nanoencapsulation and characterisation of Hypericum perforatum for the treatment of neuropathic pain	Nitin Kumar	Pharmacy	Journal of Microencapsulation	2023	0265-2048.	https://www.tandfonline.com/journals/imnc20	https://doi.org/10.1080/02652048.2023.2215306
Formulation of Phytosomes Containing Rubia cordifolia Extract for Neuropathic Pain: In Vitro and In Vivo Evaluation	Nitin Kumar, Hasan Ali, Neeraj Kant Sharma	Pharmacy	ACS Omega	2024	2470-1343	https://pubs.acs.org/journal/acsodf?ref=breadcrumb	10.1021/acsomega.4c03774
Modulation of intestinal permeability of 5-fluorouracil via phospholipid interaction based lipophilic complex designing and pharmacokinetic assessment	Anoop Kumar, Piyush Kumar Singh Arya, Amulya Jindal	Pharmacy	Journal of Dispersion Science and Technolgy	2024	0193-2691	https://www.tandfonline.com/journals/ldis20	https://doi.org/10.1080/01932691.2024.2325398
Novel therapeutic agents in clinicals trails: emerging approches in cancer therapy	Kajal Sherawat	Pharmacy	Discover Oncology	2024	2730-6011	https://link.springer.com/journal/12672	https://doi.org/10.1007/s12672-024-01195-7
Assessment of the Anti-Adipogenic Effect of Crateva religiosa Bark Extract for Molecular Regulation of Adipogenesis: In Silico and In vitro Approaches for Management of Hyperlipidemia Through the 3T3-L1 Cell Line	Nitin Kumar	Pharmacy	Current Pharmaceutical Biotechnolgy	2024	1873-4316	https://www.eurekaselect.com/journal/30	10.2174/0113892010314594240816050240
Potential Protective Effects of Acacia Nilotica (L.) against Gentamicin - Induced Nephrotoxicity by Suppressing Renal Redox Imbalance, Inflammatory Stress and Caspase-Dependent Apoptosis in Wistar Rats.	Nitin Kumar	Pharmacy	Drug and Chemical Toxicology	2024	0148-0545	https://www.tandfonline.com/journals/idct20	10.1080/01480545.2024.2388324
The Anti-ulcer Potential of Weissella cibaria Assisted Bio-fermented Product of Citrus limetta Waste Peel in Wistar Albino Rats	Nitin Kumar	Pharmacy	Recent Patents on Biotechnology	2024	0265-2048.	https://www.eurekaselect.com/issue/13726/105	10.2174/0118722083278152231121173605

Artificial Intelligence-Based Machine and Deep Learning Techniques That Use Brain Waves to Detect Depression	Mr. Sandeep Bharti	Computer Applications	Journal of Advanced Zoology	2023	0253-7214	http://jazindia.com/index.php/jaz/indexing	https://doi.org/10.17762/jaz.v44iS-5.1088
Multi-Criteria Group Decision Making Approch for scheduling algorithms selection by short term schedular using Fuzzy TOPSIS	Mr. Shubham Kumar	Computer Applications	Journal of Electrical System	2024	2147-6799	https://journal.esrgroups.org/jes/about	https://doi.org/10.52783/jes.1138
A Case Study on Scissors Manufacturing Cluster Analysis (Current Scenario & Value Chain Analysis) in Meerut City	Ms. Himani Mishra, Dr. Ankur Goel	Business Administration	Pranjana – The Journal of Management Awareness', INMANTEC Institutions, Ghaziabad. Vol. 25, 1 & 2, January-December 2023	2024	09719997(print), 09740945(online)	https://www.indianjournals.com/ijor.aspx?target=ijor:pr&type=home	10.5958/0974-0945.2023.00012.7
Energy Efficient Block Chain Solutions for Edge and Cloud Computing Infrastructures	Ms. Komal Panwar	Computer Science & Engineering	Electronic ISBN:979-8-3503-7105-5 Print on Demand(PoD) ISBN:979-8-3503-7106-2 (IEEE)	2024	ISBN:979-8-3503-7105-5	https://ieeexplore.ieee.org/document/10489584	10.1109/ICDT61202.2024.10489584
Identification of Counterfeit Currency usingMachine learning and Knowledge Discovery	Dr. Himanshu Sirohi and Dr. Neeraj Pratap	Computer Science & Engineering	International Journal of Electrical System	2024	1112-5209	https://journal.esrgroups.org/jes	https://journal.esrgroups.org/jes/article/view/5957
Enhanced Crime Detection in Smart Cities through Hybrid Machine Learning and Advanced Feature Extraction Techniques	Ayush Singhal	Computer Science & Engineering	International Journal of Intelligent Systems and Applications in Engineering	2024	2147-6799	https://ijisae.org/index.php/IJISAE	https://www.ijisae.org/index.php/IJISAE/article/view/6660/5522
Automated Crime Anomaly Detection in Smart Cities Using Sharkprey Optimization Algorithm and Ensembled-Machine Learning Approach	Ayush Singhal	Computer Science & Engineering	Nanotechnology Perceptions	2024	1660-6795	http://nano-ntp.com/index.php/nano	https://doi.org/10.62441/nano-ntp.vi.1601
Unlocking Cellular Antenna Capacity: Cell Splitting Enhanced by Machine Learning	Dr Mohd Sadim	Computer Science & Engineering	Journal of Pharmaceutical Negative Results	2024	2229-7723	https://www.pnrjournal.com/index.php/home/about	https://doi.org/10.47750/5g7tx594
Feature Extraction of Multidimensional Imagery for Façade Identification	Dr. Neeraj Pratap	Computer Science & Engineering	Journal of Chemical Health Risk	2023	2251-6727	https://jchr.org/index.php/JCHR	https://jchr.org/index.php/JCHR/article/view/2056
Advancements in Novel Architectures for Ad Hoc and Sensor Networks: A Comprehensive Review	Sanjay Kumar	Computer Science & Engineering	Journal of Ad-hoc Network and Mobile computing	2024	3048-9180	https://matjournals.com/Journal-of-Ad-hoc-Network-and-Mobile-Computing.html	www.matjournals.com

Advances in Speech and Language Processing: A Comprehensive Review	Sanjay Kumar	Computer Science & Engineering	Recent Trends in Artificial Intelligence and it's application	2024	2583-4819	https://matjournals.com/Recent-Trends-in-Artificial-Intelligence-&-it%E2%80%99s-applications.html	https://matjournals.net/engineering/index.php/RTAIA/article/view/768
Advances in Modern Sensor Network Technology	Sanjay Kumar	Computer Science & Engineering	Journal of Ad-hoc Network and Mobile computing	2024	3048-9180	https://matjournals.com/Journal-of-Ad-hoc-Network-and-Mobile-Computing.html	https://matjournals.net/engineering/index.php/JAHNMC/article/view/791
Interoperability and Standards in Web Services: Ensuring Seamless Integration across Diverse Systems	Sanjay Kumar	Computer Science & Engineering	Journal of Future internet and Hyperconnectivity	2024	3048-9210	https://matjournals.net/engineering/index.php/JFIHC/index	https://matjournals.net/engineering/index.php/JFIHC/article/view/840
CNT-TiO2 Nano Composit Films in enhanced Photocatalytic degradation of Methylene Blue	Hitesh Kumar Sharma	Applied Science	Hybrid Advances	2024	2773-207X	https://www.sciencedirect.com/journal/hybrid-advances	https://doi.org/10.1016/j.hybadv.2024.100152

Meerut Institute of Technology * MIT * Meerut *

Vegetos
https://doi.org/10.1007/s42535-024-00970-9

RESEARCH ARTICLES

Study of heterosis and inbreeding depression for bud fly infestation and its attributes in linseed (*Linum usitatissimum* L.) in central Uttar Pradesh

Rishi Pal[1]

Received: 26 August 2023 / Revised: 14 June 2024 / Accepted: 16 June 2024

Abstract
For the estimation of economic parent heterosis and inbreeding depression 49 genotypes (21 F_1 and 21 F_2 involving 7 parents) of linseed were estimated in 11 characters. The heterosis, over economic check Neelum showed positive and significant by the crosses JRF-5 × Neela, GS-234 × IC-15888, GS-234 × JRF-5, EC-1424 × GS-234, EC-1424 × IC-15888, EC-1424 × JRF-5, EC-1424 × Neela, GS-234 × Neela, IC-15888 × JRF-5, IC-15888 × Shekhar, IC-15888 × Neela, JRF-5 × Shekhar, Shekhar × Neela and IC-15888 × Neelum. For Sepal thickness, positive and significant economic heterosis was observed by 3 crosses namely JRF-5 × Shekhar, JRF-5 × Neelum and JRF-5 × NeelaFor days to maturity cross EC-1424 × Shekhar). Dough stage bud fly infestation, EC-1424 × IC-15888, EC-1424 × JRF-5, IC-15888 × Neelum, Shekhar × Neelum, IC-15888 × JRF-5, GS-234 × Neela, JRF-5 × Neelum and Neelum × Neela. Capsule per plant, (GS-234 × Shekhar, IC-15888 × Shekhar, IC-15888 × Neela and JRF-5 × Shekhar) Oil content and EC-1424 × IC-15888, IC-15888 × Neelum, JRF-5 × Neelum, Shekhar × Neelum, IC-15888 × JRF-5 and Neelum × Neela for seed yield per plant. Positive values of inbreeding depression were considered as desirable for flowering duration, days to maturity, bud length, bud width, dough stage bud fly infestation and while negative values were considered as desirable for other attributes. These cross combinations could be utilized for further use in breeding programme for improvement in yield and tolerance bud fly infestation of linseed.

Keywords Economic heterosis · Heterosis · Inbreeding depression · Linseed · Economic parent · *Linum usitatissimum* L. Neelum

Introduction

Linseed (*Linum usitatissimum* L.) belongs to the genus Linum of the family Linaceae. The somatic chromosome number of the cultivated species is 2n = 30. It is cultivated for the main products seed oil (linseed) and fibre (flax fibre) and linseed oil but recently it has gained a new interest in the emerging market of functional food due to its high content of fatty acids, alpha linolenic acid (ALA), an essential Omega-3 fatty acid and lignin oligomers, which constitute about 57% of total fatty acids in linseed (Reddy et al. 2013). World over, linseed is an important crop grown over 27.29 lakh ha with production of 25.2 lakh tons with average productivity of 923 kg/ha, while national production of 1.525 lakh tons is from 3.226 lakh ha with lower productivity of 473 kg/ha. India still ranks third in terms of area after Canada and China, but slides down to fifth place in terms of production after Canada, China, USA and Ethiopia. Average yield losses range between 19–98%, 31–59% and 22–56% due to insect-pests (Shrivastava et al. 1994, Malik 1999 and Patnaik and Lenka 2000), weeds (Mani et al. 1968 and Husain et al. 2009) and diseases (Saharan and Saharan 1999), respectively. The significant yield losses occur in linseed due to bud fly (*Dasyneura lini*) (20 to 97%), Alternaria blight (*Alternaria lini*) & powdery mildew (*Odium lini*) (up to 60%) (Srivastava et al. (1997). Since there is a need to develop varieties resistant to pest and diseases to stabilize the yield potentials of linseed varieties, studies related to heterosis in linseed crop could provide basis for the exploitation of valuable hybrid combinations in future breeding programs as earlier reported by Pali and Mehta (2014). Reddy et al. (2013). Keeping these things in view, the present research work was

✉ Rishi Pal
rishi.pal@mitmeerut.ac.in

[1] Department of Agriculture, Meerut Institute of Technology-Meerut (MIT), Baral Partapur, Meerut, Uttar Pradesh 250103, India

Published online: 11 July 2024

International Journal of Advanced Biochemistry Research

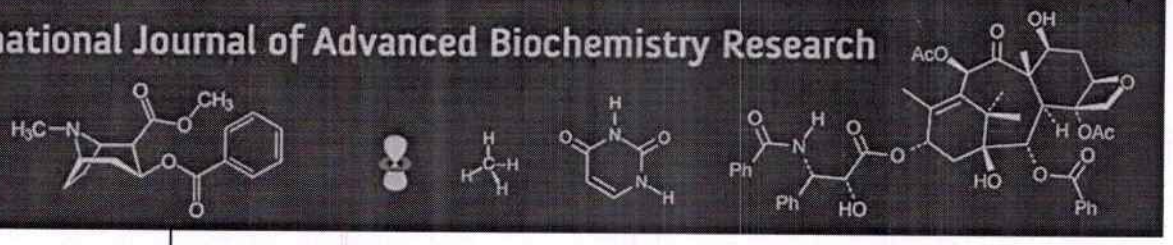

ISSN Print: 2617-4693
ISSN Online: 2617-4707
IJABR 2024; 8(4): 11-15
www.biochemjournal.com
Received: 19-01-2024
Accepted: 22-02-2024

JP Kannaujia
Department of Agriculture, Meerut Institute of Technology Meerut, Uttar Pradesh, India

Deepman Diwakar
Chadra Bhan Singh Memorial Shikshan Sansthan Jhinjhak Kanpur, Uttar Pradesh, India

NK Sharma
Krishi Vigyan Kendra, Kaushambi, Uttar Pradesh, India

SK Dubey
ICAR-ATARI Kanpur, Uttar Pradesh, India

Harikesh
Department of Agronomy, Asha Bhagwan Bux Singh Mahavidyalay, Pura Bazar Ayodhya, Uttar Pradesh, India

SN Yadav
Krishi Vigyan Kendra, Kaushambi, Uttar Pradesh, India

M Saxsena
Krishi Vigyan Kendra, Kaushambi, Uttar Pradesh, India

Monika Singh
Maharishi University of Information Technology, Lucknow, Uttar Pradesh, India

JK Yadav
Krishi Vigyan Kendra, Dhaura, Unnao, Uttar Pradesh, India

Corresponding Author:
JK Yadav
Krishi Vigyan Kendra, Dhaura, Unnao, Uttar Pradesh, India

Effect of different in-organic additives on growth of spawn and production of *Pleurotus* species (*P. djamor* and *P. sajor-caju*)

JP Kannaujia, Deepman Diwakar, NK Sharma, SK Dubey, Harikesh, SN Yadav, M Saxsena, Monika Singh and JK Yadav

DOI: https://doi.org/10.33545/26174693.2024.v8.i4a.889

Abstract
The present study is growth of spawn and yield of *Pleurotus* spp. against different inorganic additives in laboratory and crop room. Three different type inorganic additives *viz*. ferrous sulphate, zinc sulphate and magnesium sulphate @ 0.5 and 1.0% were mixed as additive with wheat grain in three replications. Maximum spawn growth of *P. djamor* (90.00 mm) was recorded in Magnesium sulphate 0.5% and zinc sulphate 0.5%. While in case of *P. sajor-caju,* maximum spawn growth (90.00 mm) was recorded in ferrous sulphate 0.5% and zinc sulphate 0.5%. The maximum growth rate of *P. djamor* (6.00 mm/day) was recorded in zinc sulphate 0.5% and magnesium sulphate 0.5%. While in *P. sajor-caju* maximum growth rate (6.00 mm/day) was recorded in zinc sulphate 0.5% and ferrous sulphate 0.5%. The maximum yield of *P. djamor* was observed in ferrous sulphate 1.0% (462.66 gm/kg of dry substrates with 46.26% biological efficiency). In case of *P. sajor-caju* maximum yield was observed in ferrous sulphate 1.0% (790.33 gm/kg of dry substrates with 79.03% biological efficiency).

Keywords: Inorganic, additives, spawn and *Pleurotus*

Introduction

Mushroom farming in India is becoming successful and also popularized day by day because of its very low input, which can bring a significant change in rural economy. The climatic conditions of the region have been found to be ideal for such an attempt. Research and field experiments on production and marketing of several varieties of mushrooms have proved its significant potentiality as a major source of income for rural people (Shahi, V. *et al*., 2018) [10].

To make Oyster mushroom cultivation more profitable and popular, different types of agro wastes, crop residues and by-products can be used with cylindrical block system, which has already been proven economically viable rather than conventional polybag method (Maniruzzaman 2004) [12]. Oyster mushroom is the third grown mushroom in the world and ranks second in India. For the successful cultivation of oyster mushroom on a small scale or commercial scale, one of the most important requirements is the mushroom seed (Spawn). This is a pure culture of the mycelium grown on a special medium. The production of spawn is done by professionals in the laboratory under controlled conditions or temperature, light and humidity. The contents of Na, K, P, Ca, Mg and Fe for each of the oven dried, vacuum dried and sun-dried mushroom powders. The results of minerals were for Na content 12.41, 9.76 and 15.32 mg/100 gm, for K content 299.5, 226.5 and 295.1 mg/100 gm, for P content 9.19,762 and 974 mg/100 gm, for Ca content 34.1, 55.5 mg/100 gm and 98.0, for Mg content 297, 254, and 297 mg/ 100 gm, for Fe content 5.24, 5.78, and 11.6, 297 mg/100 gm for each of the oven dried, vacuum dried and sun-dried mushroom powders, respectively (Maray, *et al*., 2017) [7]. It can be concluded that the highest values of minerals content in the case of sun-drying followed by oven drying and the lowest values of minerals content in the case of vacuum dehydration (Mattila *et al*., 2001) [8]. Oyster production is a meager 1200 tonnes production during 1985, the present time total production of oyster mushroom in India reached 21272 metric tonnes in 2016 (DMR, Solan 2016-17). The cultivation of oyster mushroom is now becoming popular in developing countries amongst growers due to

Uttar Pradesh Journal of Zoology

Volume 45, Issue 9, Page 20-28, 2024; Article no.UPJOZ.3373
ISSN: 0256-971X (P)

Climate Change Impact on Insect Population in Vegetable Crops: A Review

Vivek Kashyap [a], J.K. Yadav [b*], N.K. Sharma [c], S.K. Dubey [d], Rajeev Singh [d], J.P. Kannaujia [e], Shashi Shekhar [f], Vaishali Singh [g] and Deepti Singh [h]

[a] Krishi Vigyan Kendra, Deoghar (Jharkhand), India.
[b] Krishi Vigyan Kendra, Dhaura, Unnao-209881 (U.P.), India.
[c] Krishi Vigyan Kendra, Kaushambi, (U.P.), India.
[d] ICAR-ATARI Kanpur (U.P.), India.
[e] Department of Agriculture Meerut Institute of Technology Meerut (U.P.), India.
[f] J.S. University, Firozabad (UP), India.
[g] Mahatma Gandhi Kashi Vidyapeeth Krishi Vigyan Bhairav Talab VARANASI(UP), India.
[h] Department of Zoology, K.R. P.G. College, Mathura (UP), India.

Authors' contributions

This work was carried out in collaboration among all authors. All authors read and approved the final manuscript.

Article Information

DOI: 10.56557/UPJOZ/2024/v45i94019

Open Peer Review History:
This journal follows the Advanced Open Peer Review policy. Identity of the Reviewers, Editor(s) and additional Reviewers, peer review comments, different versions of the manuscript, comments of the editors, etc are available here: https://prh.mbimph.com/review-history/3373

Review Article

Received: 02/02/2024
Accepted: 05/04/2024
Published: 11/04/2024

ABSTRACT

One of the world's largest nations, India is known for its distinctive landscape, which distinguishes it as a distinct geographical entity and a global center of mega diversity. Pest populations in vegetable crops may be significantly impacted by climate change.
Additionally, warmer temperatures can lead to faster insect development and increased reproductive rates. Farmers and researchers need to monitor these changes and develop

**Corresponding author: Email: jaykumaryadav4556@gmail.com;*

ISSN: 0147-6513

Ecotoxicology and Environmental Safety 280 (2024) 116558

Contents lists available at ScienceDirect

Ecotoxicology and Environmental Safety

journal homepage: www.elsevier.com/locate/ecoenv

Genome-wide identification of MATE and ALMT genes and their expression profiling in mungbean (*Vigna radiata* L.) under aluminium stress

Dharmendra Singh [a,*], Ankita Tripathi [a], Raktim Mitra [b], Jyotika Bhati [c], Varsha Rani [d], Jyoti Taunk [b], Deepti Singh [e], Rajendra Kumar Yadav [f], Manzer H. Siddiqui [g], Madan Pal [b]

[a] Division of Genetics, ICAR-Indian Agricultural Research Institute, New Delhi 110012, India
[b] Division of Plant Physiology, ICAR, Indian Agricultural Research Institute, New Delhi 110012, India
[c] ICAR-Indian Agricultural Statistics Research Institute, New Delhi 110012, India
[d] Department of Agriculture, Meerut Institute of Technology, Meerut 250103, India
[e] Department of Botany, Meerut College, Meerut 250103, India
[f] Department of Genetics and Plant Breeding, Chandra Shekhar Azad University of Agriculture and Technology, Kanpur 208002, India
[g] Department of Botany and Microbiology, College of Science, King Saud University, Riyadh 11451, Saudi Arabia

ARTICLE INFO

Edited by Dr Muhammad Zia-ur-Rehman

Keywords:
ALMT
Aluminium
Gene expression
MATE
Phylogenetic analysis
Vigna radiata

ABSTRACT

The Multidrug and toxic compound extrusion (MATE) and aluminium activated malate transporter (ALMT) gene families are involved in response to aluminium (Al) stress. In this study, we identified 48 MATE and 14 ALMT gene families in *Vigna radiata* genome and classified into 5 (MATE) and 3 (ALMT) clades by phylogenetic analysis. All the VrMATE and VrALMT genes were distributed across mungbean chromosomes. Tandem duplication was the main driving force for evolution and expansion of MATE gene family. Collinearity of mungbean with soybean indicated that MATE gene family is closely linked to *Glycine max*. Eight MATE transporters in clade 2 were found to be associated with previously characterized Al tolerance related MATEs in various plant species. Citrate exuding motif (CEM) was present in seven VrMATEs of clade 2. Promoter analysis revealed abundant plant hormone and stress responsive cis-elements. Results from quantitative real time-polymerase chain reaction (qRT-PCR) revealed that VrMATE19, VrMATE30 and VrALMT13 genes were markedly up-regulated at different time points under Al stress. Overall, this study offers a new direction for further molecular characterization of the MATE and ALMT genes in mungbean for Al tolerance.

Abbreviations: Aa, Amino acids; ARE, Anaerobic responsive element; ART1, Al resistance transcription factor 1; ABRE, Abscisic acid responsive element; AtFRD3, *Arabidopsis thaliana* Ferric Reductase Defective 3; AtMATE, *Arabidopsis thaliana* Multidrug and toxic compound extrusion; AtALMT, *Arabidopsis thaliana* Aluminum activated malate transporters; BoMATE, *Brassica oleracea* Multidrug and toxic compound extrusion; BnALMT, *Brassica napus* Aluminum activated malate transporters; CEM, Citrate Exuding Motif; CcMATE, *Cajanus cajan* Multidrug and toxic compound extrusion; DRE, Drought responsive element; EcMATE1, *Eucalyptus camaldulensis* Multidrug and toxic compound extrusion; ERE, Ethylene responsive element; FRDL, Ferric reductase defective like; GARE, Gibberellic acid responsive element; GmFRD3b, *Glycine max* ferric reductase defective 3b; GmMATE, *Glycine max* Multidrug and toxic compound extrusion; GmALMT, *Glycine max* Aluminum activated malate transporters; HvAACT1, *Hordeum vulgare* Aluminum-Activated Citrate Transporter 1; Ka, Nonsynonymous Substitutions; Ks, Synonymous Substitutions; KDa, Kilodalton; LDL, Low density lipid; LTR, Low temperature responsive element; MBS, MYB binding site involved in drought-inducibility; MeJARE, Methyl Jasmonate responsive element; MEME, Multiple Em for motif elicitation; MBSI, MYB binding site involved in flavonoid biosynthetic genes regulation; MsALMT, Medicago sativa Aluminum activated malate transporter; MW, Molecular Weight; MYA, Million years ago; MYB, Myeloblastosis viral oncogene homolog; MYC, Myelocytomatosis viral oncogene homolog; OAs, Organic Acids; OsFRDL, *Oryza sativa* Ferric reductase defective like; QRT-PCR, Quantitative Real Time Polymerase Chain Reaction; SARE, Salicylic acid responsive element; SbMATE, *Sorghum bicolor* Multidrug and toxic compound extrusion; ScFRDL, *Secale cereale* Ferric reductase defective like; ScALMT, *Secale cereale* Aluminum activated malate transporters; STRE, Stress responsive element; TaALMT, TaALMT- *Triticum aestivum* Aluminum activated malate transporters; TaMATE, *Triticum aestivum* Multidrug and toxic compound extrusion; TC-rich repeats, cis-acting element involved in defense and stress responsiveness; VrMATE, *Vigna radiata* Multidrug and toxic compound extrusion; VrALMT, *Vigna radiata* Aluminium activated malate transporter; VuMATE, VuMATE- *Vigna umbellata* Multidrug and toxic compound extrusion; W box, WRKY binding box; WUN motif, Wound responsive motif; ZmMATE, Zea mays Multidrug and toxic compound extrusion.

* Corresponding author.
E-mail address: dharmendrapbg@rediffmail.com (D. Singh).

https://doi.org/10.1016/j.ecoenv.2024.116558
Received 21 March 2024; Received in revised form 3 June 2024; Accepted 4 June 2024
Available online 8 June 2024

ISSN: 0301-4851

Molecular Biology Reports (2024) 51:315
https://doi.org/10.1007/s11033-024-09251-9

ORIGINAL ARTICLE

Assessment of physio-biochemical assessment and gene expression analysis of sugarcane genotypes under water stress

Varsha Rani[1,2] · R. S. Sengar[1] · Chetan Chauhan[3]

Received: 24 October 2023 / Accepted: 12 January 2024

Abstract

Background Sugarcane, an economically important crop cultivated for its unique character of accumulating sucrose into its stalk and the world's major crop according to production quantity. Sugarcane production is negatively influenced by abiotic stresses because it faces all types of environments due to its long-life cycle period. Among the various abiotic stresses, drought is one of the major limiting factors creates obstacle in sugarcane production. Thus, an attempt was made to assess the molecular insights into sugarcane genotypes under water stress. A preliminary screening was done in ten sugarcane genotypes grown under semi-arid region of India through physiological, biochemical and antioxidant responses of these genotypes under two water deficit levels.

Methods In the current study, drought was imposed on ten sugarcane genotypes during their formative stage (110 DAP) by depriving them of irrigation. A pot experiment was carried out to see how several commercial sugarcane genotypes responded to water scarcity. Sugarcane received two treatments, the first after 125 days and the second after 140 days. The physio-biochemical and antioxidant responses recorded were RWC, MSI, SCMR, Proline accumulation, SOD, Catalase, Peroxidase and Lipid peroxidation. The significant variations were recorded in responses of all genotypes. On the basis of physio-biochemical, three genotypes Cos 98,014, Cos 13,235 and Colk 14,201 were selected for differential gene expression pattern analysis. The total RNA was isolated and reverse transcribe to cDNA and real time PCR was performed for expression analysis under 10 genes.

Results Under drought conditions, all sugarcane genotypes showed significantly decreased RWC, chlorophyll content, and MSI. However, when water was scarce, proline buildup, malondialdehyde (MDA) contents, enzymatic antioxidant activity (CAT, POD, and SOD), and contents all increased dramatically. Finally, in all physiological and biochemical parameters, Co 98,014 genotype displayed superior adaptation responses to drought stress, followed by Co 018, Cos 13,235, and Colk 14,201. For gene expression analysis out of 21 genes, 10 genes were expressed in sugarcane genotypes, in which 7 genes (*Shbbx2, Shbbx3, Shbbx4, Shbbx5, Shbbx8, Shbbx15* and *Shbbx20*) were upregulated and 3 genes (*Shbbx1, Shbbx16* and *Shbbx17*) were downregulated.

Conclusion The statistical analysis conducted in this study demonstrated that drought stress had a negative impact on physiological responses, including RWC, SPAD, and MSI, in sugarcane crops. However, it was found that the crops were able to survive in these stress conditions by increasing their biochemical parameters, all while maintaining their growth and function.

Keywords Drought Tolerance · Abiotic Stress · Antioxidant Defense · Oxidative Stress · Sugarcane · Gene Expression

Introduction

Sugarcane (*Saccharum spp.*) is an agriculturally important crop that holds substantial prominence in tropical and subtropical countries. Sugarcane is grown for the purpose of human consumption and the manufacturing of bioethanol, owing to its remarkable ability to accumulate sucrose. This accumulation can account for as much as 65% of the dry mass of its stem [1]. The prevailing sources of biofuels on a global scale are primarily obtained from either sugarcane in Brazil or maize in the United States. The utilisation of plant biomass for the production of second-generation ethanol presents a feasible option in comparison to first-generation biofuels. This is due to the considerable presence of polysaccharides within the biomass, which make up around 75% of its composition, as reported by Gomez et al. [2]. The

Extended author information available on the last page of the article

Published online: 20 February 2024

Assessment of physio-biochemical assessment and gene expression analysis of sugarcane genotypes under water stress

Varsha Rani

Department of Agricultural Biotechnology, Sardar Vallabhbhai Patel University of Agriculture and Technology, Meerut, 250110, India

Department of Agriculture, Meerut Institute of Technology, Meerut, 250103, India

Abstract

Background

Sugarcane, an economically important crop cultivated for its unique character of accumulating sucrose into its stalk and the world's major crop according to production quantity. Sugarcane production is negatively influenced by abiotic stresses because it faces all types of environments due to its long-life cycle period. Among the various abiotic stresses, drought is one of the major limiting factors creates obstacle in sugarcane production. Thus, an attempt was made to assess the molecular insights into sugarcane genotypes under water stress. A preliminary screening was done in ten sugarcane genotypes grown under semi-arid region of India through physiological, biochemical and antioxidant responses of these genotypes under two water deficit levels.

IJRCS

International Journal of Robotics and Control Systems
Vol. 3, No. 4, 2023, pp. 1007-1020
ISSN 2775-2658
http://pubs2.ascee.org/index.php/ijrcs

ASCEE

Optimizing Solar Energy Harvesting: Supervised Machine Learning-Driven Peak Power Point Tracking for Diverse Weather Conditions

Zaiba Ishrat [a,1,*], Kunwar Babar Ali [b,2], Satvik Vats [c,3], Surender Kumar [d,4]

[a] Meerut Institute of Technology, Meerut, Bypass Road Bahgpat Crossing, Meerut, 250005, U.P. India
[b] Meerut Institute of Engineering and Technology, N.H. 58, Delhi Roorkee Highway, Meerut, 250005, U.P. India
[c] Graphic Era Hill University, Road Sociuety Area, Celement Town, Dehradun, 248002, Uttrakhand, India
[d] IIMT College of Engineering, Knowledge Park III, Greater Noida, 201310, U.P, India
[1] zaibaishrat01@gmail.com; [2] kunwarbabrali1@gmail.com; [3] Svats@gehu.ac.in; [4] skladhoura88@gmail.com
* Corresponding Author

ARTICLE INFO

Article history
Received October 03, 2023
Revised November 24, 2023
Accepted December 14, 2023

Keywords
PV System (PVS);
MxPPT;
SGPRA;
Matlab/Simulink

ABSTRACT

Solar Power is one of the significant prevalent forms of clean energy due to its perceived to be pollution-free and easily accessible. The market for renewable energy was established by the rapid development in electrical energy consumption and the diminution of conventional energy resources (CER). Under varying weather condition extracted energy from solar system is not constant and maximum. This study suggests the applicability of machine learning algorithm (MLA) in Peak power point tracking (P3T) methods to maximize power of a PV arrangement under varying weather conditions. Machine learning methods optimize peak power point tracking in solar photovoltaic systems by bringing agility, data-driven decision-making, and increased accuracy. MLAs improve the overall efficiency, stability, and dependability of these systems by handling the unpredictability of solar energy production under varying weather circumstances and PSCs Because MLAs are able to learn and adjust to non-linear relationships between solar intensity and PVS output. In this study, the squared multiple squared exponential Gaussian process regression method SGPRA tested in three rapidly varying ecological conditions. The performance of ML-P3T methods is validated using Matlab/Simulink, and the simulation outcome are compared with one of the most used algorithms, the variable step size incremental conductance algorithm (VINA). The Matlab/Simulink findings show that SGPRA operates significantly better under varying weather circumstances, harnessing more peak power efficiency > 90%, shorter tracking time 0.13 sec, a mean error of 0.042, and superior stability.

1. Introduction

Massive interest in the use of green energy resources (GER) has been sparked by the rise in demand, rising costs of fossil fuels, and concern about environmental issues. Because it is so readily available, solar energy is one of them [1], [2]. It appears encouraging that solar energy power will expand from 227 GW in 2015 to 1362 GW by 2030 [38], [39].

Despite the advantages that a PV system (PVS) can provide, PVS has certain drawbacks; including a high installation cost, poor energy conversion efficiency, and unpredictable power output due to a reliance on constantly shifting climatic circumstances [3], [25]. The most commercial solar panels' efficiency falling between 15% and 22%, a sizable amount of sunshine does not get converted into electrical power. When a solar panel is partially shaded, either the system as a whole or specific sections of it are, resulting in uneven lighting. This may occur as a result of adjacent structures, trees, or even cloud cover. In addition to low ouput power PSCs also responsible for mismatch in power loses. There are several peaks on the P-V characteristics (PVC) curve under Partial shading conditions (PSCs) [31], including a number of local minima and one GP (Global Peak). As a result, some MxPP algorithms must be created that can haul out the utmost amount of power from PVS and transmit it to the load while operating in a variety of environmental conditions [4]. However, under PSCs, several MxPPT strategies were unable to follow GMxPP. As a result, the PVS experienced power losses and operated with low efficiency [4]-[6].

Various approaches to tracking maximum power have been presented, as seen in the literature. Swarm optimization algorithms, artificial intelligence algorithms, and conventional algorithms can all be used to classify these techniques [1], [6], [7], [26]. Hill climbing (HCA), perturb and observe (PnOA), incremental conductance (ICA), open circuit voltage [8], [9], [23], short circuit current method [23], are all straightforward techniques that work well in stable weather conditions. The P&OA exhibit the swinging around the topmost point which is overawed by INCA however, under NUW conditions but INCA is unable to track the MxPP. The author suggests a fixed voltage [7]-[9], open circuit voltage [9], and short circuit current method [8], but they are all offline methods and unrealistic methods because they call for constant solar radiation and temperature.

AI-based strategies like ANN [1], [32], FLC [10], and ANFIS [12] are utilized to get beyond the limitations of classical algorithms. Although they require a significant internal storage area, ANN-based approaches [1], [32] have the advantage of monitoring the GMxPP under PSC. A unique FLC-MxPPT has been proposed that does not require a mathematical model of the PVS but rather a professional with knowledge of the fuzzification process [10]. N. Priyadarshi, et al. [11] employed ANFIS to take advantage of FLC and ANN advantages.

Researchers have employed optimization strategies to track the GMxPP under PSC, such as the CSA with Golden Search Algorithm [17], PSOA [12], [16], ACO [18], [21], GA [13] but the mathematical computational complexity is very high. The efficiency of CSA depends on tuning of parameters i. e. population size and probability of finding new nest which is very difficult to decide in NUW. In PSOA [12], [16] the inertia weight and acceleration coefficients in PSOA are usually static, making it thought-provoking for the algorithm to adjust quickly in NUW. GA comprise functions like crossover and mutation, which are computational complex and like CSA this algorithm is also parameter sensitive. The MLA [15], [19], [20], [24], [30], [33] is used by the researchers. The researcher proposed a multiple linear regression model for forecasting of power under varying weather [24]. The model predict the power with less than 6% error as an actual power. A study is published to propose the systematic literature review of Deep learning in solar power tracking [27]. These techniques give good convergence speed and tracking efficiency, but the computational complexity is quite high for the suggested algorithms.

Squared Gaussian Process Regression algorithm (SGPRA), an enhanced ML-MxPPT technique, is introduced in this study and correlated with variable step size incremental conductance algorithm (VINA) utilizing real-time data under PSC. This study recommended cascading the MxPPT and PID controllers (PIDC) to rectify and optimize the large flaws into smaller flaws. Additionally, it increases the MxPPT algorithm's precision, which ultimately raises the PV panel's effectiveness. This paper's primary contribution is as follows:

(i) Emphasizing the MxPPT controllers' significance within non uniform weather conditions (NUW).

(ii) Harnessing MxPP for real-time data using SGPRA-MxPPT approaches.

(iii) Using a PIDC to lower the inaccuracy and thereby improve MxPPT controller performance.

(iv) Using SGPRA enhance the tracking rate and tracking efficiency under non uniform weather condition (NUW).

(v) Using SGPRA technique decreases the fluctuation around the MxPP therefore negligible power losses.

The outline of this study is organized as follows: Section II discuss the designing of proposed system, segment III explains MLA, flow chart and proposed algorithm under NUW. Section IV discuss the simulation result analysis and finally concludes the research paper.

2. Design and Methodology

The MSX -60W solar panel data set [40] was utilized by the author to test the squared Guassian regression model (SGPRA.The suggested strategy splits the PV panel data set into an 80% and 20% ratio randomly. SGPRA is trained on 80% of the data and tested on 20% of the data. Solar insolation and temperature are employed as key features to train the model, while ref maximum panel current is the desired parameter. "Table 1" shows he MSX-60W solar module's PV model specifications [22].

To obtain the equilibrium PVS and load impedances, the Boost Converter is used. In order to control the transmission of electricity, the duty cycle (Dc) is used to change its ON/OFF condition [25]. The duty ratio, which can be stated as a ratio or percentage, is the percentage of time that an electrical device is used. Using Equation (1), Dc is computed where average output and input voltages of the converter are represented by Vout and Vin. Equations (2), (3), and (4), used to establish the suitable values for inductors and capacitors [35]. Table 2 shows the parameters of designed boost converter.

$$Vo = Vi \div (1 - Dc) \tag{1}$$

$$L = \frac{Dc * Vi}{f * 2 * \mathrm{d}IL} \tag{2}$$

$$C1 = \frac{4ViDc}{\mathrm{d}Vi\ Ri.f} \tag{3}$$

$$C2 = \frac{2Vo\ Dc}{dVoRof} \tag{4}$$

The suggested network is fully depicted in Fig. 1, which includes the PV panel, MxPPT methods, the PID controller [34], the PWM generator, the Boost DC-DC converter, and the 60 Ohms load resistor. PID controller, which is the most popular, is utilized to enhance system capabilities like steadiness, voltage management, swiftness, and precision [34]. For the tuning of PID controller Ziegler-Nichols" approach is used. The parameter of tuned PID controller is given in Table 3.

3. Supervised Machine Learning Algorithm

MLA is a subfield of AI that allows a computer algorithm to anticipate events more precisely without its exclusively designing to do so. In order to anticipate new response values, MLA use chronological data as input. Regression algorithm is a supervised algorithm [36]. Squared Gaussian process regression SGPRA is based on the idea of Gaussian processes, which are a set of haphazard variables with a mutual Gaussian distribution for any finite number of them. A mean function and a covariance function also referred to as a kernel function, describe a Gaussian process [23], [27]-[29]. The squared exponential kernel, also acknowledged as the radial basis function, is the covariance function used in the squared exponential GPR use (5).

$$M((x1, x2), (x1', x2')) = ¥\text{^}2 * exp(-0.5 * (||x - x'||\text{^}2 / L\text{^}2)) \quad (5)$$

Table 1. PV module specification of MSX-60W pv module [22]

PV module specification	Value
Voc open circuit voltage	21.1volt
Isc short circuit current in amp	3.8A
Impp panel maximum current in ampere	3.5A
Vmpp Panel max output voltage in volt	17.1volt
K_s (boltzman constant)	1.38×10^{-23} J/K
N (series cell)	36
q (electron charge)	1.6×10^{-19} coulomb
n is the constant	1.3
Isc short circuit current	3.8A
Tr (reference temperature)	25 °C
Gr (reference Sun radiation)	1000 watt/m^2
Series Resistor Rx	0.00181 ohm
Shunt Resistor Ry	400 ohm
Temperature coefficient of current Ki	.003 mA/°C
Temperature coefficient of voltage Kv	-.08 mA/ °C
Maximum output power	60W

Table 2. Parameters of boost converter

Parameter	Value
Vi (Maximum Panel output voltage)	51.3 volt
Ro	60 ohm
L	29 mH
F (Switching frequency)	25 khz
dI_L (current ripple)	10% of I_L
dV_i (voltage ripple)	1% of Vo
C_2	260 microfarad
C_1	34.11 microfarad

Table 3. Performance & robustness parameter of PID controller

Stability	Rise Time	Overshoot	Settling Time	Peak	Gain margin
Stable	0.0251sec	4.20%	0.0649	1.01	67.5deg

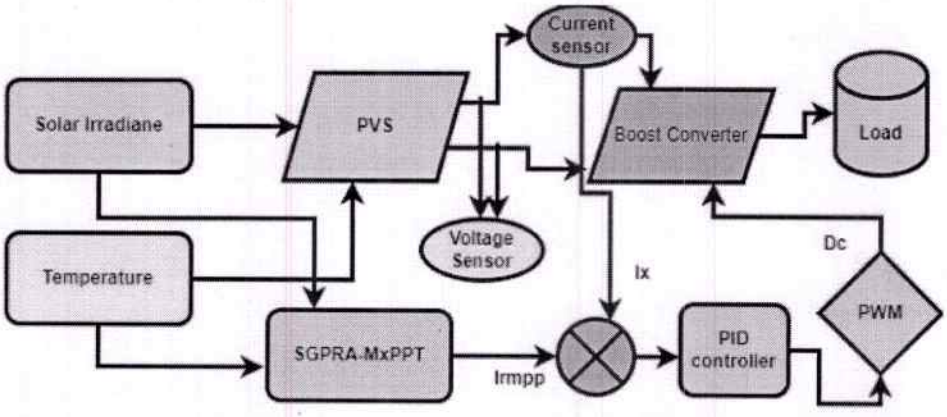

Fig. 1. Proposed block diagram of SGPRA-MxPPT

Here, $(x1, x2)$ and $(x1', x2')$ shows the two points input features in space, ¥^2 is the variance, $||x - x'||$^2 is the squared Euclidean distance between the points, and L is the length scale. Estimate the parameters of the covariance function (¥^2 and L) using techniques like maximum likelihood

estimation. To make the predictions for a test input $(x1^*, x2^*)$ compute the covariance vector among the investigation point and the training points: $M\_^* = [M((x1^*, x2^*), (x1, x2))]$ for each training point $(x1,\ x2)$. Compute the predictive mean $(£(x^*))$ and predictive variance $(¥\hat{}2(x^*))$ using equation (6) and (7) [23], [29].

$$£(x^*) = M\_\hat{}T * (M + ¥\hat{}2\_n * L)\hat{}(-1) * y \quad (6)$$

$$¥\hat{}2(x) = M(x^*, x^*) - M\_\hat{}T * (M + ¥\hat{}2\_n * L)\hat{}(-1) * M\_ \quad (7)$$

Here, $M(x^*, x^*)$ represents the covariance between the test point and its self. Proposed model's efficacy is computed by correlated the anticipated values with the actual target values using appropriate evaluation metrics (e.g., MSE, R-squared) for regression tasks [26]-[29]. Fig. 2 displays the flow of SGPRA algorithm.

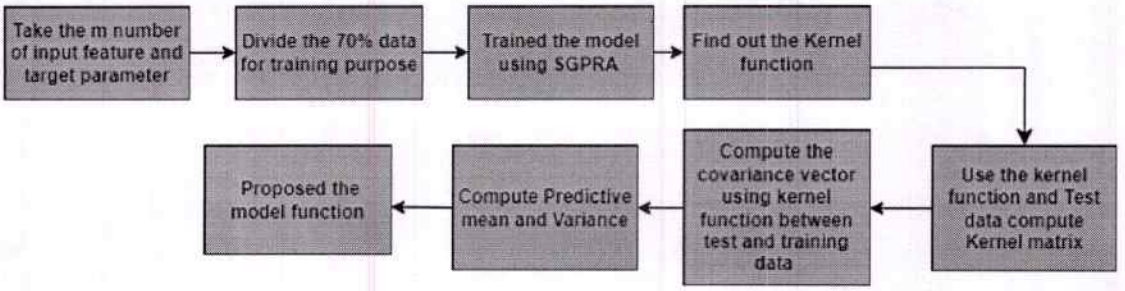

Fig. 2. Flow chart of SGPRA algorithm

The SGPRA used data set of MSX-60W for training and testing purpose. The Table 4 shows the error result during validation and testing duration, Fig 3 (a) and Fig. 3 (b) shows the plot of response of model during training and testing phase and Fig. 4 (a), (b) residual error during training and testing phase. The extracted model for the prediction of new value to unknown input parameter is trainedModel.predictFcn = @(x) gpPredictFcn(predictorExtractionFcn(x));

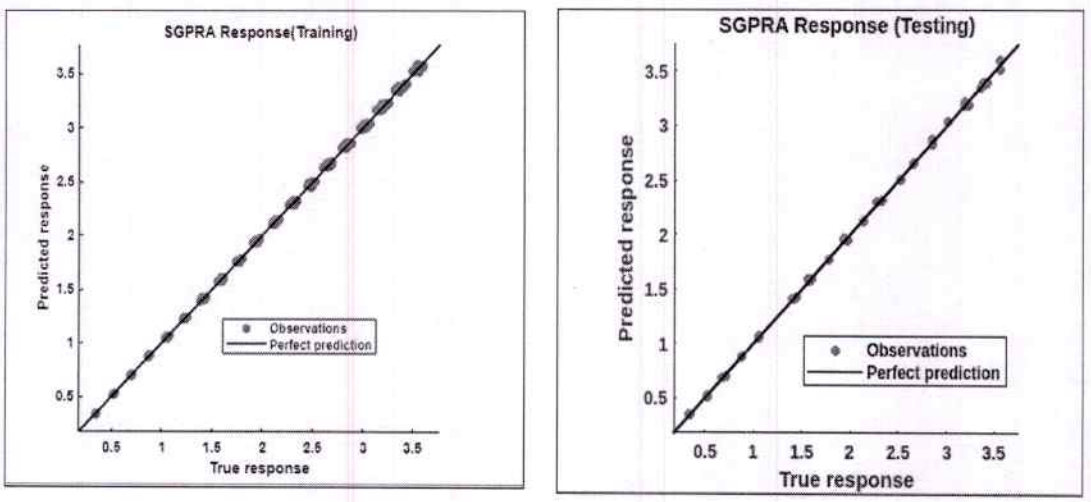

(a) (b)

Fig. 3. SGPRA Response during training (a), testing (b)

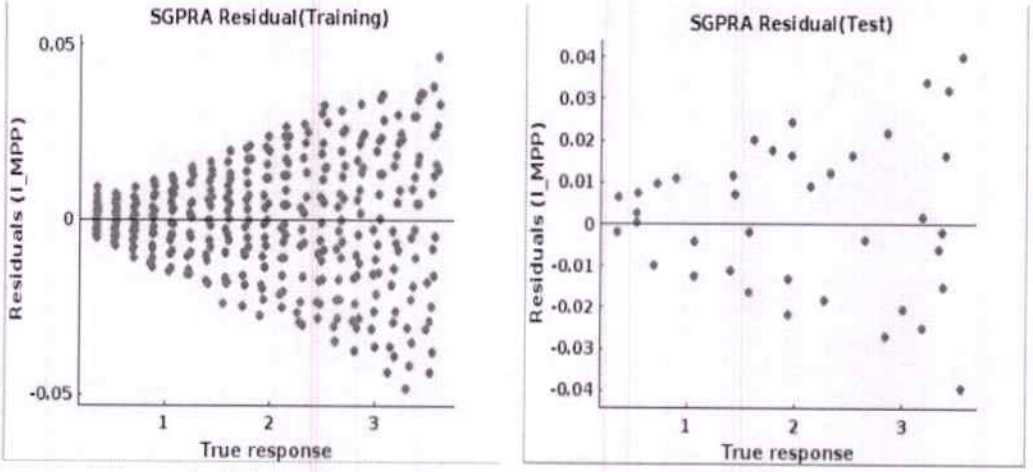

(a) (b)

Fig. 4. Residual during training (a), testing (b)

3.1. Proposed MxPPT Algorithm

Author uses SGPRA model to track MxPP of a PVS using. The proposed MxPPPT algorithms steps are given below. Fig. 5 shows the proposed SGPRA-MxPPT algorithm flow chart.

(i) Measure the panel voltage Vx and current Ix for an incident illumination and temperature value.

(ii) Calculate the panel instantaneous power Px.

(iii) Compute the predicted maximum current Irmpp using the SGPRA model for incident radiation and temperature.

(iv) If measured instantaneous current Ix <Irmpp then increase the Ix by adjusting duty duration Dd.

(v) If measured instantaneous current Ix >Irmpp then decrease the Ix by adjusting duty duration Dd.

(vi) Continue the process until Irmpp=Ix

(vii) Calculate Px at when objective achieved and display maximum power of PVS.

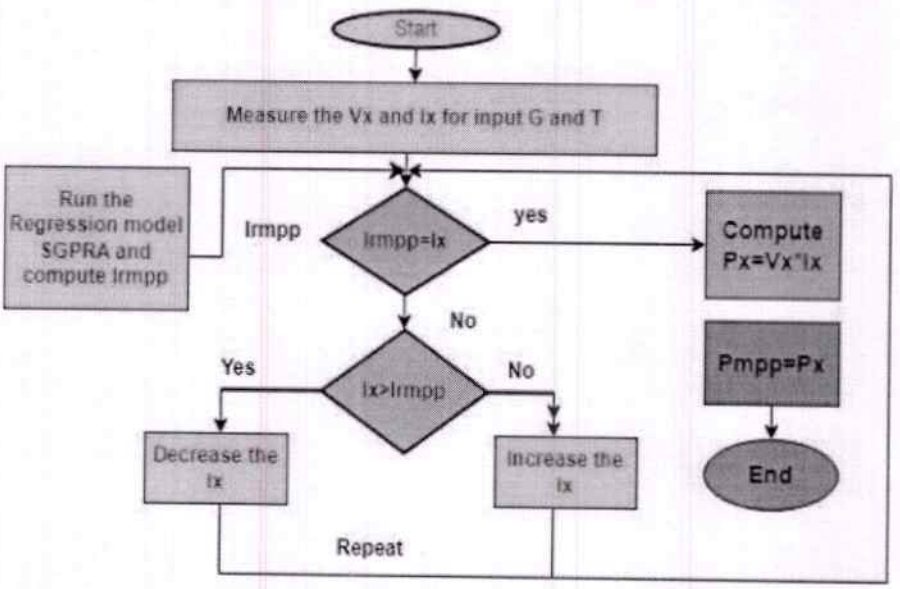

Fig. 5. SGPRA-MxPPT Algorithm flow chart

Table 4. SGPRA Result analysis during training and testing phase

Regression constant	Value	Error	Training Result (Validation)	Error	Testing Result
Variance	1.00	RMSE	0.016791	RMSE	0.01461
Mean	0.00	MSE	0.000281	MSE	0.000213
		MAE	0.013081	MAE	0.0115
Training Time ----------2.35 sec					
Prediction speed----------19000obs/sec					

4. Result and Discussion

A PVS system of MSX -60W 3×1 photo panel connected in series. Fig. 6 (a) and (b) shows the PVC of PVS under different solar insolation. When array is subjected to UWC (1000w/m^2 solar illumination and 25 °C temperature) than average power (P_a) from the array is 179.5 Watt, if panel is subjected to NUW1 (1000w/m^2 to 800w/m^2 to 600 w/m^2 at 25 °C) than average power (Pa)is 143Watt and under NUW2 (800w/m^2 to 600w/m^2 to 400 w/m^2 at 25 °C) average power is 108 Watt. The simulation of model on Matlab/Simulink under UWC, NUW1 and NUW2 as exposed in Fig. 7 is performed. The Table 5 shows the result of 3×1 MSX-60W PVS under UWC, NUW1 and NUW2 without MxPPT controller. In Table 5 No of peak shows the global and minor peak in variable weather conditions, Vmp is the maximum voltage at global peak, Imp is maximum current at global peak and Pm is the mean power which is the average of total power under the plot. Fig. 8 (a), (b), and (c) demonstrate the result analysis under non uniform weather conditions without MxPPT controller.

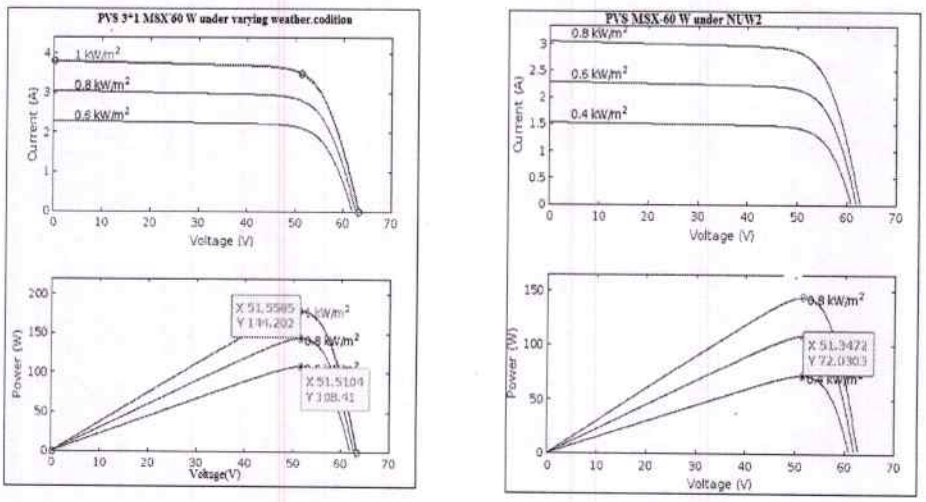

(a) (b)

Fig. 6. V-I & P-V curve of array under NUW1 (a), NUW2 (b)

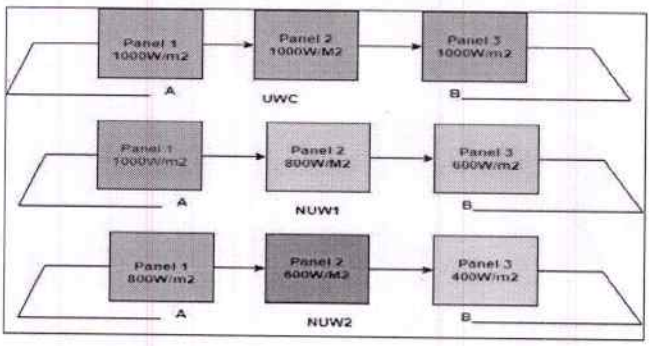

Fig. 7. UWC, NUW1 and NUW2

Simulation result analysis of PVS without MxPPT under UWC shows one global peak (GP) at 178.8 watt, NUW1 3 peaks with GP at 126W and in NUW2 3 peaks with GP at 90W. For the same operating conditions Simulation run under UWC, NUW1 and NUW2 using SGPRA controller and VINA-MxPPT controller. The Fig. 9 (a, b & c) displays the results of SGPRA-MxPPT under UWC, NUW1 and NUW2 and Fig. 10 (a, b & c) shows the response of VINA under UWC, NUW1 and NUW2. The time required to stable the algorithm under UWC, NUW1 and NUW2 is 0.13s by SGPRA and 0.26 s by VINA although fluctuation around the stable value using SGPRA algorithm are negligible small as publicized in Fig. 11 a and b. Table 6 shows the response analysis under three operating condition for both the MxPPT Controller.

Table 5. Response analysis of MSX-60W PVS without MxPPT controller

Operating Condition	No of Peak	Maximum Voltage (Vmp)	Maximum Current (Imp)	Max Power (Pmp)	Mean Power (Pm)
UWC	1	51.1	3.50	178.8Watt	83.84W
NUW1	3 (GP, LP1, LP2)	51.20	2.98	126 Watt	64.61W
NUW2	3 (GP, LP1, LP2)	51.19	2.25	90 Watt	46.69W

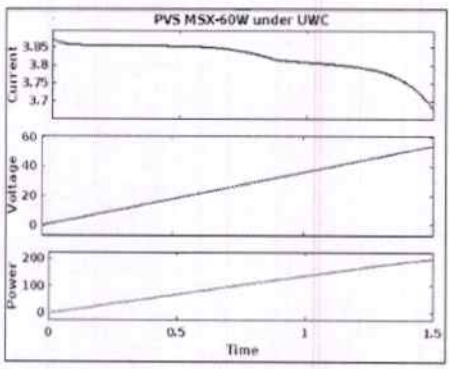

(a)

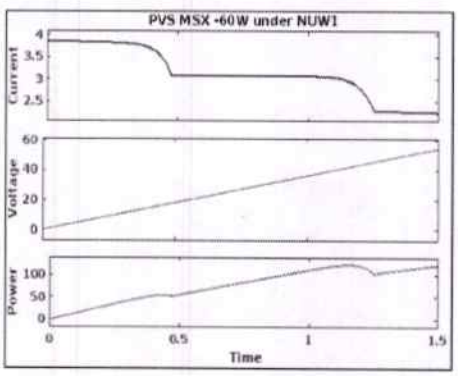

(b)

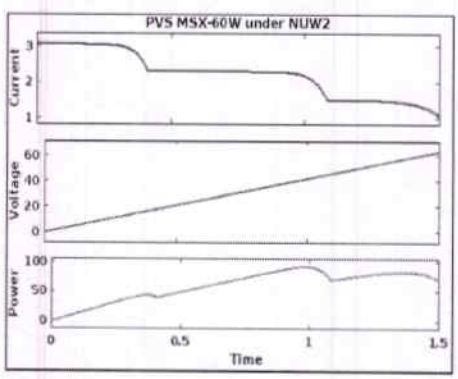

(c)

Fig. 8. Response under UWC (a), NUW1 (b), NUW2 (c)

$$Efficiency = (Px/Pa) * 100 \quad (8)$$

The comparative analysis of simulation result SGPRA-MxPPT and VINA-MxPPT in Table 6 shows that SGPRA controller exhibits improved performance in terms of maximum power, mean power and transit time. The means power efficacy of projected controller can be computed by using equation (8), where Pa is the maximum average power of an actual solar panel in UWC, NUW1 and NUW2 conditions i. e. 179.5W, 143W and 108W and Px is the mean power using MxPPT controllers

show in. Fig. 12 shows the mean efficiency of SGPRA-MxPPT, VINA-MxPPT and Fig. 13 shows the tracking duration for proposed MxPPT.

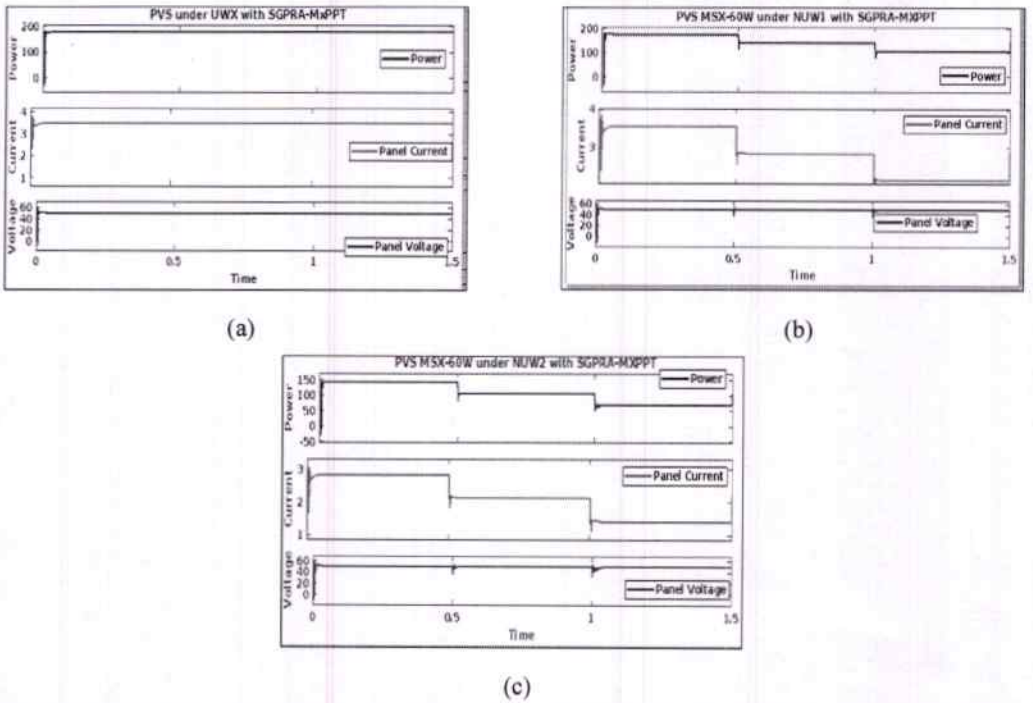

Fig. 9. PVS under UWC with SGPRA-MxPPT (a), PVS under NUW1 with SGPRA-MxPPT (b), PVS under NUW2 with SGPRA-MxPPT (c)

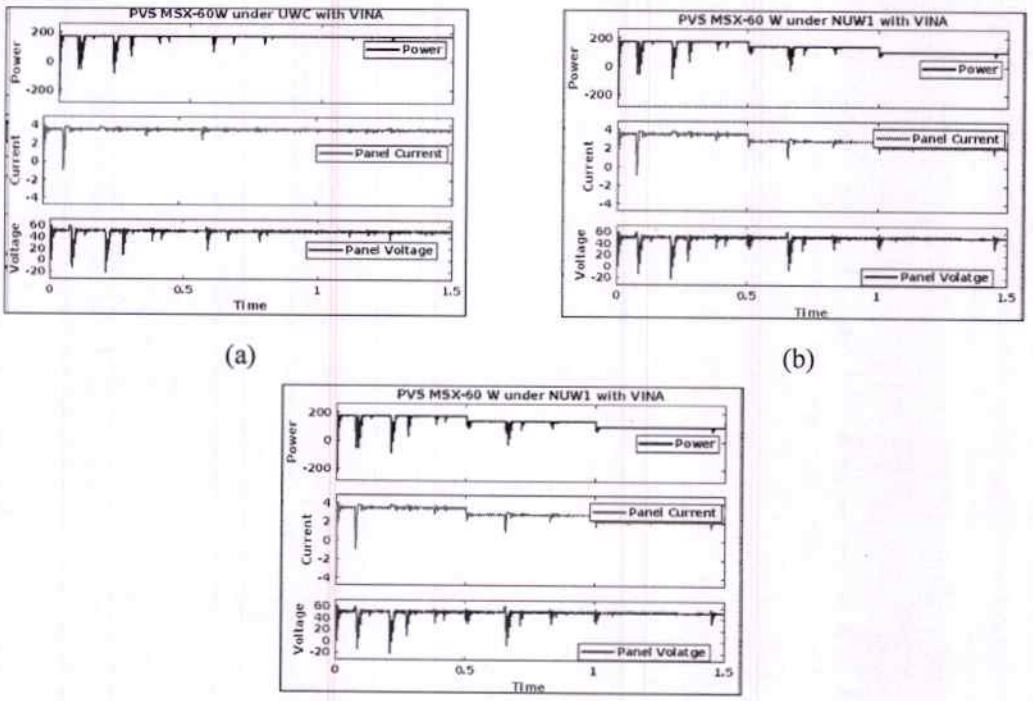

Fig. 10. PVS under UWC with VINA (a), PVS under NUW1 with VINA (b), PVS under NUW2 with VINA (c)

The Table 6 shows that mean power Px using UWC, NUW1 and NUW2 is more than the mean power Pm without using MxPPT controller. The Table 5 and Table 6 demonstrates that maximum tracking power (Pmp) and mean power (Px) by using MxPPT controller is more than the without MxPPT controller. The SGPRA-MxPPT mean Power Px is 179.3W, 143.4W, and 106.6W and VINA Px are 173.7W, 137.6W, and 103.6W.

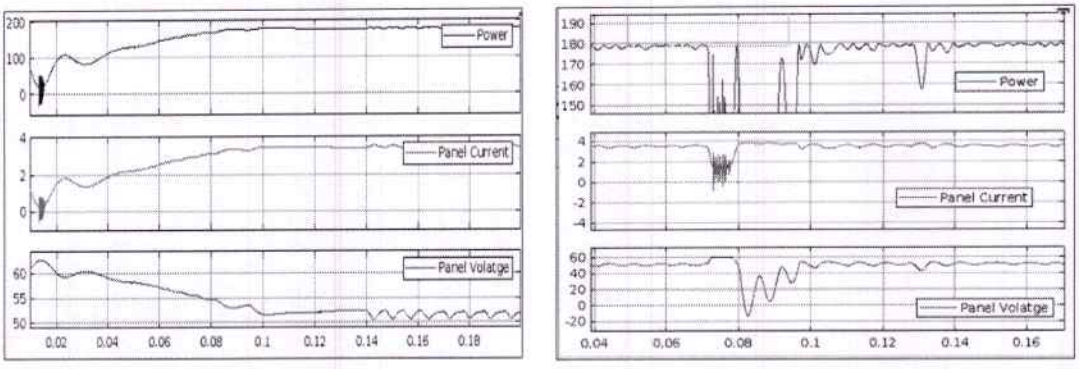

(a) (b)

Fig. 11. Oscillation for SGPRA-MxPPT (a), Oscillation for VINA-MxPPT (b)

Table 6. Comparative analysis of results with SGPRA-MxPPT and VINA-MxPPT

Environment Condition	MxPPT Controller	Vmax (V)	Imax (A)	Pmax (watt)	Mean Power Px (watt)	Time	Efficiency $=(Px/Pa)*100$
UWC (1000w/m², 25c)	SGPRA	50.9	3.51	179.3	179.3	0.13s	99.86%
NUW1 (1000, 800, 00W/m²25c)		50.29	2.829	158.8	142.4	0.13s	99.58%
NUW2 (800, 600, 400W/m²25 c)		50.29	2.136	143.6	106.6	0.16s	99.02%
UWC (1000w/m², 25c)	VINA	49.92	3.49	178.8	173.7	0.23s	96.74%
NUWC1 (1000, 800, 600W/m² 25c)		49.78	2.79	105.09	137.6	0.25s	96.21%
NUWC2 (800, 600, 400W/m²25 c)		47.32	2.11	71.07	103.2	0.28s	95.31%

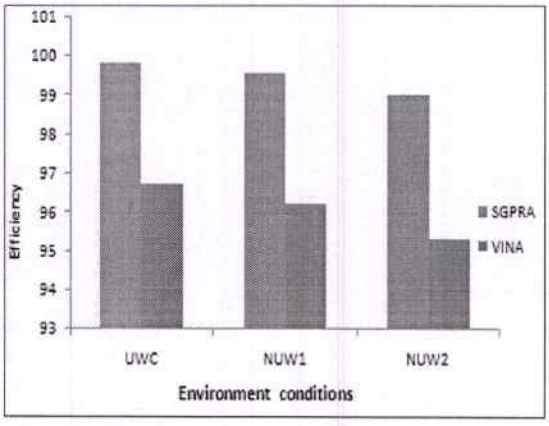

Fig. 12. Means efficiency of MxPPT controller

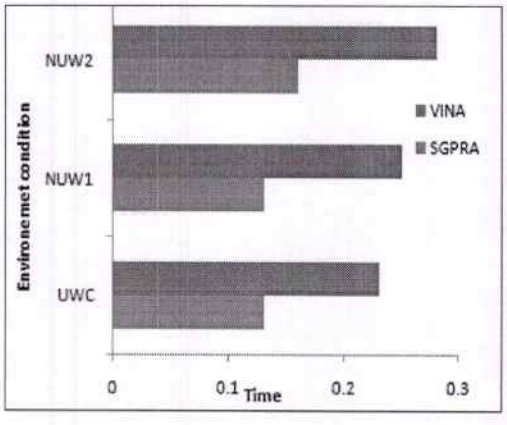

Fig. 13. Tracking duration of MxPPT controller

5. Conclusion

This research introduces a novel regression machine learning-based MxPPT controller. It resolves a number of underlying issues that the bulk of MxPPT algorithms typically have. The primary aim of the MxPPT-Controller is to track the utmost power point with the least variation around steady state power under varying solar illumination in the shortest amount of time. The following conclusions are find out by the authors in presented paper:

- A New ML-MxPPT controller proposed that shows the mean power approximate equals to Solar Panel mean Power.
- Under different environmental conditions, the suggested MxPPT controller's efficiency in MATLAB is greater than 99%, with 0.13 sec tracking time and barely perceptible oscillations around stable maximum power.
- Comparing the SGPRA-MxPPT controller's performance to that of other advanced methods In order to prove its superiority, VINA used a 0.26-second tracking duration with a high tracking efficiency.

Author's intended hardware setup in upcoming works and experimental result to prove the advantage of MLA in the field of MxPPT under varying environment situation.

Data Availability: The statistics utilized to help out the result of this research are integrated in the article and mentioned in reference section.

Acknowledgements: The authors are very grateful to the research department of MIET, Meerut and MIT Meerut, India for offering a good exploration surroundings and facilities.

Conflicts of Interest: The authors declare that they have no conflicts of interest to this work.

References

[1] A. K. Podder, N. K. Roy, and H. R. Pota, "MPPT methods for solar PV systems: a critical review based on tracking nature," *IET Renewable Power Generation*, vol. 13, no. 10, pp. 1615-1632, 2019, https://doi.org/10.1049/iet-rpg.2018.5946.

[2] N. A. Kamarzaman and C. W. Tan, "A comprehensive review of maximum power point tracking algorithms for photovoltaic systems," *Renewable and Sustainable Energy Reviews*, vol. 37, pp. 585–598, 2014, https://doi.org/10.1016/j.rser.2014.05.045.

[3] M. Mosa, M. B. Shadmand, R. S. Balog, and H. A. Rub, "Efficient maximum power point tracking using model predictive control for photovoltaic systems under dynamic weather condition," *IET Renewable Power Generation*, vol. 11, no. 11, pp. 1401-1409, 2017, https://doi.org/10.1049/iet-rpg.2017.0018.

[4] R. J. Mustafa, M. R. Gomaa, M. Al-Dhaifallah, and H. Rezk, "Environmental Impacts on the Performance of Solar Photovoltaic Systems," *Sustainabilty*, vol. 12, no. 2, p. 608, 2020, https://doi.org/10.3390/su12020608.

[5] N. Karami, N. Moubayed, and R. Outbib, "General review and classification of different MPPT Techniques," *Renewable and Sustainable Energy Reviews*, vol. 68, pp. 1–18, 2017, https://doi.org/10.1016/j.rser.2016.09.132.

[6] M. Seyedmahmoudian *et al.*, "State of the art artificial intelligence based MPPT techniques for mitigating partial shading effects on PV systems-A review," *Renewable and Sustainable Energy Reviews*, vol. 64, pp. 435–455, 2016, https://doi.org/10.1016/j.rser.2016.06.053.

[7] A. R. Jordehi, "Maximum power point tracking in photovoltaic (PV) systems: a review of different approaches," *Renewable and Sustainable Energy Reviews*, vol. 65, pp. 1127-1138, 2016, https://doi.org/10.1016/j.rser.2016.07.053.

[8] R. Ahmad, A. F. Murtaza, and H. A. Sher, "Power tracking techniques for efficient operation of photovoltaic array in solar applications – A Review," *Renewable and Sustainable Energy Reviews*, vol. 101, pp. 82-102, 2019, https://doi.org/10.1016/j.rser.2018.10.015.

[9] B. Bendib, H. Belmili, and F. Krim, "A survey of the most used MPPT methods: conventional and advanced algorithms applied for photovoltaic systems," *Renewable and Sustainable Energy Reviews*, vol. 45, pp. 637-648, 2015, https://doi.org/10.1016/j.rser.2015.02.009.

[10] T. Radjai, L. Rahmani, S. Mekhilef, and J. P. Gaubert, "Implementation of a modified incremental conductance MPPT algorithm with direct control based on a fuzzy duty cycle change estimator using dSPACE," *Solar Energy*, vol. 110, pp. 325-337, 2014, https://doi.org/10.1016/j.solener.2014.09.014.

[11] N. Priyadarshi, F. Azam, A. K. Sharma, and M. Vardia, "An adaptive neuro- fuzzy inference system-based intelligent grid-connected photo-voltaic power generation," *Advances in Computational Intelligence*, vol. 988, pp. 3–14, 2020, https://doi.org/10.1007/978-981-13-8222-2_1.

[12] W. Hayder, E. Ogliari, A. Dolara, A. Abid, M. B. Hamed, and L. Sbita, "Improved PSO: A Comparative Study in MPPT Algorithm for PV System Control under Partial Shading Conditions" *Energies*, vol. 13, no. 8, p. 2035, 2020, https://doi.org/10.3390/en13082035.

[13] Y. Shaiek M. B. Smida, A. Sakly, and M. F. Mimouni, "Comparison between conventional methods and GA approach for maximum power point tracking of shaded solar PV generators," *Solar Energy*, vol. 90, p. 107-122, 2013, https://doi.org/10.1016/j.solener.2013.01.005.

[14] M. K. Behera, I. Majumder, and N. Nayak, "Solar photovoltaic power forecasting using optimized modified extreme learning machine technique," *Engineering Science and Technology an International Journal*, vol. 21, no. 3, pp. 428-438, https://doi.org/10.1016/j.jestch.2018.04.013.

[15] M. Takruri *et al.*, "Maximum power point tracking of PV system based on machine learning," *Energies*, vol. 13, no. 3, p. 692, 2020, https://doi.org/10.3390/en13030692.

[16] D. D. Martínez, R. T. Codorniu, R. Giral, and L. V. Seisdedos, "Evaluation of particle swarm optimization techniques applied to maximum power point tracking in photovoltaic systems," *International Journal Circuit Theory and Applications*, vol. 49, no. 7, pp. 1849-1867, 2021, https://doi.org/10.1002/cta.2978.

[17] D. A. Nugraha, K. L. Lian, and Suwarno, "A Novel MPPT Method Based on Cuckoo Search Algorithm and Golden Section Search Algorithm for Partially Shaded PV System," *Canadian Journal of Electrical and Computer Engineering*, vol. 42, no. 3, pp. 173-182, 2019, https://doi.org/10.1109/CJECE.2019.2914723.

[18] H. Rezk, A. Fathy, and A. Y. Abdelaziz, "A comparison of different global MPPT techniques based on meta-heuristic algorithms for photovoltaic system subjected to partial shading conditions," *Renewable and Sustainable Energy Reviews*, vol. 74, pp. 377-386, 2017, https://doi.org/10.1016/j.rser.2017.02.051.

[19] M. S. Nkambule, A. N. Hasan, A. Ali, J. Hong, and Z. W. Geem, "Comprehensive evaluation of machine learning MPPT algorithms for a PV system under different weather conditions," Journal Electrical Engineering Technology, vol. 16, no. 1, pp. 411-427, 2021, https://doi.org/10.1007/s42835-020-00598-0.

[20] R. Sharmin, S. S. Chowdhury, F. Abedin, and K. M. Rahman, "Implementation of MPPT Technique of Solar Module with Supervised Machine Learning," *Frontiers in Energy Research*, vol. 10, p. 932653, https://doi.org/10.3389/fenrg.2022.932653.

[21] R. K. Phanden, L. Sharma, J. Chhabra, and H. İ. Demir, "A novel modified ant colony optimization based maximum power point tracking controller for photovoltaic systems," *Materials Today Proceeding*, https://doi.org/10.1016/j.matpr.2020.06.020.

[22] K. Nallathambi, S. S. Dash, S. Padmanaban, S. Paramasivam, and P. K. Morati, "Maximum Power Point Tracking Implementation by Dspace Controller Integrated Through Z-Source Inverter Using Particle Swarm Optimization Technique for Photovoltaic Applications," *Applied Sciences*, vol. 8, no. 1, p. 145, 2018, https://doi.org/10.3390/app8010145.

[23] Y. Xie, C. Zhu, W. Jiang, J. Bi, and Z. Zhu, "Analyzing Machine Learning Models with Gaussian Process for the Indoor Positioning System", *Mathematical Problems in Engineering*, vol. 2020, 2020, https://doi.org/10.1155/2020/4696198.

[24] P. Pourmalekia, W. Agutub, A. Rezaei, and N. Pourmaleki, "Techno-Economic Analysis of a 12-kW Photovoltaic System Using an Efficient Multiple Linear Regression Model Prediction," *IJRCS International Journal of Robotics and Control Systems*, vol. 2, no. 2, pp. 370-378, 2022, https://doi.org/10.31763/ijrcs.v2i2.702.

[25] M. L. Katche, A. B. Makokha, S. O. Zachary, and M. S. Adaramola, "A Comprehensive Review of Maximum Power Point Tracking (MPPT) Techniques Used in Solar PV Systems," *Energies*, vol. 16, no. 5, p. 2206, 2023, https://doi.org/10.3390/en16052206.

[26] J. P. Ram, N. Rajasekar, and M. Miyatake, "Design and overview of maximum power point tracking techniques in wind and solar photovoltaic systems: A review," *Renewable and Sustainable Energy Reviews*, vol. 73, pp. 1138-1159, 2017, https://doi.org/10.1016/j.rser.2017.02.009.

[27] M. Phiri, M. Mulenga, A. Zimba, and C. I. Eke, "Deep Learning Techniques for Photovoltaic SolarTracking Systems: A Systematic Literature Review," *Research Square*, 2023, https://doi.org/10.21203/rs.3.rs-2539961/v1.

[28] F. Lubbe, J. Maritz, and T. Harms, "Evaluating the Potential of Gaussian Process Regression for Solar Radiation Forecasting: A Case Study," *Energies*, vol. 13, no. 20, p. 5509, 2020, https://doi.org/10.3390/en13205509.

[29] B. Zazoum, "Solar photovoltaic power prediction using different machine learning methods," *Energy Reports*, vol. 8, pp. 19-25, 2022, https://doi.org/10.1016/j.egyr.2021.11.183.

[30] K. R. Ahmed *et al*, "Application of Hybrid Nanostructure for Photo and Bioenergy Applications," *International Journal of Photoenergy*, vol. 2022, 2022, https://doi.org/10.1155/2022/1123251.

[31] K. S. Awan, T. Mahmood, M. Shorfuzzaman, R. Ali, and R. M. Mehmood, "A Machine Learning Based Algorithm to Process Partial Shading Effects in PV Arrays," *Computers, Materials & Continua*, vol. 68, no. 1, pp. 29-43, 2021, https://doi.org/10.32604/cmc.2021.014824.

[32] A. G. Olabi *et al.*, "Artificial neural networks applications in partially shaded PV systems," *Thermal Science and Engineering Progress*, vol. 37, p. 101612, 2023, https://doi.org/10.1016/j.tsep.2022.101612.

[33] Z. Ishrat, S. Vats, K. B. Ali, O. Ahmad Shah, and T. Ahmed, "A Comprehensive Study on Conventional HPPT Techniques for Solar PV System," *2023 International Conference on Computational Intelligence, Communication Technology and Networking (CICTN)*, pp. 315-321, 2023, https://doi.org/10.1109/CICTN57981.2023.10140264.

[34] A. Khaled, H. Aboubakeur, B. Mohamed, and A. Nabil, "A Fast MPPT Control Technique Using PID Controller in a Photovoltaic System," *2018 International Conference on Applied Smart Systems (ICASS)*, pp. 1-5, 2018, https://doi.org/10.1109/ICASS.2018.8652062.

[35] X. Wang and F. Blaabjerg, "Harmonic Stability in Power Electronic-Based Power Systems: Concept, Modeling, and Analysis," *IEEE Transactions on Smart Grid*, vol. 10, no. 3, pp. 2858-2870, 2019, https://doi.org/10.1109/TSG.2018.2812712.

[36] S. Sun, Z. Cao, H. Zhu, and J. Zhao, "A Survey of Optimization Methods from a Machine Learning Perspective," *IEEE Transactions on Cybernetics*, vol. 50, no. 8, pp. 3668-3681, 2020, https://doi.org/10.1109/TCYB.2019.2950779.

[37] C. E. Rasmussen, "Gaussian Processes in Machine Learning," *Advanced Lectures on Machine Learning*," vol. 3176, pp. 63-71, https://doi.org/10.1007/978-3-540-28650-9_4.

[38] M. S. Raboaca *et al.*, "Concentrating Solar Power Technologies," *Energies*, vol. 12, no. 6, p. 1048, https://doi.org/10.3390/en12061048.

[39] S. Fadhel *et al.*, "PV shading fault detection and classification based on I-V curve using principal component analysis: Application to isolated PV system," vol. 179, pp. 1-10, 2019, https://doi.org/10.1016/j.solener.2018.12.048.

[40] N. Al-Rousan, N. A. M. Isa, and M. K. M. Desa, "Advances in solar photovoltaic tracking systems: A review," *Renewable and sustainable energy reviews*, vol. 82, pp. 2548-2569, 2018, https://doi.org/10.1016/j.rser.2017.09.077.

International Journal of Current Engineering and Technology
E-ISSN 2277 – 4106, P-ISSN 2347 – 5161

Available at http://inpressco.com/category/ijcet

Research Article

Design and Simulation of Hybrid Tee and 180⁰ Ring Hybrid Coupler for S Band

Ashish Tripathi#*

#Electronics and Communication Engineering Department, Dr.A.P.J Abdul Kalam Technical University, Lucknow (U.P) (formerly Uttar Pradesh Technical University), India, *Meerut institute of Technology, Partapur Meerut (U.P) India

Received 16 June 2023, Accepted 20 July 2023, Available online 22 July 2023, **Vol.13, No.4 (July/Aug 2023)**

Abstract

Hybrid tee is widely used component in microwave system, the four arms of a conventional Hybrid tee direct at four directions, which occupy much space and give inconvenience to the assemblage of a system. In this paper a design of waveguide having width =50.0 mm, Height =20.0 mm, Length=75.0 mm as well as solution frequency =4.0 GHz. Material assign for Hybrid tee is vacuum which relative permittivity =1 as well as relative permeability =1. We make four arms at different position, such as first arms located at position -25.0,-10.0, 0.0, second arms locate at position -25.0,-10.0, 0.0, third and fourth arms locate at position -25.0,-10.0, and 0.0. Each arm is 900 positions from each other's.1800 ring hybrid coupler a type of coupler used in RF and Microwave system. Its simplest form it is a 3dB coupler and is thus an alternative to a Hybrid tee.RogersRT/duroid 5870™ is used which relative permittivity 2.33 used. HFSS is a high performance full wave electromagnetic (EM) field simulator for arbitrary 3D volumetric passive device Modeling. It employs the finite Element Method (FEM), adaptive Meshing and brilliant graphics. This paper reports for Hybrid Tee for S band that a signal incident on the different port split equally between port 2 and 3, but the resulting signal are 1800 out of phase. Also 1800 Ring Hybrid Coupler for S band is a four port networks with a 1800 phase shift between two output ports but it can also be operated so that output port are in phase. Both the Structures are first designed using HFSS and then Simulated.

Keywords: *Microwave system, waveguide, hybrid coupler.*

1. Introduction

Waveguide E-plane tee is an important passive element in microwave and millimetre wave engineering. Tee junctions are generally used to split the line power into two or combine the power from two lines with proper consideration of phase. However, because of the complicated structure and small size, good performance E-plane tee at Microwave frequencies such as at X-band or higher frequencies is difficult to realize on the other hand, a precise field analysis on waveguide E- plane tee is also difficult. So, proper numerical analysis of waveguide tee junction will help to analyse the power distribution between different ports along with phase of transmission coefficient. Several works already made significant contributions in this field. [1] Made a comparative analysis of planar SIW magic tee with traditional rectangular tee. Novel four planar magic tee was proposed by [2] for networking applications using waveguide slab filled waveguide phase shifter.

The Present author [3] also analyzed magic tee structure in X- band for useful practical applications, which is matched with finding of others [4].Experimental results[5] are well fitted with the recently available numerical studies. She first presented the detailed analytical model [6] for tee structures using hybrid finite-element model-expansion method.

As HFSS is an interactive software package for calculating the electromagnetic behaviour of a structure, so one can compute basic electromagnetic field quantities, generalized S-parameters and S-parameters renormalized to specific port impedances, the eignmodes, or resonances, of a structure [7]. HFSS is high-performance full wave electromagnetic field simulators for arbitrary 3D volumetric passive device Modelling Proper material are always chosen prior to the simulation for future experimental works.

2. Designing

A. Construction

Let us design Hybrid Tee and 180⁰ Ring Hybrid Coupler as Shown in fig and fig

*Corresponding author's ORCID ID: 0000-0000-0000-0000
DOI: https://doi.org/10.14741/ijcet/v.13.4.3

CERTIFICATE OF PUBLICATION

It is certified that the research article

Design and Simulation of Hybrid Tee and 180° Ring Hybrid Coupler for S Band

Submitted by

Ashish Tripathi

was accepted and was published in our *Refereed* **International Journal of Current Engineering and Technology** **(ISSN: 2277 – 4106)** in **Vol.13, No.4 (July/Aug 2023)** at page no. 327-333 and is available at:
https://inpressco.com/category/ijcet/vol-13-no-4-july-aug-2023/

INPRESSCO® International Press Corporation

Article Grade: Good

NAAS India

Date: 14.09.2023

IJCET Global Impact Factor: 7.151

D. Mhatre

DR D. Mhatre Editor

Meerut Institute of Technology MIT Meerut

Journal of
Fluid Mechanics and Mechanical Design

e-ISSN: 2582-9165
Volume-5, Issue-3 (September-December, 2023)

Contemporary Research in Solid Mechanics

Gaurav Kumar*
Assistant Professor, Department of Mechanical Engineering, Meerut Institute of Technology, Meerut, Uttar Pradesh, India

*Corresponding Author: gauravnirmal78600@gmail.com

Received Date: December 21, 2023

Published Date: January 4, 2023

ABSTRACT

The study of force and matter's motion is known as mechanics. The study of force and matter motion in solid states is known as solid mechanics. Naturally, mechanics interests physicists. Quantum mechanics, statistical mechanics, and the theory of relativity are considered the three greatest contributions to physics in the 20th century. The dynamics of chemical reactions, the generation of molecular aggregates, crystal formation, the polymerization of bigger molecules, and other processes are among the topics that fascinate chemists. Biomechanics, which connects biologists, are interested in structure to function at all levels of the hierarchy, from biomolecules to cells, tissues, organs, and persons. Living cells are manufacturers of proteins with internal machinery that moves and performs tasks in a systematic manner in accordance with the rules of mechanics, despite the fact that they are not homogenous continuums.

Keywords- Biomechanics, Biomolecules, Dynamics, Machinery, Mechanics

INTRODUCTION

A solid is any substance that, in the course of an industrial or natural process or action, can endure for a predefined amount of time under a substantial degree of shearing force. What distinguishes solids from fluids is this: Despite the fact that normal stress is the normal force per material plane unit area in question is directed perpendicular to the plane across which it acts in fluids. Shearing stresses are defined as shearing forces per unit area. In contrast to normal forces, shearing forces act parallel to the material plane rather than perpendicular to it [1].

As a result, solid mechanics studies shear stress, deformation, and structural and material failure. The following are the most often discussed subjects in the field of solid mechanics:

Structures' stability is the study of whether a structure can revert to a particular equilibrium following a disruption or partial or total failure.

Chaos and Dynamical Systems: managing mechanical systems that are extremely sensitive to their beginning location thermomechanics: the study of materials using thermodynamics-derived models.

Biomechanics is the application from organic materials like bones and cardiac tissue to solid mechanics.

Geomechanics: the application of solid mechanics to geological materials, such as rock, ice, and soil solids and structures vibrating - studying the propagation of vibration and waves from vibrating particles and structures; this is important for fracture and damage mechanics in the fields of mechanical, civil, mining, aerospace, and maritime/marine engineering handling the physics of crack development in solid materials. Composite materials are materials composed of many compounds, such as fiber glass, reinforced concrete, and reinforced polymers. Solid mechanics is applied to these materials [2-5].

Computational mechanics or the numerical solutions to mathematical problems, including the variational formulations and the finite element method (FEM), that comes from several schools of solid mechanics

Experimental mechanics is the creation and

Journal of
Modern Thermodynamics in Mechanical System

e-ISSN: 2582-5771
Volume-5, Issue-3 (September-December, 2023)

The Consequence of Stress on the Microstructure of Low Carbon Sheets

Gaurav Kumar*
Assistant Professor, Department of Mechanical Engineering, Meerut Institute of Technology, Meerut, Uttar Pradesh, India

*Corresponding Author: gauravnirmal78600@gmail.com

Received Date:December 20, 2023

Published Date:January 05, 2024

ABSTRACT

Under plane stress circumstances, the impact effects of low carbon steel stress on the microstructure and failure morphology are investigated experimentally and numerically in this study. The analysis discovered large grain extensions at the fracture location as well as an endless cycle of tension and stress around the microstructure matrix's pearlitic faces. Concentrations of stress and strain on the pearlite at the limited area are primarily responsible for the oblique fractures seen in the microstructure's stress and strain patterns.

Ferrite, which is carbon dissolved in alpha-iron, is the primary component in a solid solution phase of low-carbon steels to form a cubic crystal with a body core. Ferrite, The better machinability of low-carbon steel compared to other carbon and alloyed steels is mostly due to the softest phase of steel. The amount of pearlite in the steel microstructure rises with the metal's carbon content. The alternating stacking process creates the microconstituent pearlite. Two minerals are ferrite and iron carbide, also known as cementite. Therefore, compared to low-carbon steels, medium-carbon steels are more challenging to manufacture. In the cementite network, high-carbon steels with carbon content greater than 0.8% produce a pearlitic matrix. The dense pearlite concentration and the rigid, brittle cementite network are the main reasons why high-carbon steels are difficult to machine.

Keywords- Carbon steels, Cubic crystal, Low carbon, Network, Steels

INTRODUCTION

Low-carbon steel is a type of steel commonly used in vehicle body components, structural Pipeline sheets, shapes, structures, bridges, tin cans, and other components. They can be machined, welded, and are less expensive to create [1]. Microscopic defects caused by manufacturing and operational processes invariably exist in engineering structures, and combined stress can cause these flaws to multiply and spread throughout the material and environmental factors, causing a part to separate into two or more pieces—a catastrophic failure [2-4]. Nucleation is frequently used to aid in the ultimate separation process, which is usually very short. Three interconnected mechanisms—void nucleation; the microscopic features of ductile failure are caused by void formation and void coalescence [5, 6]. The experimental research and interpretation of data utilizing simulation software to determine Special consideration has been given to the mechanical behaviour of materials when subjected to complicated loading conditions [7]. The Mackenzie group [8] looked into how the stress state affected the commencement of ductile failure and found that stress triaxiality has an inverse relationship with the threshold plastic strain needed to cause ductile failure. Additionally, he thought that the chemistry relating to void formation and flow characteristics might account for the observed variations in fracture toughness and how thickness affects it [9]. According to Nath and Uttam, brittle fracture was brought about by a notch being introduced into the material [10]. In shear stress loops that have mild steel materials, the shear morphology and failure site have been determined to arise from an angular bearing at a 45-degree angle to the tensile axis [11]. A new finite element analysis method for simulating ductile failure. It was founded on the ductile fracture model is characterized by the phenomenological stress-modified fracture strain model. The effects of stress are examined in this

Azerbaijan Pharmaceutical and Pharmacotherapy Journal.

DOI https://doi.org/10.61336/appj/22-2-01

Academic Publishing: Shifting Paradigm from Print to Digital Publication

Neeraj Kant Sharma[1]

[1]Department of Pharmacy Meerut Institute of Technology, Meerut, India

Corresponding author: Neeraj Kant Sharma (e-mail: sharma25neeraj@gmail.com).

Two facets of academic publishing pose significant challenges. One relates to the relative ease of online publishing compared to the traditional difficulties faced when establishing print-based journals in the pre-internet era. On the other front, the trend in publishing is shifting towards "open-access," driven by user expectations and the preferences of funding bodies. Both of these developments are facilitated by the information revolution, which has enabled a substantial and continually expanding segment of the global population to access an extensive network of internet-connected resources and to share their own ideas with the world, a concept that might have seemed fantastical just a few decades ago. Neither of these developments should be viewed as inherently negative.

Accessibility to research databases has increased significantly over the past two decades, thanks to the infrastructure development of information technology tools and procedures. This progress has also accelerated the publication of newly developed research and methodologies. With journals transitioning from the conventional practice of print publications to web platforms, researchers now have numerous opportunities to select and publish their research in reputable periodicals more expeditiously.

The shift to digital publication has had a profoundly positive impact on scholars worldwide, making scholarly publications more accessible and of higher quality on a global scale. The availability of additional creative online and digital content expands the possibilities for the comprehensive accessibility and usability of all research components, including processes, resources, and data.

Our journey into the realm of online publishing, with one foot grounded in established norms and protocols and the other stepping into the experimental and exhilarating world of previously unimaginable possibilities, especially with the advent of the internet and the web, has been characterized by a blend of vigilance and courageous innovation. We not only dare to dream but also take action by integrating software, text, images, video, and sound to create dynamic representations of our ideas and knowledge, striving to express our ideas as vividly as possible.

In today's world, researchers frequently collaborate across institutional and geographical boundaries. Online publication offers the advantage of information sharing, enabling works to be discussed, revised, and reissued. Knowledge progresses as a result of the sharing of new ideas, theories, and discoveries.

The possibilities in the new realm of information exchange are intriguing, notwithstanding their complexity. To comprehend the future of publishing, one must consider not only the current environment that defines the roles of authors, readers, publishers, and third-party institutions in the publication process but also the potential ramifications of innovative technologies that allow for the unprecedented exchange of knowledge and information.

OPEN ACCESS PUBLISHING

There is a widely shared consensus that scientific knowledge should be accessible to everyone. However, accessing articles from many reputable journals can be costly, limiting the benefits to numerous academics and institutions. The traditional route to making a lasting impact on scientific literature is no longer solely through subscription-based print publications. Instead, various opportunities are emerging for optometric educators, physicians, vision scientists, healthcare practitioners, and even our students to share their work within an open access environment.

Section A-Research paper

Hepatoprotective Activity of *Lagenaria siceraria* Leaf Extract against Carbon Tetrachloride-Induced Damage in Rats

Neeraj Kant Sharma*[1], Priyanka[2], Nisha[3], Suneel kumar[4], Nitin Kumar[1], Hasan Ali[1],

[*1]Department of Pharmacy, Meerut Institute of Technology, Meerut, Uttar Pradesh, India

[2]Kalka Institute for Research and Advanced Studies, Meerut, Uttar Pradesh, India

[3] KC College of Pharmacy, Nawanshahr, Punjab

[4] School of Pharmacy Mangalayatan University, Aligarh, Uttar Pradesh, India

***Name and address of corresponding author**:

Neeraj Kant Sharma

Department of Pharmacy, Meerut Institute of Technology

Meerut-250103, UP, India

Telephone: +91-9897693004

Email: neerajkant.sharma@mitmeerut.ac.in

Abstract

Traditionally, the juice and decoction of aerial part and leaves of *Lagenaria siceraria* was used for cure and management of hepatic disorders in South Asia. There is a scarcity of scientific details to justify the traditional claim for hepatoprotective potential of leaves of *L. Siceraria*. In the present research work, the hepatoprotective potential was evaluated for methanolic extract of *L. siceraria* leaves (LSME) against carbon tetrachloride induced hepatotoxicity in albino rats. The levels of hepatic biochemical markers were estimated in treated groups. The treatment with LSME (50 mg/kg) altered back the normal levels of biochemical markers as well as done the significant improvement in the damaged hepatatocytes. The levels of endogenous liver antioxidant enzymes, catalase, superoxide dismutase and glutathione contents were increased significantly. There was also recorded the significant ($P<0.001$) depletion in serum glutamic-pyruvic transaminase, serum glutamic-oxaloacetic transaminase, Alkaline- phosphatase and total bilirubin in LSME treated group. From these results, it is suggested that methanolic extract of *L. siceraria* leaves possesses hepatoprotective properties.

Key Words *Lagenaria siceraria*, carbon tetrachloride, Hepatoprotective effect, biochemical enzymes.

Introduction

Liver is the largest vital organ to facilitate intense metabolism and excretion. It plays the vital role in the maintenance, performance and regulating homeostasis of the body. Various biochemical pathways of growth, immunity, energy and reproduction are passed through the liver [1]. The major functions of the liver are metabolism of carbohydrate, protein and fat, detoxification, bile secretions and storage of some vitamins. So, keeping the liver healthy is an

International Journal of All Research Education and Scientific Methods (IJARESM), ISSN: 2455-6211, Volume 11, Issue 10, October-2023, Available online at: www.ijaresm.com

Formulation and Evaluation of Transdermal Patches Containing Glibenclamide of Enhanced Diabetes Management

Simran[1], Mamta Gupta[2], Pankaj Kumar Jangra[3], Amit Singh[4], Dr. Arshad Ahmad[5], Km. Shiva[6*]

[1]Assistant Professor, Meerut Institute of Technology, Meerut Uttar Pradesh
[2]Assistant Professor, B.S.A. College of Engineering and Technology, Mathura Uttar Pradesh
[3]Associate Professor, N.K.B.R College of Pharmacy and Research Center Phaphunda, Meerut Uttar Pradesh
[4]Ph.D. Scholar, IIMT College of Medical Science, Ganga Nagar Meerut Uttar Pradesh
[5]Professor, Shri Gopichand College of Pharmacy, Ahera Baghpat Uttar Pradesh
[6]Assistant Professor, NGI College of Pharmacy, Meerut Uttar Pradesh

***Corresponding Author:** Km. Shiva

----------**********----------

ABSTRACT

The purpose of this work was to develop a matrix-type transdermal treatment system containing the drug glibenclamide and various ratios of hydrophilic and hydrophobic polymeric systems using the solvent evaporation technique. Oleic acid and isopropyl myristate were used in different doses to increase the transdermal permeability of Glibenclamide. Transdermal matrix patches created using different solvent evaporation techniques and Eudragit RS100 and HPMC100M ratios. All of the created formulations were assessed for weight variation, thickness, drug content, moisture content, moisture uptake, flatness, and in-vitro drug release. By using differential scanning calorimetry and infrared spectroscopy, the physicochemical compatibility between the drug and the polymers was confirmed, and there was no incompatibility. A drug and polymer compatibility analysis can be carried out using FTIR. F3 was the optimal formula from the entire formulation batch. demonstrates linear zero order release over a period of 24 hours with cumulative drug diffusion of 88.34% from patches measuring 4 cm2. Conclusion: When the concentration of the polymer (HPMC100M) increases in the primary layer, the rate of in vitro diffusion also rises, and the concentration of the eudragit Rs100 also rises. Increases cause the drug diffusion to decline. For patches, it offers better, more controlled medication release.

Keywords: Matrix Type Transdermal Patch, In-Vitro Permeation Study, Eudragit RS 100, Glibenclamide

INTRODUCTION

Transdermal medication administration refers to the topical delivery of drugs to healthy, unbroken skin for systemic therapy or for the focused treatment of tissues beneath the surface. For transdermal products, the goal of dosage design is to optimize the flux through the skin into the systemic circulation [1].

Transdermal drug delivery has several advantages over oral route of administration, including avoiding first-pass metabolism, maintaining drug delivery, maintaining a constant and prolonged drug level in plasma, minimizing inter- and intra-patient variability, and enabling interruption or termination of treatment.The development of a transdermal delivery method for currently existing drug molecules improves the therapeutic benefit, as well as the safety, effectiveness, and adherence of the patient [1,2].Self-contained, discrete dosage forms, commonly referred to as "patches," deliver the medicine to the systemic circulation at a controlled rate through the skin when placed on healthy skin [12].

In order to accurately administer the drug and release it into the bloodstream at a predetermined rate, a transdermal patch is a medicated adhesive patch that is put directly to the skin. an epidermal transdermal patch customized membrane to control the rate of drug absorption from the body's liquid reservoir patch is able to enter the body through the skin and Bloodstream[3]. Regulated drug delivery eliminates pulsed drug entry into the systemic circulation in addition to enabling continuous medicine delivery with short biological half-lives. By using transdermal medicine delivery into the patient and ensuring a stable blood-level profile to lessen systemic side effects, controlled release enables multi-day dosage [4,5].

JOURNAL OF DISPERSION SCIENCE AND TECHNOLOGY
https://doi.org/10.1080/01932691.2023.2266010

Cytotoxicity and bioavailability assessment from thiamin-phospholipid complexation loaded Ajwain oil based self nanoemulsifying system

Anoop Kumar[a], Amulya Jindal[a,b], and Piyush Kumar Singh Arya[a,b]

[a]Meerut Institute of Engineering and Technology, Meerut, India; [b]Meerut Institute of Technology, Meerut, India

ABSTRACT

Poor bioavailability (<5%) of thiamin hydrochloride (TH) primarily relates to its impaired permeability across gut mucosa. To modulate its permeability, a dual system based approach consisting of phospholipid complexation embedded into a self nanoemulsifying system was investigated. Thiamin-Phospholipid Complex (TPC) was developed and its Ajwain oil (AJO)-based self nanoemulsifying formulations (SNFs) were evaluated. Formation of TPC complexation was resulted from molecular interactions held between free bases of thiamin and phospholipid (PL). FTIR characterization reveals that the amino group (-NH_2) in the free base of thiamin was physically interacted to phosphate linkage in PL. Single endothermic event in TPC & TH, reveals complexation between PL & free bases as interpreted from DSC data. Their corresponding melting point was 127 °C and 258 °C, respectively. Heat of fusion (ΔH_f) in TPC was higher than TH or PL. TPC exhibits a poor conductive environment over TH when diluted with ethanol/Tween20 (T2) medium. Lipophilic character of TPC was confirmed from partition coefficient (log P). Exact combination where ternary components produced fully dilutable nanoemulsion system, was identified using ternary diagram drawn between AJO (incorporated with TPC) as oil phase, and Tween20/Polyethylene glycol 600 (PEG600) as Surfactant/co-surfactant (S_{mix}) at ratios 1:1; 1:2 & 2:1. Seven TPC-loaded self nanoemulsifying formulations (SNFs) were designed which, upon subjected to aqueous phase dilution yielded nanoemulsion with droplet size range 95–190 nm with zeta potential −1.78 ± 0.10 mV. Conductivity and Refractive index (RI) data of SNFs were in the range of 98 ± 7.0 to 231 ± 27 μS/cm and 1.458 to 1.463 units, respectively. In vitro TH release from SNF was determined in hydrochloric (HCl) buffer at pH 1.2, and in phosphate buffer solution (PB) at pH 6.8, data interpretation reveals that TPC delayed the release pattern compared to TH and could be attributed to lipophilic behavior of TPC. Intestinal permeability of drug was assessed from optimized SNF (F1) vs. TH across intestinal gut sac model (Apical to basolateral A→B) resulted in a significant difference in permeability coefficient (1.09×10^{-5}cm/h). Antioxidant potential of SNF was demonstrated in the DPPH method. MTT assay of TPC formulation conducted on MCF-7 and MDA-MB-231 (Breast cancer) cell lines showed the developed system from AJO possessed cytotoxicity effect. Pharmacokinetic assessment showed that optimized SNFs produced more than four-fold enhancement in bioavailability over control (TH solution) in the Wistar rat model. Meanwhile Area under curve (AUC) data obtained from TPC (in coarse emulsion) vs.TH produced a significant difference ($p < 0.001$). It can be concluded that developed SNFs *via* phospholipid complexation produced lipophilic transformation of TH and its SNFs modulated permeability as well as bioavailability enhancement of thiamin.

ARTICLE HISTORY
Received 20 July 2023
Accepted 25 September 2023

KEYWORDS
Thiamin-phospholipid complex; phospholipid; permeability; bioavailability; Ajwain oil; cytotoxicity

CONTACT Amulya Jindal amulyajindal05@gmail.com Department of Pharmaceutical Technology, Meerut Institute of Engineering and Technology (MIET), NH-58, Delhi-Roorkee Highway, Meerut-250005, Uttar Pradesh, India.

pharmaceuticals

MDPI

Article

Rubia cordifolia L. Attenuates Diabetic Neuropathy by Inhibiting Apoptosis and Oxidative Stress in Rats

Sweeti Bana [1], Nitin Kumar [2], Ali Sartaj [3], Abdulsalam Alhalmi [4], Ashraf Ahmed Qurtam [5], Fahd A. Nasr [5], Mohammed Al-Zharani [5], Neelam Singh [6], Praveen Gaur [7], Rosaline Mishra [7], Snigdha Bhardwaj [8], Hasan Ali [2] and Radha Goel [9,*]

1 Department of Pharmacology, Lloyd School of Pharmacy, Greater Noida 201306, India; sweetybanapharm8755@gmail.com
2 Department of Pharmacy, Meerut Institute of Technology, Meerut 250103, India; nitin_23106@yahoo.co.in (N.K.); hasanmesra@gmail.com (H.A.)
3 Department of Pharmaceutics, Lloyd School of Pharmacy, Greater Noida 201306, India; sartaz005@yahoo.com
4 Department of Pharmaceutics, School of Pharmaceutical Education and Research, Jamia Hamdard, New Delhi 110062, India; asalamahmed5@gmail.com
5 Department of Biology, College of Science, Imam Mohammad Ibn Saud Islamic University (IMSIU), Riyadh 11623, Saudi Arabia; aaqurtam@imamu.edu.sa (A.A.Q.); faamohammed@imamu.edu.sa (F.A.N.); mmyalzahrani@imamu.edu.sa (M.A.-Z.)
6 Department of Pharmacy, ITS College of Pharmacy, Muradnagar 201206, India; singhneelam16@gmail.com
7 Department of Pharmacy, Metro College of Health Sciences and Research, Plot No.-41, Knowledge Park-III, Uttar Pradesh 201306, India; gaurpharm@gmail.com (P.G.); rosalinemishra.mchsr@gmail.com (R.M.)
8 Department of Pharmacy, Noida Institute of Engineering and Technology, Greater Noida 201306, India; snigs1990@gmail.com
9 Department of Pharmacology, Lloyd Institute of Management & Technology, Plot No.-11, Knowledge Park-II, Greater Noida 201306, India
* Correspondence: radhamit2006@gmail.com

Citation: Bana, S.; Kumar, N.; Sartaj, A.; Alhalmi, A.; Qurtam, A.A.; Nasr, F.A.; Al-Zharani, M.; Singh, N.; Gaur, P.; Mishra, R.; et al. *Rubia cordifolia* L. Attenuates Diabetic Neuropathy by Inhibiting Apoptosis and Oxidative Stress in Rats. *Pharmaceuticals* **2023**, *16*, 1586. https://doi.org/10.3390/ph16111586

Academic Editors: Francesca Bosco and Lorenza Guarnieri

Received: 18 September 2023
Revised: 12 October 2023
Accepted: 6 November 2023
Published: 9 November 2023

Abstract: Background: Diabetic neuropathy is a debilitating manifestation of long-term diabetes mellitus. The present study explored the effects of the roots of *Rubia cordifolia* L. (*R. cordifolia* L.) in the Wistar rat model for diabetic neuropathy and possible neuroprotective, antidiabetic, and analgesic mechanisms underlying this effect. Materials and Methods: Rats were divided into five experimental groups. An amount of 0.25% carboxy methyl cellulose (CMC) in saline and streptozotocin (STZ) (60 mg/kg) was given to group 1 and group 2, respectively. Group 3 was treated with STZ and glibenclamide simultaneously while groups 4 and 5 were simultaneously treated with STZ and hydroalcoholic extract of the root of *R. cordifolia*, respectively. Hot plate and cold allodynias were used to evaluate the pain threshold. The antioxidant effects of *R. cordifolia* were assessed by measuring Thiobarbituric acid reactive substances (TBARS), reduced glutathione (GSH), catalase (CAT), and superoxide dismutase (SOD). At the end of the study, sciatic nerve and brain tissues were collected for histopathological study. Bcl-2 proteins, cleaved caspase-3, and Bax were assessed through the Western blot method. Results: *R. cordifolia* significantly attenuated paw withdrawal and tail flick latency in diabetic neuropathic rats. *R. cordifolia* significantly ($p < 0.01$) improved the levels of oxidative stress. It was found to decrease blood glucose levels and to increase animal weight in *R. cordifolia*-treated groups. Treatment with *R. cordifolia* suppressed the cleaved caspase-3 and reduced the Bax:Bcl2 ratio in sciatic nerve and brain tissue compared to the diabetic group. Histopathological analysis also revealed a marked improvement in architecture and loss of axons in brain and sciatic nerve tissues at a higher dose of *R. cordifolia* (400 mg/kg). Conclusion: *R. cordifolia* attenuated diabetic neuropathy through its antidiabetic and analgesic properties by ameliorating apoptosis and oxidative stress.

Keywords: antioxidants; antidiabetic; diabetic neuropathy; *Rubia cordifolia*; streptozotocin; caspase-3; Bax:Bcl2 ratio; brain tissue; sciatic nerve tissue

JOURNAL OF MICROENCAPSULATION
2023, VOL. 40, NO. 6, 402–411
https://doi.org/10.1080/02652048.2023.2215306

Taylor & Francis
Taylor & Francis Group

RESEARCH ARTICLE

Nanoencapsulation and characterisation of *Hypericum perforatum* for the treatment of neuropathic pain

Radha Goel[a], Nitin Kumar[b], Neelam Singh[c] and Rosaline Mishra[d]

[a]Lloyd Institute of Management & Technology, Greater Noida, India; [b]Department of Pharmacy, Meerut Institute of Technology, Meerut, India; [c]Department of Pharmaceutics, I.T.S. College of Pharmacy, Muradnagar, India; [d]Department of Pharmachemistry, Metro College of Health Sciences and Research, Greater Noida, India

ABSTRACT

Aim: This work aimed to encapsulate *Hypericum perforatum* extract (HPE) into nanophytosomes (NPs) and assess the therapeutic efficacy of this nanocarrier in neuropathic pain induced by partial sciatic nerve ligation (PSNL).

Methods: Hydroalcoholic extract of *Hypericum perforatum* was prepared and encapsulated into NPs by thin layer hydration method. Particle size, zeta potential, TEM, differential scanning calorimetry (DSC), entrapment efficiency (%EE), and loading capacity (LC) of NPs were reported. The biochemical and histopathological examinations were measured in the sciatic nerve.

Results: Particle size, zeta potential, %EE, and LC were 104.7 ± 1.529 nm, −8.93 ± 1.71 mV, 87.23 ± 1.3%, and 53.12 ± 1.7%, respectively. TEM revealed well-formed and distinct vesicles. NPHPE (NPs of HPE) was significantly more effective than HPE in reducing PSNL-inducing pain. Antioxidant levels and sciatic nerve histology were reversed to normal with NPHPE.

Conclusions: This study demonstrates that encapsulating HPE with phytosomes is an effective therapeutic approach for neuropathic pain.

ARTICLE HISTORY
Received 3 January 2023
Accepted 15 May 2023

KEYWORDS
Nanophytosomes; *Hypericum perforatum*; neuropathic pain; sciatic nerve; antioxidants

1. Introduction

Neuropathic pain is one of the many factors that contribute to the global burden of disease (Sukmawan *et al.* 2021). It is caused by damage to somatosensory nervous system and affects around 7% of the population (Szok *et al.* 2019). Several traditional drugs, including opioids, anticonvulsants, NSAIDs, and antidepressants, are available for neuropathic treatment, but they do not provide acceptable pain relief in many individuals. Most of these people want safe treatment, as they are concerned about serious side effects such as dizziness, nausea, vomiting, stomach ache, heartburn, etc. with the traditional therapy for neuropathic pain. Hence, in this prospect, herbal therapy may thus give a high-level alternative with superior therapeutic results and fewer adverse effects in the future (Kumar *et al.* 2021).

Hypericum perforatum L. (Hypericaceae), mainly known as St. John's wort, is a perennial herb that has recently gained popularity as one of the world's most commonly used medicinal plants (Birt *et al.* 2009, Huang *et al.* 2013). The extracts of *Hypericum perforatum* are employed as medical natural agents because they have a wide range of therapeutic actions, including antidepressant, antiinflammatory, antibacterial, antioxidant, wound healing, and pain relief (Güneş and Tıhmınlıoğlu 2017). It is regarded a safe herbal medicinal agent because it is well tolerated and has few negative effects (Woelk 2000). Recently, *Hypericum perforatum* has also been found to be useful in treatment of oxaliplatin-induced neuropathic pain (Cinci *et al. 2017*). One of the studies found that taking *Hypericum perforatum* extract (HPE) orally can improve morphine antinociception in conditions of neuropathic pain (Zeliou *et al.* 2017). Hypericin is the major bioactive component for the most of HPE functional characteristics. As hypericin is sensitive to high temperatures and pH, it can be encapsulated to improve its stability (Greeson *et al.* 2001).

Traditional herbal preparations have low solubility, stability, and bioavailability, all of which limit their efficiency in therapeutic products (Mathur 2013). Nano-phytosomes are a new lipid-based drug delivery system that overcomes the drawbacks of traditional drug delivery system. Nanophytosomes (NPs) are advanced form of herbal products that are more easily

CONTACT Radha Goel radhamit2006@gmail.com Lloyd Institute of Management & Technology, Plot No.-11, Knowledge Park-II, Greater Noida, Uttar Pradesh 201306, India

ACS OMEGA

http://pubs.acs.org/journal/acsodf

Article

Formulation of Phytosomes Containing *Rubia cordifolia* Extract for Neuropathic Pain: *In Vitro* and *In Vivo* Evaluation

Nitin Kumar,* Radha Goel, Mohd Nazam Ansari, Abdulaziz S Saeedan, Hasan Ali, Neeraj Kant Sharma, Vaishali M. Patil, Dinesh Puri, and Monika Singh

Cite This: *ACS Omega* 2024, 9, 25381−25389

Read Online

ACCESS | Metrics & More | Article Recommendations

ABSTRACT: This study aimed to develop a delivery system for the dried aqueous extract of *Rubia cordifolia* leaves (RCE) that could improve the neuroprotective potential of RCE by improving the bioavailability of the chief chemical constituent rubiadin. Rubiadin, an anthraquinone chemically, is a biomarker phytoconstituent of RCE. Rubiadin is reported to have strong antioxidant and neuroprotective activity but demonstrates poor bioavailability. In order to resolve the problem related to bioavailability, RCE and phospholipids were reacted in disparate ratios of 1:1, 1:2, and 1:3 to prepare phytosome formulations PC1, PC2, and PC3, respectively. The formulation PC2 showed particle size of 289.1 ± 0.21 nm, ζ potential of −6.92 ± 0.10 mV, entrapment efficiency of 72.12%, and *in vitro* release of rubiadin of 89.42% at pH 7.4 for a period up to 48 h. The oral bioavailability and neuroprotective potential of PC2 and RCE were assessed to evaluate the benefit of PC2 formulation over the crude extract RCE. Formulation PC2 showed a relative bioavailability of 134.14% with a higher neuroprotective potential and significantly ($p < 0.05$) augmented the nociceptive threshold against neuropathic pain induced by partial sciatic nerve ligation method. Antioxidant enzyme levels and histopathological studies of the sciatic nerves in various treatment groups significantly divulged that PC2 has enough potential to reverse the damaged nerves into a normal state. Finally, it was concluded that encapsulated RCE as a phytosome is a potential carrier system for enhancing the delivery of RCE for the efficient treatment of neuropathic pain.

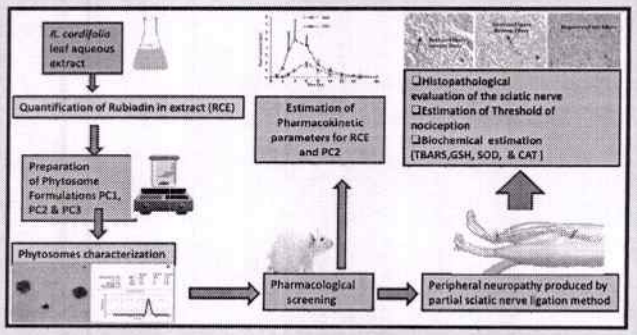

1. INTRODUCTION

Out of all the pain and suffering, neuropathic pain (NP), which is caused by injury or damage to the nerves, and manifests as tingling, shooting, burning, stabbing pain, or shocking, is the most horrifying. Diabetes is the most common cause of neuropathy. It may also be caused by other health conditions like cancer, hypertension, anxiety, poor nutrition, and intake of some anticancer and antimycobacterial drugs, for example, Paclitaxel, Vincristine, Dapsone, Isoniazid, Rifampin, etc. To treat NP, a wide range of drugs are available, including opioids, NSAIDs, antidepressants, and anticonvulsants. Serious side effects are present in the majority of these adverse effects despite the need for safe treatment. The use of antidepressants and NSAIDs increases the risk of gastrointestinal adverse effects like peptic ulcer, acidity, and diarrhea. Herbs are a natural source of many bioactive compounds, including specific glycosides and polyphenols, which act as potent antioxidants *in vivo* to mediate the suggested health benefits.[1,2] Therefore, in terms of the possibility of a successful therapeutic outcome, herbal treatment might offer a better alternative.

A member of the Rubiaceae family *Rubia cordifolia* includes the chemical compound *rubiadin*, a derivative of hydroxy anthraquinone. For a very long time, *R. cordifolia* has been used as an antibacterial and to treat rheumatoid arthritis, uterine pain, and joint pain.[3] Furthermore, *R. cordifolia* has been linked to hepatoprotective, nephroprotective, antineoplastic, anti-ulcer, anti-inflammatory, and antidysenteric properties.[4] *R. cordifolia* root extract demonstrated antioxidant and anti-hyperglycemic effects in a previous study.[5,6] In a different study, the aqueous root extract of *R. cordifolia* was tested for its antidiabetic properties using a diabetic rat model that was induced using streptozocin .[7] Additionally, the alcohol extract from *R. cordifolia* demonstrated antioxidant and antihyperglycemic properties in a different study.[8] According to other studies, *R. cordifolia* root extract has shown strong antioxidant and antidiabetic properties. Poor stability and absorption have been observed in a number of herbal compounds, including

Received: April 19, 2024
Revised: May 13, 2024
Accepted: May 16, 2024
Published: May 27, 2024

https://doi.org/10.1021/acsomega.4c03774
ACS Omega 2024, 9, 25381−25389

JOURNAL OF DISPERSION SCIENCE AND TECHNOLOGY
https://doi.org/10.1080/01932691.2024.2325398

Taylor & Francis
Taylor & Francis Group

Modulation of intestinal permeability of 5-fluorouracil via phospholipid interaction based lipophilic complex designing and pharmacokinetic assessment

Anoop Kumar[a], Piyush Kumar Singh Arya[a,b], and Amulya Jindal[a,b]

[a]Department of Pharmaceutical Technology, Meerut Institute of Engineering and Technology, Meerut, India; [b]Department of Pharmacy, Meerut Institute of Technology, Meerut, India

ABSTRACT

5-Fluorouracil (5-FU) is a poorly bioavailable anti-tumor drug with impaired permeability function across gut mucosa. To modulate the permeability of 5-FU, a 5-FU-phospholipid based lipophilic complexes was developed. 5-fluorouracil-phospholipid complexes (FUPLCs) complexes were prepared at weight ratios (1:1, 1:2 and 2:1) of phospholipid (PL) and 5-FU using solvent evaporation method. FTIR characterization showed that FUPLCs were formed from molecular interaction held between 5-FU & PL; as change in the vibrational frequencies of PL appeared at 1227, 1085 and 1051 cm^{-1} were shifted to 1224, 1069 and 1037 cm^{-1} for >P=O, >ONH-, and -NH-OH- respectively. Melting endotherm of 5-FU appeared at 287 °C and was shifted to 278 °C in the complex. XRD pattern of FUPLC was crystalline; and indicates phospholipid (amorphous solid) occupied into crystal lattice of 5-FU. FUPLCs produce distinct conductive species in comparison to 5-FU and allow changes in the electrical conductivity pattern due to changes in the molecular orientations when diluted in Tween 20/ethanol environment. Furthermore, partition coefficient measurement confirmed the lipophilic character of complexes. *In vitro* drug release studies demonstrated that complexes produce delayed release patterns over 5-FU in phosphate buffer at pH 6.8, HCl buffer at pH 1.2 and distilled water. These variations in drug release patterns could reflect hydrophobic nature of complexes. FUPLC gave higher drug permeability ($p < 0.001$) across the intestinal sac than the 5-FU solution. P_{eff} value from FUPLCs (1:1; and 1:2) and 5-FU was 8.0×10^{-5} and 4.0×10^{-5} cm/sec respectively in apical to basolateral direction (A→B). Modulation of drug permeability in FUPLC could relate to the lipophilic character of 5-FU/PL interaction. Pharmacokinetic assessment in the Wistar rat model showed that complex (1:1) produced three-fold enhancement in the $AUC_{(0\text{-}120min)}$ over 5-FU administered orally. Designing lipophilic carriers based on drug/PL interaction produces changes in the 5-FU release and modulates the intestinal permeability and bioavailability. Lipophilic carrier of 5-FU viz. FUPLCs could be employed in the designing of nanoemulsion, (Self-emulsifying drug delivery system) SEDDS or (Self-Nanoemulsifying drug delivery system) SNEDDS system for bioavailability enhancement of BCS class III.

GRAPHICAL ABSTRACT

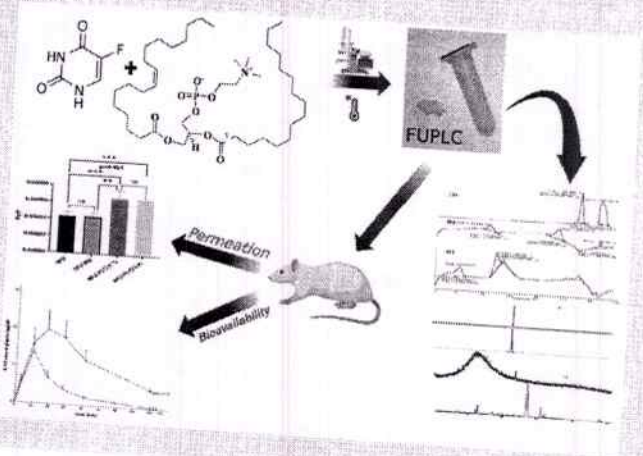

ARTICLE HISTORY
Received 22 September 2023
Accepted 24 February 2024

KEYWORDS
5-Fluorouracil; permeability; phospholipid; 5-Fluorouracil-phospholipid complex; lipophilic carrier

CONTACT Piyush Kumar Singh Arya aryapeeyush4@gmail.com Meerut Institute of Engineering and Technology, NH 58 Near Baghpat Byepass, Meerut 250005, Uttar Pradesh, India.

Discover Oncology

Review

Novel therapeutic agents in clinical trials: emerging approaches in cancer therapy

Deepak Chandra Joshi[1] · Anurag Sharma[2] · Sonima Prasad[3] · Karishma Singh[4] · Mayank Kumar[5] · Kajal Sherawat[6] · Hardeep Singh Tuli[7] · Madhu Gupta[8]

Received: 15 January 2024 / Accepted: 25 July 2024
Published online: 11 August 2024

Abstract
Novel therapeutic agents in clinical trials offer a paradigm shift in the approach to battling this prevalent and destructive disease, and the area of cancer therapy is on the precipice of a trans formative revolution. Despite the importance of tried-and-true cancer treatments like surgery, radiation, and chemotherapy, the disease continues to evolve and adapt, making new, more potent methods necessary. The field of cancer therapy is currently witnessing the emergence of a wide range of innovative approaches. Immunotherapy, including checkpoint inhibitors, CAR-T cell treatment, and cancer vaccines, utilizes the host's immune system to selectively target and eradicate malignant cells while minimizing harm to normal tissue. The development of targeted medicines like kinase inhibitors and monoclonal antibodies has allowed for more targeted and less harmful approaches to treating cancer. With the help of genomics and molecular profiling, "precision medicine" customizes therapies to each patient's unique genetic makeup to maximize therapeutic efficacy while minimizing unwanted side effects. Epigenetic therapies, metabolic interventions, radio-pharmaceuticals, and an increasing emphasis on combination therapy with synergistic effects further broaden the therapeutic landscape. Multiple-stage clinical trials are essential for determining the safety and efficacy of these novel drugs, allowing patients to gain access to novel treatments while also furthering scientific understanding. The future of cancer therapy is rife with promise, as the integration of artificial intelligence and big data has the potential to revolutionize early detection and prevention. Collaboration among researchers, and healthcare providers, and the active involvement of patients remain the bedrock of the ongoing battle against cancer. In conclusion, the dynamic and evolving landscape of cancer therapy provides hope for improved treatment outcomes, emphasizing a patient-centered, data-driven, and ethically grounded approach as we collectively strive towards a cancer-free world.

Keywords Cancer · Cancer therapy · Checkpoint inhibitor · Kinase inhibitor · CAR-T cell therapy · Cancer vaccines · Epigenetic therapies

✉ Deepak Chandra Joshi, Deepakjoshi024@gmail.com; ✉ Madhu Gupta, madhugupta98@gmail.com | [1]Department of Pharmacy, School of Chemical Sciences and Pharmacy, Central University of Rajasthan, Bandar Sindri, Dist., Ajmer, Rajasthan, India. [2]Invertis Institute of Pharmacy, Invertis University Bareilly Uttar Pradesh, Bareilly, India. [3]Chandigarh University, Ludhiana-Chandigarh State Highway, Gharuan, Mohali, Punjab 140413, India. [4]Institute of Pharmaceutical Sciences, Faculty of Engineering and Technology, University of Lucknow, Lucknow, India. [5]Himalayan Institute of Pharmacy, Road, Near Suketi Fossil Park, Kala Amb, Hamidpur, Himachal Pradesh, India. [6]Meerut Institute of Technology, Meerut, Uttar Pradesh, India. [7]Department of Bio-Sciences & Technology, Maharishi Markandeshwar Engineering College, Maharishi Markandeshwar (Deemed to Be University), Mullana, Ambala, India. [8]Department of Pharmaceutics, School of Pharmaceutical Sciences, Delhi Pharmaceutical Sciences and Research University, New Delhi, India.

Send Orders for Reprints to reprints@benthamscience.net

Current Pharmaceutical Biotechnology, 2025, *26*, 778-794

RESEARCH ARTICLE

Assessment of the Anti-adipogenic Effect of *Crateva religiosa* Bark Extract for Molecular Regulation of Adipogenesis: *In Silico* and *In vitro* Approaches for Management of Hyperlipidemia Through the 3T3-L1 Cell Line

Monika Singh[1,*], Monika Sachdeva[2] and Nitin Kumar[3]

[1]*Department of Pharmacology, I.T.S. College of Pharmacy, Ghaziabad, U.P., Affiliated with Dr. A.P.J. Abdul Kalam Technical University, Lucknow, India;* [2]*Department of Pharmacy, Raj Kumar Goel Institute of Technology, Ghaziabad U.P., Affiliated with Dr. A.P.J. Abdul Kalam Technical University, Lucknow, India;* [3]*Department of Pharmacy, Meerut Institute of Technology, Meerut, Affiliated with Dr. A.P.J. Abdul Kalam Technical University, Lucknow, India*

Abstract: ***Aims:*** This study aimed to determine the phytoconstituents of *Crateva religiosa* bark (CRB) and evaluate the hypolipidemic effect of bioactive CRB extract by preventing adipocyte differentiation and lipogenesis.

Background: After performing the preliminary phytochemicals screening, the antioxidant activity of CRB extracts was determined through a DPPH (2, 2-diphenyl-1-picrylhydrazyl) assay. Ethyl acetate extract (CREAE) and ethanol extract (CRETE) of CRB were selected for chromatographic evaluation.

Methods: The antihyperlipidemic potential was analyzed by molecular docking through the PKCMS software platform. Further, a 3T3-L1 cell line study *via in vitro* sulforhodamine B assay and western blotting was performed to confirm the prevention of adipocyte differentiation and lipogenesis

Results: The total phenolic contents in CREAE and CRETE were estimated as 29.47 and 81.19 µg/mg equivalent to gallic acid, respectively. The total flavonoid content was found to be 8.78 and 49.08 µg/mg, equivalent to quercetin in CREAE and CRETE, respectively. CRETE exhibited greater scavenging activity with the IC_{50} value of 61.05 µg/ mL. GC-MS analysis confirmed the presence of three bioactive molecules, stigmasterol, gamma sitosterol, and lupeol, in CRETE. Molecular docking studies predicted that the bioactive molecules interact with HMG-CoA reductase, PPARγ, and CCAAT/EBP, which are responsible for lipid metabolism. *In vitro,* Sulforhodamine B assays revealed that CRETE dose-dependently reduced cell differentiation and viability. Cellular staining using 'Oil Red O' revealed a decreased lipid content in the CRETE-treated cell lines. CRETE significantly inhibited the induction of PPARγ and CCAAT/EBP expression, as determined through protein expression *via* western blotting.

Conclusion: The influence of CRETE on lipid metabolism in 3T3-L1 cells is potentially suggesting a new approach to managing hyperlipidemia.

ARTICLE HISTORY

Received: March 05, 2024
Revised: June 16, 2024
Accepted: July 02, 2024

DOI:
10.2174/0113892010314594240816050240

Keywords: 3T3-L1 cell lines, *in vitro*, *in silico*, antihyperlipidemic, adipocyte, GC-MS analysis.

1. INTRODUCTION

Hyperlipidemia is characterized by increased levels of lipids, including cholesterol and triglycerides, in the blood circulation [1]. Metabolic disorders are a significant danger for the treatment of cardiovascular diseases and many metabolic illnesses. Due to the variety of bioactive composites, natural products, such as plant extracts, have attracted increased interest as potential therapeutic agents for treating hyperlipidemia [2]. The cause of hyperlipidemia may be oxidative stress, which was investigated in this study using both *in vitro* and *in silico* approaches [3].

In vitro, study was performed on the 3T3-L1 cell line. Fibroblasts were isolated from the embryo of a mouse. Therefore, the murine preadipocyte cell line is a common tool for analyzing the various steps involved in adipogenesis through the differentiation of these preadipocytes. Phenotyp-

*Address correspondence to this author at the Department of Pharmacology, I.T.S. College of Pharmacy, Ghaziabad, Affiliated with Dr. A.P.J. Abdul Kalam Technical University, Lucknow, India; E-mail: monikas@its.edu.in

1389-2010/25 $65.00+.00

DRUG AND CHEMICAL TOXICOLOGY
https://doi.org/10.1080/01480545.2024.2388324

Taylor & Francis
Taylor & Francis Group

RESEARCH ARTICLE

Potential protective effects of *Acacia nilotica* (L.) against gentamicin - induced nephrotoxicity by suppressing renal redox imbalance, inflammatory stress and caspase-dependent apoptosis in Wistar rats

Radha Goel[a], Nitin Kumar[b], Rosaline Mishra[c], Gaurav Kumar[a], Neelam Singh[d], Snigdha Bhardwaj[e] and Dinesh Puri[f]

[a]Department of Pharmacology, Lloyd Institute of Management & Technology, Greater Noida, India; [b]Department of Pharmacy, Meerut Institute of Technology, Meerut, India; [c]Department of Pharmacy, Metro College of Health Sciences and Research, India; [d]Department of Pharmacy, Noida Institute of Engineering and Technology (Pharmacy Institute), Greater Noida, India; [e]Department of Pharmaceutics, KIET School of Pharmacy, Ghaziabad, Delhi-NCR, India; [f]Department of Pharmaceutics, Graphic Era Hill University, Dehradun, India

ABSTRACT

Gentamicin-induced nephrotoxicity limits its therapeutic use as an effective aminoglycoside. Herbal drugs have a distinct place in the world of pharmaceuticals since they are safe, effective, and cost-efficient. *Acacia nilotica* (L.) has long been recognized for its antihypertensive, antioxidant, anti-inflammatory, and antiplatelet aggregatory benefits in traditional medicine. Still, the protective effect of *Acacia nilotica* on gentamicin-induced nephrotoxicity is still unknown. Thus, the goal of this research was to examine the protection of ethanolic extract of *Acacia nilotica* (ANE) against nephrotoxicity triggered by Gentamicin.

Thirty-six rats were randomly divided into six groups containing six rats in each group. The distilled water were given in control group. The rats in groups two and three were administered metformin and gentamicin respectively. In groups five and six, rats were administered ANE at doses of 100 and 200 mg/kg. Ten days of daily treatments were given. The urea, creatinine, uric acid, and LDH levels were analyzed on serum, whereas histological evaluation, MDA, GSH, SOD, CAT, TNF-α, IL-6, and caspase-3, were performed on kidney tissue on day 11. The gentamicin-treated group exhibited a significantly elevated MDA, and lower levels of antioxidant enzymes. Kidney function markers, inflammatory markers and caspase-3 expression were significantly elevated in the gentamicin-treated group. ANE significantly restored kidney function biomarkers, upregulated biochemical levels, inhibited TNF-α, caspase-3, cytokine expression, and reduced histological lesions.

In conclusion, ANE has the ability to prevent gentamicin-induced nephrotoxicity and reduce nephrotoxic damage. As such, it may represent an effective therapy for patients receiving gentamicin treatment.

ARTICLE HISTORY
Received 23 March 2024
Revised 14 July 2024
Accepted 30 July 2024

KEYWORDS
Acacia nilotica; gentamicin; nephrotoxicity; oxidative stress; cytokine; caspase-3

Introduction

The aminoglycoside antibiotic gentamicin (GM) is used extensively across the world to treat severe infections in humans and animals that are brought on by gram-negative bacteria (Ahmed & Mohamed, 2019). However, ototoxicity and nephrotoxicity are the major adverse effects that may abrogate the use of GM (Tavafi, 2012). Gentamicin-induced nephrotoxicity is a multifactorial condition that manifests as high levels of creatinine, urea, uric acid, and LDH in the serum, along with apoptosis and severe proximal renal tubular necrosis (Hoffmann et al., 2010).

The nephrotoxicity caused by GM is linked with the onset of kidney inflammatory cascades, oxidative stress, associated pathological signaling pathways, apoptosis, necrosis and alterations in protein oxidation and lipid peroxidation (Balakumar et al., 2010). Almost 30% of patients experience symptoms of nephrotoxicity after 7 days of treatment with GM therapy (Patereson et al., 1998). The precise processes underlying GM-induced nephrotoxicity remain unclear. On the other hand, it has been demonstrated that GM initiates the production of free radicals (Cuzzocrea et al., 2002, Yanagida et al., 2004), which results in cell death in a variety of clinical conditions, including several models of renal disorders. According to reports, direct tubular necrosis, mostly located in the proximal tubule, is a characteristic of GM-induced nephrotoxicity (Cuzzocrea et al., 2002).

Systematic research has shown that GM increases renal cortical MDA levels and suppresses the actions of kidney antioxidants such as CAT, SOD, and GSH. Consequently, substances that can inhibit oxidative stress, inflammatory cascades, and apoptosis may be used as GM-induced nephrotoxicity preventives. It was found that Acetate, a short-chain fatty acid produced by gut bacteria might be beneficial

CONTACT Radha Goel radhamit2006@gmail.com Department of Pharmacology, Lloyd Institute of Management & Technology, Plot No.-11, Knowledge Park-II, Greater Noida, India

Send Orders for Reprints to reprints@benthamscience.net

Recent Patents on Biotechnology, 2024, 18, 344-357

RESEARCH ARTICLE

The Anti-ulcer Potential of *Weissella cibaria* Assisted Bio-fermented Product of *Citrus limetta* Waste Peel in Wistar Albino Rats

Monika Singh[1], Shreshtha Singh[1], Dinesh Puri[2,*], Shalini Kapoor Sawhney[1], Nitin Kumar[3], Mohd. Yasir[4] and Pankaj Nainwal[2]

[1]*Department of Pharmacology, I.T.S College of Pharmacy, Murad Nagar, Ghaziabad, Uttar Pradesh, India;* [2]*School of Pharmacy, Graphic Era Hill University, Dehradun, Uttarakhand, India;* [3]*Department of Pharmacy, Meerut Institute of Technology, Meerut, Uttar Pradesh, India;* [4]*Department of Pharmacy, College of Health Science, Arsi University, Asella Oromia region, Ethiopia*

Abstract: ***Background:*** There are patents available related to fermented food and beverages which enhance to human health. *Citrus limetta* (Mosambi) has a high content of flavonoids and exhibits antioxidant activity, which could stimulate the digestive system and be useful for gastroprotective activity. It supports digestion by neutralizing the acidic digestive juices and reducing gastric acidity.

Objective: This study explored the potential of using waste peel extract from *Citrus limetta* to prevent ulcers. The study specifically sought to assess the anti-ulcer properties of fermented and non-fermented extracts and compare them. Further, the study looked at the potential benefits of treating or preventing ulcers with *Citrus limetta* waste peels and whether fermentation affected the efficacy of the treatment.

Methods: Thirty female Wistar albino rats were equally distributed into five different groups. Group 1 received distilled water (20 ml/kg/b.w); Group 2 received indomethacin (mg/kg/b.w); Group 3 received omeprazole (20 mg/kg/b.w); Group 4 received aqueous extract of Mosambi peel (400 mg/kg/b.w) and Group 5 received fermented product of extract of Mosambi peel (400 mg/kg/b.w).

Results: Findings explored that, compared to non-fermented citrus fruit juice, bio-fermented exhibited less gastric volume (1.58 ± 0.10 ml *vs.* 1.8 ± 0.14 ml), reduced MDA levels (355.23 ± 100.70 µmol/mg protein *vs.* 454.49 ± 155.88 µmol/mg protein), and low ulcer index (0.49 ± 0.07 *vs.* 0.72 ± 0.14).

Conclusion: The results suggest that the bio-fermented product of *Citrus limetta* peel has better anti-ulcer potential against peptic ulcer induced by indomethacin in Wistar albino rats compared to non-fermented.

ARTICLE HISTORY

Received: August 19, 2023
Revised: October 14, 2023
Accepted: October 25, 2023

DOI:
10.2174/0118722083278152231121173605

Keywords: Citrus fruit waste, fermented and non-fermented product, indomethacin, peptic ulcer, gastric acidity, bio-fermented product.

1. INTRODUCTION

An imbalance between the synthesis of gastroprotective substances like mucous, prostaglandins, bicarbonates, and luminal acid may lead to the formation of ulcers [1, 2]. Ulcers characterize superficial injury of tissue from skin or mucous membrane. Of all types of ulcers, peptic ulcers are seen among many people. It is one of the most significant problems in the world and commonly affecting approximately 10 to 15% of the population. It is observed that men are more vulnerable to duodenal ulcers compared to women [3, 4]. Fruit juice is a significant component of the global food

*Address correspondence to this author at the School of Pharmacy, Graphic Era Hill University, Dehradun, U.K.-248002, India; E-mail: puridinesh105@gmail.com

1872-2083/18 $65.00+.00

JAZ INDIA

Journal of Advanced Zoology

ISSN: 0253-7214

Volume 44 Issue S-5 Year 2023 Page 1028:1044

Artificial Intelligence-Based Machine and Deep Learning Techniques That Use Brain Waves to Detect Depression

Uruj Jaleel[1*], Parbhat Gupta[2], Dr. Praveen Kumar Gupta[3], Sandeep Bharti[4], Jyoti Sehrawat[5], Ajit Singh[6]

[1,3]Alliance College of Engineering & Design, Alliance University, Central Campus Bengaluru, Karnataka, India

[2]SRM Institue of Science and Engineering, NCR Campus, Modinagar, UP, India

[4]Meerut Institute of Technology, Meerut, UP, India

[5,6]Dr. K. N. Modi Institute of Enfineering and Technology, Modinagar, UP, India

Email: parbhatg@srm.edu.in[2], praveenkumar.gupta@alliance.edu.in[3], sandeep.bharti@mitmeerut.ac.in[4], jyotisehrawat4990@gmail.com[5], myemailajit@gmail.com[6]

**Corresponding author's E-mail: dr_urujjaleel@yahoo.com*

Article History

Received: 06 June 2023
Revised: 05 Sept 2023
Accepted: 18 Oct 2023

Abstract

Electroencephalogram (EEG) lsignal-based lemotion lrecognition lhas lattracted lwide linterests in lrecent lyears land lhas lbeen lbroadly ladopted in lmedical, laffective lcomputing, land lother lrelevant lfields. Depression has lbecome la lleading lmental ldisorder lworldwide. Evidence lhas lshown lthat lsubjects lwith ldepression lexhibit ldifferent lspatial lresponses in lneurophysiologic lsignals lfrom lthe lhealthy lcontrols lwhen lthey lare lexposed lto lpositive land lnegative. Depression isla common lreason lfor an increase in lsuicide lcases lworldwide. EEG lplays an important lrole in lE-healthcare lsystems, lespecially in lthe lmental lhealthcare larea, lwhere lconstant land lunobtrusive lmonitoring lis ldesirable. EEG lsignals lcan lreflect lactivities lof lthe lhuman lbrain land lrepresent different lemotional lstates. Mental lstress lhas lbecome la lsocial lissue land lcould lbecome la lcause lof lfunctional ldisability lduring lroutine lwork. This lResearch presents ldeep llearning ltechnique lfor ldetecting ldepression lusing lEEG. The lalgorithm lfirst lextracts lfeatures lfrom lEEG lsignals land lclassifies lemotions lusing lmachine land ldeep llearning ltechniques, in lwhich ldifferent lparts lof la ltrial lare lused lto ltrain lthe lproposed lmodel land lassess lits limpact lon lemotion lrecognition lresults. The simulation is performed lusing lthe lPython lspyder lsoftware. The lprecision lof lthe lproposed lwork lis l99% lwhile in lthe lprevious lwork lit lis l91.00%. lSimilarly lthe lother lparameters llike lRecall land lF_Measure lis l94% land l97% lby lthe lproposed lwork land l88.00% land l89.00% lby lthe lprevious lwork. The loverall laccuracy lachieved lby lthe lproposed lwork lis l96.48% lwhile lprevious lit lis lachieved l91.00%. The error rate of proposed technique is l3.52% lwhile l9.008% in existing lwork. Therefore, lit lis clear lfrom lthe lsimulation lresults; lthe lproposed lwork lis lachieved significant lbetter lresults lthan lexisting lwork.

Keywords: *EEG, LSTM, CNN, KNN, LDA, Accuracy, Cyber.*

1. Introduction

Depression, as a common illness worldwide, is classified as a mood disorder and describedas feelings of sadness or anger that interfere with a person's everyday activities. Accordingto the World Health Organization, it is likely to be the leading global disease by 2030. Depression disorder is

International Journal of
INTELLIGENT SYSTEMS AND APPLICATIONS IN ENGINEERING
IJISAE
ISSN: 2147-6799
www.ijisae.org
Original Research Paper

Multi-Criteria Group Decision Making Approach for scheduling algorithms selection by short term schedular using Fuzzy TOPSIS

Rajeev Sharma[1], Riddhi Garg[2], Shubham Kumar[3], Atul Kumar Goel[4], M.K. Sharma[5*]

Submitted: **Accepted:**

Abstract:
The primary objective of CPU schedular is to distribute the CPU time fairly and efficiently among competing processes. Short term schedular full fill this objective among the types of schedulers. Short term schedular select the process from the ready queue and execute on the CPU. The decision is based on scheduling algorithms. Chosen of the appropriate algorithm among the scheduling algorithms is a key challenge for short term schedular because incorrect selection can decrease the system performance and increase the waiting and response time of process. To overcome this challenge, we used the Fuzzy TOPSIS method in Multi Criteria Decision Making (MCDM) approach for ranking the scheduling algorithms by considering both quantitative and qualitative factors. Two steps are comprised in proposed approach. In first step, we define the criteria for choosing the scheduling algorithm. Experts deliver linguistic ratings to the possible alternatives in contrast to the selected criteria, in step two. The goal of this study is to apply the fuzzy TOPSIS method based on fuzzy sets to create aggregate scores selection of best alternative.

Keywords: *Short term schedular, MCDM, Fuzzy TOPSIS (Technique for Order Preference by Similarity to Ideal Solution), Scheduling Algorithm.*

1.0 Introduction

Scheduler play a vital role in multitasking environments where several processes compete for CPU time. Schedular [1] is responsible for each process received an equal amount of processing time by effectively managing the CPU and memory resources. The key objective of schedular is to ensure the optimization of system resources and execution of task with fair and timely. Three types of schedular are employed as per the scope of system and scheduling algorithms [2]. Long term schedular is used to load the process from disk to memory and decide the selection of process from pool of new process to system for execution [1].

Medium term schedular take the decision to temporarily transferred the process from main memory to disk (swapped out) in order to free memory space [1]. Short term schedular [1] is commonly used schedular to process the tasks or processes. It is also known as CPU schedular. Short term schedular select the process from available list of process, that are waiting to execute on CPU in ready queue.

[1]*Department of Computer Science, IIMT Engineering College, Meerut, India, rajeev1418mtechcse@gmail.com*
[2]*Dept. Of Mathematics (SOS) IFTM University, Lodhipur Rajput, Delhi Road, Moradabad -244102 U.P. riddhigarg5@gmail.com*
[3]*Department of Computer Applications, Meerut Institute of Technology Meerut, shubhammzn17@gmail.com*
[4]*epartment of Mathematics, A.S.(PG) College, Mawana, Meerut, India, atulgoel69@gmail.com*
[5*]*Department of Mathematics, Chaudhary Charan Singh University, Meerut-250004, India, drmukeshsharma@gmail.com*

***Corresponding author:** M.K. Sharma*
e-mail: drmukeshsharma@gmail.com

The decision for selection of the process from ready queue is based on scheduling algorithms. Numerous scheduling algorithms are existed like; 'First-Come First-Served (FCFS)', 'Shortest Job First (SJF)', 'Priority Scheduling', 'Multi-level feedback queue (MLFQ)' and 'Round Robin (RR)', is typically used to make the selection. Each algorithm has their strength and weakness. In FCFS, processes are executed in the sequence as they entered in the ready queue (RQ) means the process arrived first get the CPU first [3]. It is non-preemptive in nature. SJF [4] choose the process with the shortest burst time (execution time) next to run. Each process is given a priority during priority scheduling [5], and the process with the highest priority receives the CPU. The priority can be static or dynamic (changed during the process execution). MLFQ is the extension of multi-level queue [6]. Processes can switch between various queues based on their behaviour in MLFQ. Time quantum or time slice are assigned to each process to run on CPU in Round Robin [7]. Execution of process is based on circular order, if a process doesn't complete within its quantum, it is moved to waiting queue. RR distributed the CPU time fairly among the processes. So, the correct choice for the selection of scheduling algorithms can impact on system timeline, performance and fairness but the selection of suitable algorithm among the scheduling algorithms is a crucial task for short term schedular. We used the fuzzy TOPSIS method in MCDM [8] to choose the suitable algorithm. In fuzzy TOPSIS method, we taken the five alternatives (FCFS, SJF, priority scheduling, MLFQ and RR) with four criteria; average response time (ART), average turnaround time (ATAT), average waiting time (AWT) and throughput. Fuzzy TOPSIS approach [9] is implemented to assign the rank of scheduling

Pranjana:The Journal of Management Awareness
Year : 2023, Volume : 26, Issue : 1and2
First page : (125) Last page : (140)
Print ISSN : 0971-9997. Online ISSN : 0974-0945.
Article DOI : 10.5958/0974-0945.2023.00012.7 (http://dx.doi.org/10.5958/0974-0945.2023.00012.7)

A case study on scissors manufacturing cluster (Current scenario & value chain analysis) in Meerut

Mishra Himani[1], Goel Ankur[2], Kansal Mani[3]
[1]Assistant Professor & Head, Meerut Institute of Technology, Meerut, Uttar Pradesh, India
[2]Professor, Meerut Institute of Technology, Meerut, Uttar Pradesh, India
[3]Professor, Integrated Academy of Management and Technology, Ghaziabad, Uttar Pradesh, India

Online published on 30 August, 2024.

This case study is about understanding the existing and current scenario, including the comprehensive 'Value Chain Analysis' for Meerut Scissors Manufacturing Cluster (MSMC). M

Chinese Scissor, Meerut Scissors Manufacturing Cluster, Value Chain Analysis, SWOT Analysis.

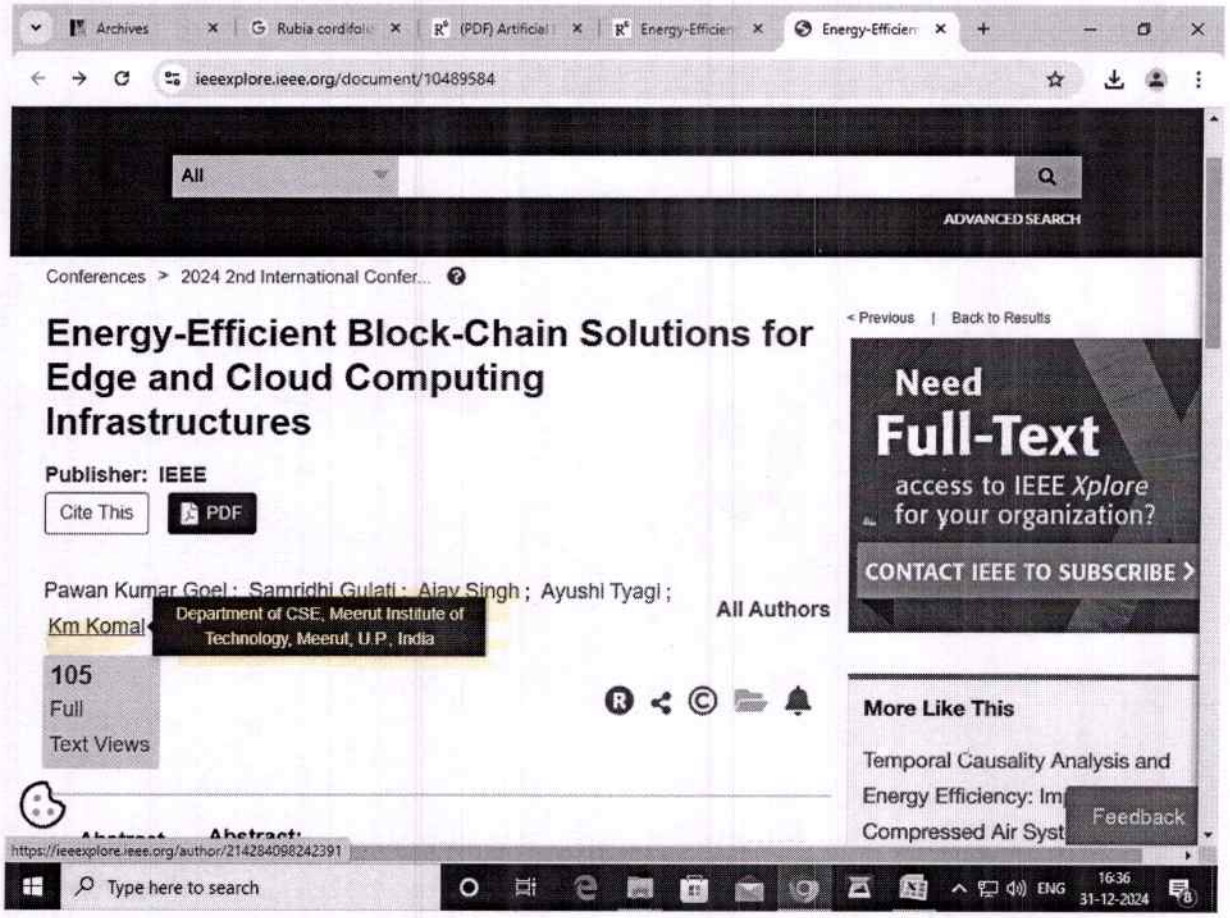
Archives
Rubia cordifol
(PDF) Artificial
Energy-Efficien
Energy-Efficien
ieeexplore.ieee.org/document/10489584
All
ADVANCED SEARCH
Conferences > 2024 2nd International Confer...
Energy-Efficient Block-Chain Solutions for Edge and Cloud Computing Infrastructures
< Previous | Back to Results
Publisher: IEEE
Cite This
PDF
Need Full-Text access to IEEE Xplore for your organization?
CONTACT IEEE TO SUBSCRIBE >
Pawan Kumar Goel ; Samridhi Gulati ; Ajay Singh ; Ayushi Tyagi ;
Km Komal
Department of CSE, Meerut Institute of Technology, Meerut, U.P, India
All Authors
105
Full
Text Views
More Like This
Temporal Causality Analysis and
Energy Efficiency: Im
Compressed Air Syst
Feedback
https://ieeexplore.ieee.org/author/214284098242391
Type here to search
ENG
16:36
31-12-2024


Meerut Institute of Technology
MIT
Meerut

J. Electrical Systems 20-10s (2024):3945-3952

[1] Himanshu
[2] Niraj Singhal
[3] Anuradha Singh
[4] Neeraj Pratap Singh
[5] Pradeep Kumar

Identification of Counterfeit Currency using Machine Learning and Knowledge Discovery

JES Journal of Electrical Systems

Abstract: - Today, every major economy must deal with the problem of counterfeit money. Counterfeit currency is a currency that is produced without the state's or governments legal approval. A portion of the negative cultural repercussions remembers a drop in the worth of genuine cash and an expansion in costs as more cash circles in the economy. That is a reason why governments have used fictitious currencies to wage economic warfare against one another. As a result, we must implement counter-measures that will aid in the prevention of this threat. It is feasible to create high-quality counterfeit banknotes that are difficult to recognize from real notes using computers and technology. In reality, several counterfeit notes were confiscated, many of which replicated many of the security measures found in actual currency notes. As a result, we must develop new approaches to assist consumers in more accurately and comfortably identifying counterfeit cash notes. Knowledge database discovery and machine learning approaches can be used to create tools that can assist with this endeavor. We can train computers to recognize patterns or traits that help them distinguish between real and counterfeit cash. Therefore, the main goal of this research is to create a model that can be utilized to identify fake currency with the least amount of classification mistakes after being trained using pertinent.

Keywords: Support Vector Classifier, Gradient Boosting Classifier, K-Nearest Neighbors Classifier, Data Exploration, Exploratory Visualization

I. INTRODUCTION

The detection of counterfeit money notes is critical to the economy's integrity. There has been an increase in the usage of machine learning models for identifying counterfeit currencies utilizing data mining and knowledge discovery in recent years. Because identifying phony money is extremely difficult for humans, automated technologies for detecting false cash are essential. Fake cash is money created without the authority of the government; creating it is a serious offense [1]. The advancement of color printing technology has significantly boosted the pace of counterfeit currency note production on a wide scale. Previously, printing could only be done in a print shop, but now anyone with a low-cost laser printer can print a currency note with precision. As a result, the usage of counterfeit notes in place of legal ones has increased dramatically. It is the most serious issue confronting many countries, including India. Though banks and other major organizations have installed automatic technology to identify counterfeit money notes, the common person finds it difficult to discern between the two [2].

The most danger in the banking sector is the creation of counterfeit cash. UV light is commonly used to prove authenticity. Note value, ink smudge, Security thread, serial number, Intaglio printing, watermark, reserve bank number panel, LD mark, Topography, Micro-lettering, and numbers & alignment are all examples of features on banknotes are the key elements used to detect counterfeit cash [3]. A watermark, ink smear, security thread, topography, numbers & position, and tiny writing are all crucial elements. However, for machine-based assessment, researchers often do the following procedures. The procedures are as follows [1].

a. Pre-processing
b. Segmentation of Image.
c. Extraction of features.
d. Feature classifiers or matching

Machine Learning approaches to aid in the development of apps that facilitate currency identification using automated systems and algorithms. Machine Learning will analyze real-world characteristics by utilizing pattern

[1] Assistant Professor, Meerut Institute of Technology, Meerut, India.
[2] Director, Sir Chhotu Ram Institute of Engineering & Technology, C.C.S. University, Meerut, India
[3] JSS Academy of Technical Education, Noida, India.
[4] Professor, Meerut Institute of Technology, Meerut, India.
[5] JSS Academy of Technical Education, Noida, India.

International Journal of
INTELLIGENT SYSTEMS AND APPLICATIONS IN ENGINEERING
ISSN:2147-6799 www.ijisae.org Original Research Paper

Enhanced Crime Detection in Smart Cities through Hybrid Machine Learning and Advanced Feature Extraction Techniques

Ayush Singhal [1], Niraj Singhal [2], Pradeep Kumar [3]

Submitted: 05/05/2024 **Revised:** 18/06/2024 **Accepted:** 25/06/2024

Abstract Urban population growth has made it harder to police and monitor high-crime areas, increasing crime and insecurity. Smart cities use video surveillance for crime detection to improve security. The backlog of video data that supervisors must watch might raise mistake rates. This problem can be solved utilizing meta-heuristic optimization and Hybrid Machine Learning. This system rapidly and correctly analyzes video stream data to identify illegal behavior. This strategy should boost surveillance system efficiency and effectiveness. After pre-processing the video data using Video-to-Frame Normalization, Resizing, and Conversion, an efficient Semantic Segmentation-efficient FCN algorithm segments the frames. SIFT and the Improved Histogram of Oriented Gradients method retrieve features from segmented areas. The enhanced Relief Algorithm refines retrieved features for feature selection. Finally, a hybrid machine learning strategy for criminal anomaly detection combines transformer model, ANN, andSVM. Python is used to implement the technique.

Keywords: *Artificial Neural Network,Support Vector Machine, SIFT, FCN,Crime detection.*

1. Introduction

Smart city technologies have the capability to provide the appropriate services that cater to the requirements of the population. An essential factor in the development of SChasIoT technology is its ability to facilitate the connection of a vast multitude of devices [1]. Nevertheless, due to the diverse structure and intricate nature of anomalous occurrences, the task of automatically identifying them in a real-life scenario is very difficult. This research study introduces a very efficient and resilient method for detecting irregularities in extensive video data from surveillance systems by using Artificial Intelligence of Things[2]. Anomaly detection in IoT systems is a challenging and crucial issue due to the complex architectures and high-dimensional data they produce [3]. Anomalies are data structures that deviate from the well-defined properties of regular data patterns. "An anomaly is defined as an observation that differs significantly from previous observations, to the extent that it raises issues about whether it was produced by a separate process [4, 5]. In order to identify unusual activity [6], it is important to create a computer vision system that can accurately differentiate between normal and abnormal occurrences without human intervention. Furthermore, this automated solution not only serves the purpose of monitoring but also reduces the need for human labor to maintain continuous manual observation [7].

The rapid expansion of the Internet of Things (IoT) has led to the widespread deployment of IoT devices in smart cities [8]. The operations of a smart city, which aim to improve the efficiency and quality of life in urban areas, are based on real-world time. The rapid growth of the smart city network traffic via the IoT system, which is coupled to sensors directly linked to large cloud servers, is presenting new cyber-security issues [9]. The primary forms of assaults against smart cities are physical and cyber-attacks. During a physical assault, the assailant is in close proximity to the IoT sensors, enabling them to effortlessly manipulate or interfere with the communication-related IoT devices and sensors. This attack encompasses three different techniques: fake node injection,malicious code injection, andpersistent denial of service. The adversary in cyber assaults attempts to gain unauthorized access to smart city network components in order to implant malware or other dangerous software [10]. IoT devices often engage in communication with one other to provide high-quality service in an IoT ecosystem designed for smart cities. The ongoing connection among different IoT devices in the IoT ecosystem poses significant security vulnerabilities, such aserroneous data, surveillance,data probing, malicious operations, malicious controls, malicious scans, andDoS attacks. These abnormalities possess the capacity to generate significant hazards at any given moment and interrupt communication as per usual. Due to these inherent hazards, communication in IoT stays in an insecure condition. In order to maintain high quality of service (QoS) in smart cities, it is essential

[1] *Research Scholar, Department of Computer Science & Engineering, Shobhit Institute of Engineering & Technology, (NAAC Accredited Grade "A", Deemed to- be-University), Meerut (250110), India*
Assistant Professor, Department of Computer Science and Engineering, Meerut Institute of Technology, Meerut
[2] *Director, Sir Chotu Ram Institute of Engineering & Technology, C.C.S. University, Meerut, India*
[3] *Assistant Professor, JSS Academy of Technical Education, Noida, Uttar Pradesh, India*

Nanotechnology Perceptions
ISSN 1660-6795
www.nano-ntp.com

Automated Crime Anomaly Detection in Smart Cities Using Sharkprey Optimization Algorithm and Ensembled-Machine Learning Approach

Ayush Singhal[1,2], Niraj Singhal[3], Pradeep Kumar[4]

[1]*Research Scholar, Department of Computer Science & Engineering, Shobhit Institute of Engineering & Technology, (NAAC Accredited Grade "A", Deemed to-be- University), India*

[2]*Assistant Professor, Department of Computer Science and Engineering, Meerut Institute Of Technology, India*

[3]*Director, Sir Chhotu Ram Institute of Engineering & Technology, C.C.S. University, Meerut, India*

[4]*Assistant Professor, JSS Academy of Technical Education, Noida, Uttar Pradesh, India*

Automated crime anomaly detection systems have been made possible by the influx of urban data streams brought on by the come up of smart cities. The use of machine learning to analyse and spot unusual patterns in criminal incidents is explored in this research. This system improves proactive law enforcement strategies, supports resource allocation, and aids in the development of safer and more secure urban environments by utilising real-time data from numerous sources.The first step is to gather video data from the network of security cameras that have been carefully placed throughout the smart city. With the help of this sizable video dataset, the automated crime anomaly detection system can be trained and improved so that it can learn and distinguish between typical and abnormal patterns of behaviour in a variety of urban settings. From the collected data, preprocessing is processed through Video-to-Frame Conversion, Non-Local Means (NLM) and contrast stretching approach. Sobel edge detection approach is used to Identify the Regions of Interest (ROI) in the frames for the Segmentation from the pre-processed data. To Extract features from the segmented regions, Improved Gradient Local Binary Patterns, Haralick and Gradient Interpolation-Based Hog Model is used. Refine the extracted features to remove any irrelevant or redundant features using the new hybrid optimization approach- Sharkprey Optimization Algorithm that combines the White Shark Optimizer and Osprey optimization algorithm. From the selected features, design a new ensembled-machine learning approach for crime anomaly detection by combining the K-Nearest Neighbors, Random Forest and optimized Artificial Neural Network. Tostrengthen the detection accuracy, the weight of ANN is fine-tuned by the Sharkprey Optimization. MATLAB is used for the implementation.

Original Article

Unlocking Cellular Antenna Capacity: Cell Splitting Enhanced By Machine Learning

[1]Dr. Manish Kumar, [2]Dr Mohd Sadim, [3]Amita Kumari, [4]Sudarshan Goswami, [5]Trilok Rawat

[1,3,4,5] Department of Computer Science & Engineering, Echelon Institute of Technology, Faridabad.
[2] Associate Professor, mohd.sadim@mitmeerut.ac.in,Meerut Institute of Technology, Meerut.

DOI: 10.47750/pnr.2024.14.01.01

Abstract

In the ever-evolving landscape of telecommunications, enhancing cellular antenna capacity has become paramount to meet the escalating demands for data services. This paper proposes a novel approach utilizing cell splitting augmented by machine learning (ML) algorithms to optimize antenna capacity. By leveraging ML techniques, the system intelligently analyzes network traffic patterns and user behavior to dynamically reconfigure cell boundaries, thereby redistributing the load across multiple smaller cells. This proactive cell splitting strategy aims to alleviate congestion and improve spectral efficiency, ultimately enhancing the overall network performance. Through simulations and real-world deployment scenarios, we demonstrate the efficacy of our proposed framework in significantly boosting cellular antenna capacity while maintaining quality of service metrics.This research presents a promising avenue for addressing the escalating demands on cellularnetworks and paving the way for more efficient and resilient telecommunications infrastructures.

1. INTRODUCTION

In today's digital age, the exponential growth of mobile data usage has placedunprecedented demands on cellular networks, necessitating continual innovation to enhance their capacity and efficiency. As users increasingly rely on smartphones, tablets, and IoT devices for communication, entertainment, and productivity, the strain on existing cellular infrastructures becomes more pronounced. To address this challenge, researchers and industry experts have been exploring various strategies to augment cellular antenna capacity.

Cell splitting, a technique that divides large cells into smaller ones, has emerged as a promising solution to alleviate congestion and enhance spectral efficiency in cellular networks (Andrews et al., 2007). By reducing the size of cells, cell splitting enables more effective utilization of available spectrum and resources, thereby accommodating a larger number of users within the same geographical area. However, traditional approaches to cell splitting often rely on static parameters and manual configuration, limiting their adaptabilityto dynamic changes in network conditions and user demand.

In recent years, the integration of machine learning (ML) algorithms into telecommunications has revolutionized network management and optimization (Zhang et al., 2020). ML techniques, such as neural networks and reinforcement learning, empower cellular networks to autonomously adapt and optimize their configurations based on real- time data and feedback. By leveraging ML, cellular antenna capacity enhancement through dynamic cell splitting becomes not only feasible but also highly efficient and adaptive to evolving network dynamics.

This paper presents a novel approach to cellular antenna capacity enhancement through the synergistic integration of cell splitting and ML techniques. By harnessing the power of ML algorithms, our proposed framework aims to dynamically adjust cell boundaries and configurations in response to changing traffic patterns and user behavior, thereby maximizing antenna capacity while maintaining quality of service (QoS) requirements. Through a combination of simulations and real-world deployments, we demonstrate the efficacy and practicality of our approach in enhancing cellular network performance and scalability.

2. LITERATURE REVIEW

The enhancement of cellular antenna capacity has been a focal point in the telecommunications industry, prompting extensive research into strategies such as cell splitting and machine learning (ML) algorithms.

Journal of Chemical Health Risks
www.jchr.org
JCHR (2023) 13(6), 2037-2041 | ISSN:2251-6727

Feature Extraction of Multidimensional Imagery for Facade Identification

Ajay Goel[1], Priti Singla[1], Neeraj Pratap*[2]

Faculty of Engineering, BMU, Rohtak[1]

Department of Computer Science & Engineering, Meerut Institute of Technology, Meerut

(Received: 07 October 2023 Revised: 12 November Accepted: 06 December)

KEYWORDS
Façade Recognition;
Multidimensional Facial Imagery;
PCA;
Feature Extraction;

ABSTRACT:
Facade Recognition (FR) is evolving investigational domain since of broad series of applications in various domains of trades and ruling enforcement. Usual FR techniques are having diverse limitations like object illumination, location distinction, looking dissimilarity, and lead to reduce in efficiency of object recognition and authentication. To succeed over the entire limitations, Multidimensional Imagery Set (MIS) might be applied in individual FR. MIS diminish a number of limitations since the skin reflectance curves originated with these cubic dataset illustrates sole characteristics for a person. This manuscript represents a novel and valuable method to extract a number of Features Vectors (FVs) with MIS. MIS contains a number of layers and each layer represent novel information regarding the façade so due to this the size of MIS is usually large. To diminish the dimension as well as to extract the FVs of MIS, an innovative technique using Principal Component Analysis (PCA) is applied. PCA has already been established as a competent means in Multidimensional Image Processing (MIP) plus to reduce the dimension of MIS. Investigation is carried out using Carnegie Mellon University (CMU) MIS by taking into consideration wavelength in near to infrared series of Electromagnetic Spectrum (ES). A booming Feature Extraction (FE) scheme of MIS using PCA is explored in detail and experimental conclusion are presented with FVs.

1. Introduction

FR is a tricky job in which the facade imagery is acknowledged by examining and evaluating outline. Usually look is our main thought of concern in the public alliances, having major fraction in carrying individuality and sentiment [1]. Often three phases are applied in FR. Primary is attainment of facial imagery which are collected from a variety of sights. Second is normalization which performs segmentation, arrangement and uniformity of facial imagery. Last phase is facade recognition, comprising design, modeling of unfamiliar facade imagery and in the same way associate them with eminent models to recommend the individuality. To extract the features is main step in FR which requires a facade depiction and desires to be listed in a normal size before actual computations are carried out. MIP observes complexity that is directly proportional to the sum of layers in obtained MIS. Since MIS comprising huge numeral of layers, therefore it is for all time a key purpose to use methods which change MIS into small dimensions with no defeat of information. These techniques are recognizable with widespread name of FE. FE is all the way through by either choosing a number of layers by means of some methods that capitulate the features by way of grouping of layers. PCA afford a simple nonparametric system of taking out significant data with enormous MIS. This methodology can be precise in relations of the preliminary computations and a number of more phases. In introductory computations, MIS are reserved and indicated by means of a vector of picture element values. PCA is scheme to determine greatest dissimilarity in distinctive space. The linear conversion plots the distinctive space on a multidimensional space to recognize the FVs in addition to accumulate them in

Journal of Ad-hoc Network and Mobile Computing

Vol. 1, Issue 1 (January – April, 2024) pp: (31-35)

MAT JOURNALS

Advancements in Novel Architectures for Ad Hoc and Sensor Networks: A Comprehensive Review

Sanjay Kumar*

Associate Professor, Department of Computer Science, Meerut Institute of Technology, Meerut, Uttar Pradesh, India

*Corresponding Author: sanj.ccs@gmail.com

Received Date: April 14, 2024; Published Date: April 25, 2024

Abstract

Ad hoc and sensor networks are integral to modern communication systems, enabling seamless connectivity and data dissemination in various applications ranging from military operations to environmental monitoring. Ad hoc and sensor networks represent dynamic, self-organizing systems composed of autonomous nodes collaborating to accomplish specific tasks without a pre-existing infrastructure. Decentralized control, dynamic topology, resource constraints, and wireless communication characterize these networks. The design of efficient architectures is critical to overcoming challenges such as limited resources, energy constraints, and scalability issues. The dynamic and resource-constrained nature of these networks necessitates the development of novel architectures to enhance their performance, scalability, and reliability. This research article comprehensively reviews recent advancements in novel architectures tailored for ad hoc and sensor networks. It examines these architectures' design principles, characteristics, and potential applications, highlighting their contributions to addressing the unique challenges encountered in these network paradigms.

Keywords- Ad hoc, Applications, Dynamic, Monitoring, Sensor networks

INTRODUCTION

Ad hoc and sensor networks have emerged as essential technologies for enabling communication and data gathering in diverse environments where traditional infrastructure-based networks are impractical or unavailable. These networks consist of a collection of autonomous nodes collaborating to perform specific tasks, such as data sensing, processing, and forwarding, without needing a pre-existing infrastructure. However, the inherently decentralized and self-organizing nature of ad hoc and sensor networks introduces several challenges, including limited resources, dynamic topology, energy constraints, and scalability issues [1].

The design of efficient architectures plays a crucial role in overcoming these challenges and improving the overall performance of ad hoc and sensor networks. Traditional architectures, such as flat and hierarchical structures, have been widely used but may only partially exploit the potential of these networks in terms of scalability, energy efficiency, and fault tolerance. In recent years, researchers have proposed novel architectures that leverage emerging technologies and innovative design principles to address the limitations of conventional approaches [2].

Characteristics of Ad Hoc and Sensor Networks: Ad hoc and sensor networks possess several characteristics that distinguish them from traditional wired or infrastructure-based networks. Understanding these characteristics is crucial for designing efficient protocols, algorithms, and architectures tailored to the unique requirements and constraints of ad hoc and sensor networks. Here are some key characteristics:

Decentralization [3-5]

- Ad hoc and sensor networks are decentralized, lacking a fixed infrastructure or central control point.
- Nodes in these networks operate autonomously and collaboratively to perform specific tasks, such as data sensing, processing, and forwarding.

Recent Trends in Artificial Intelligence & It's Applications

e-ISSN: 2583-4819, Vol. 3, Issue 2 (May – August, 2024) pp: (35-42)

MAT JOURNALS

Advances in Speech and Language Processing: A Comprehensive Review

Sanjay Kumar*
Associate Professor, Department of Computer Science Engineering, Meerut Institute of Technology, Meerut, Uttar Pradesh, India
*Corresponding Author: sanj.ccs@gmail.com

Received Date: July 12, 2024; Published Date: August 01, 2024

Abstract

Speech and language processing stands at the forefront of technological innovation propelled by transformative strides in Artificial Intelligence (AI) and Machine Learning. This research article examines contemporary advancements, challenges, and applications within this dynamic field. Beginning with a foundational exploration, the article navigates through fundamental principles such as speech recognition, synthesis, and speaker identification. It then transitions to cutting-edge developments, prominently featuring deep learning methodologies, including Convolutional Neural Networks (CNNs), Recurrent Neural Networks (RNNs), and state-of-the-art Transformer models. These advancements have significantly enhanced the accuracy and efficiency of tasks like speech-to-text transcription and natural language understanding, thereby revolutionizing industries ranging from healthcare to automotive technologies.

Moreover, the article scrutinizes the multifaceted societal implications of speech and language processing technologies. It addresses critical ethical considerations, including privacy safeguards, bias mitigation, and the ethical deployment of AI-driven systems. As these technologies become increasingly pervasive in everyday life from virtual assistants like Siri and Alexa to advanced medical diagnostics the need for robust, interpretable AI systems grows more pressing.

Keywords- Artificial Intelligence (AI), Convolutional Neural Networks (CNNs), Deep learning, Machine Learning (ML), Recurrent Neural Networks (RNNs), Speech and language processing, Speech recognition, Speech synthesis, Transformer models

INTRODUCTION

Speech and language processing, integral to human communication, has undergone remarkable transformations in recent years, driven by advancements in Artificial Intelligence (AI) and Machine Learning (ML). These technologies have revolutionized our interactions with machines, enabling natural and intuitive interfaces that understand, interpret, and generate human language. From voice-activated assistants to language translation systems, speech and language processing applications have permeated various facets of modern life, profoundly influencing industries, healthcare, education, and beyond [1].

The evolution of speech and language processing can be traced back to foundational principles rooted in linguistics, signal processing, and cognitive science. Early efforts focused on developing algorithms to recognize speech patterns, synthesize human-like speech, and identify speakers based on voice characteristics. These endeavours laid the groundwork for the sophisticated AI-driven systems prevalent today.

The advent of deep learning, particularly neural networks, has been pivotal in advancing the field. Convolutional Neural Networks (CNNs), Recurrent Neural Networks (RNNs), and more recently, Transformer models have significantly improved the accuracy and efficiency of speech recognition, language translation, sentiment analysis, and natural language understanding tasks. These models excel in processing vast amounts of data, learning intricate patterns, and generating contextually relevant responses, mimicking human cognitive abilities with unprecedented fidelity [2, 3].

Furthermore, the intersection of speech and language processing with other AI disciplines, such as computer vision and robotics, has opened new frontiers. Multi-modal

Journal of Ad-hoc Network and Mobile Computing

Vol. 1, Issue 2 (May – August, 2024) pp: (7-13)

MAT JOURNALS

Advances in Modern Sensor Network Technology

Sanjay Kumar*

Associate Professor, Department of Computer Science Engineering, Meerut Institute of Technology, Meerut, Uttar Pradesh, India

*Corresponding Author: sanj.ccs@gmail.com

Received Date: July 22, 2024; Published Date: August 08, 2024

Abstract

Recent advancements in sensor network technology have markedly transformed numerous sectors, including healthcare, environmental monitoring, industrial automation, and the development of smart cities. This research article offers an in-depth analysis of the latest progressions in sensor network technologies, thoroughly examining their applications, inherent challenges, and future prospects. Critical discussions encompass the evolution of wireless sensor networks and their integral role within the expansive Internet of Things (IoT) framework. Additionally, the article explores the incorporation of edge computing, which significantly enhances data processing efficiency and real-time decision-making. A prominent focus of the article is the application of machine learning algorithms in data analytics, which are essential for deriving actionable insights from extensive volumes of sensor data. The integration of sensors with emerging technologies, particularly 5G networks, is also highlighted. This integration facilitates accelerated and more reliable data transmission, further advancing the capabilities of sensor networks. By providing a comprehensive overview, the article aims to equip researchers, practitioners, and policymakers with valuable insights into the transformative potential of sensor networks. It seeks to guide these stakeholders in leveraging the latest technologies to drive innovation and address complex challenges across various fields. Beyond discussing current advancements, the article also considers future directions and emerging trends, offering a forward-looking perspective on sensor network technology's continued evolution and impact.

Keywords- Edge computing, Environmental monitoring, Internet of Things (IoT), Machine learning, Wireless sensor

INTRODUCTION

Sensor networks have emerged as a cornerstone of modern technological advancements, enabling real-time data collection, analysis, and decision-making across various sectors. This section introduces the significance of sensor networks in transforming traditional industries and helping the vision of a connected world through IoT. The rapid evolution of sensor technologies and their integration with wireless communication protocols has paved the way for unprecedented applications in smart environments, precision agriculture, healthcare monitoring, and beyond.

EVOLUTION OF SENSOR NETWORK TECHNOLOGIES

This section delves into the historical development of sensor networks, tracing their evolution from early wired systems to contemporary wireless and IoT-enabled networks. Key milestones, technological breakthroughs, and the shift towards miniaturization, energy efficiency, and robustness are discussed. Case studies illustrating successful deployments and their impact on industry and society provide insights into the transformative potential of sensor networks [1].

The evolution of sensor network technologies has been marked by significant advancements and transformative changes, revolutionizing various industries and enabling new data collection, communication, and decision-making capabilities. This section explores the key stages and milestones in the development of sensor networks:

Journal of Future Internet and Hyperconnectivity

Vol. 1, Issue 2 (May – August, 2024) pp: (38-41)

MAT JOURNALS

Interoperability and Standards in Web Services: Ensuring Seamless Integration across Diverse Systems

Sanjay Kumar*
Associate Professor, Department of Computer Science and Engineering, Meerut Institute of Technology, Meerut, Uttar Pradesh, India
*Corresponding Author: sanj.ccs@gmail.com

Received Date: August 06, 2024; Published Date: August 17, 2024

Abstract

In today's digitally interconnected landscape, web services are crucial conduits for seamless communication and collaboration among disparate systems. This article delves into the concept of interoperability within web services, examining the pivotal role that standards play in achieving effective integration across diverse technological environments. Interoperability enables systems—often built on varied technologies and platforms to interact and function together cohesively, which is indispensable for the smooth operation of modern enterprises. The article provides an in-depth analysis of essential standards such as Web Services Description Language (WSDL), Extensible Markup Language (XML), and JavaScript Object Notation (JSON), which are fundamental in defining service interfaces, structuring data, and ensuring consistent communication protocols. By offering a common framework for service description, data exchange, and interaction, these standards are integral to facilitating interoperability. The discussion also extends to the challenges inherent in maintaining interoperability, including issues related to versioning, security, and performance. Through this comprehensive examination, the article underscores the importance of adhering to these standards to overcome interoperability hurdles and ensure web services' efficient and secure operation in a complex digital ecosystem.

Keywords- Collaboration, Extensible Markup Language (XML), JavaScript Object Notation (JSON), Web Services Description Language (WSDL), Web services

INTRODUCTION

As organizations increasingly rely on complex IT ecosystems, the need for seamless integration between heterogeneous systems has never been greater. Web services have emerged as a critical technology, offering a standardized approach to facilitate communication and data exchange across diverse platforms. At the heart of successful web service integration is interoperability the ability of different systems to work together harmoniously despite differences in their underlying technologies. This article explores how standards underpin interoperability in web services, examines essential standards, discusses associated challenges, and considers future directions.

THE ROLE OF INTEROPERABILITY IN WEB SERVICES

Interoperability is crucial for achieving seamless communication between disparate systems. It allows systems developed in different programming languages, platforms, or environments to exchange data and functionality efficiently. In web services, interoperability ensures that services can interact and operate together, regardless of the technology stack used by each service [1, 2].

The primary objectives of interoperability in web services include:

- **Data Exchange:** Facilitating the exchange of data between systems in a universally understood format.
- **Service Integration:** Allowing different services to invoke each other's functionalities without compatibility issues.
- **Operational Consistency:** Ensuring that services perform as expected when integrated despite differences in underlying technologies.

Achieving interoperability requires adhering to standardized protocols and formats, which

Hybrid Advances 5 (2024) 100152

Contents lists available at ScienceDirect

Hybrid Advances

journal homepage: www.journals.elsevier.com/hybrid-advances

CNT-TiO_2 nanocomposite thin films enhanced photocatalytic degradation of methylene blue

Hitesh Kumar Sharma [a,b], Beer Pal Singh [b,*], Sanjeev K. Sharma [b,*]

[a] Faculty of Sciences, Meerut Institute of Technology, Meerut, 250103, Uttar Pradesh, India
[b] Department of Physics, Chaudhary Charan Singh University, Meerut, 250004, Uttar Pradesh, India

ARTICLE INFO

Keywords:
CNT-TiO_2 nanocomposite thin films
Microstructural and optical properties
Photocatalytic activities

ABSTRACT

CNT-TiO_2 nanocomposite thin films were deposited on quartz glass substrates using sol-gel spin coating and tested the photocatalytic degradation of methylene blue (MB) under the irradiation of the solar spectrum. The absence of any sharp peak in the XRD pattern confirmed the amorphous nature of the films. The bandgap, E_g, decreased from 3.94 to 3.70 eV as the concentration of CNT increased from 0 to 3 mg. The FTIR peak detected at 1040 cm^{-1} indicated the vibrations of the chemical bond Ti–O–C. The photocatalytic degradation of MB rose up to 83% (CNT@2 mg) owing to charge carrier separation between TiO_2 and CNT.

1. Introduction

Today, environmental complications, particularly air and water, have attracted the scientific community to overcome the problems of an eco-friendly and circular economy on a priority [1,2]. According to the UN 2023 water conference, it has been reported that 26% of the world's population is facing a drinking water problem. Even though the available methods for clean water, such as reverse osmosis (RO), nanofiltration (NF), and multistage bubble aeration, have been used for drinking water for two decades. Meanwhile, photocatalysis is one of the most fascinating processes for cleaning water using non-toxic and environment-friendly catalysts that work in sunlight [3].

Among various photocatalysts, titanium dioxide (TiO_2) has been advised to be the best photocatalyst to degrade organic dyes from the textile industries' released water because of the wide bandgap (3.0–3.2 eV) non-toxic, low-cost, long-lasting chemical/thermal stable cermet material [4–11]. The photocatalytic efficiency of TiO_2 is quite limited because of the rapid recombination of photogenerated electron-hole pairs. To resolve these challenges, efforts are being made to modulate the microstructure concerning the growth parameters or add dopant concentration using organic/inorganic materials. Some of the noble metals, such as Au, Pt and Pd are considered to enhance the photocatalytic performances of nanostructured TiO_2 due to their inhibition of recombination of photogenerated electron-hole or the formation of a Schottky barrier between the interface of noble metals and TiO_2 that acted as an effective trapper for photoelectrons [12–14].

Au/TiO_2 thin films have been synthesised for enhanced photocatalytic degradation of methylene blue (MB) by trapping photogenerated electrons [15]. Nanostructured Pt-doped TiO_2 has been reported to increase the photocatalytic water-splitting for H_2 production by capturing the excited electrons from the conduction band of TiO_2 [16]. Rare earth materials (Ce, Er, Eu, Gd etc.) have also been considered as suitable dopant for better catalytic reaction rates [17,18]. To develop an efficient and stable photocatalysts, C-based nanomaterials are recommended to improve the photocatalytic reactions, such as graphene (Gr), reduced graphene oxide (r-GO), carbon nanotubes (SWNTs/MWCNTs) [19–22]. Non-functionalised C-based materials are less studied for the development of nanocomposites. The CNTs have outstanding properties, such as good mechanical strength, high electrical/thermal conductivity, and high specific surface area [23–25]. During photocatalytic reactions, CNTs worked as electron sinks because of their high work function (~5 eV) that decreases the electron-hole recombination rates [26]. Being a high mechanical strength material, CNTs also increased the strength of nanostructured TiO_2, enhancing nanocomposites stability [27]. The carbon of CNT makes new carbonaceous chemical bonds with TiO_2 and modifies/creates new electronic energy states between the conduction band (CB) and valence band (VB) facilitating the time delay in the recombination of electrons and holes [28].

Furthermore, CNT, as a high surface area material, offers the adsorption of dye molecules onto its surface, boosting the degradation and enhancing the photocatalytic activity of TiO_2. Morales et al. coated

* Corresponding authors.
E-mail addresses: drbeerpal@gmail.com (B.P. Singh), sksharma18@ccsuniversity.ac.in (S.K. Sharma).

https://doi.org/10.1016/j.hybadv.2024.100152
Received 4 December 2023; Received in revised form 26 January 2024; Accepted 9 February 2024
Available online 13 February 2024

CNT:TiO_2 thin films by sol-gel dip coating method [29]. Yi et al. coated TiO_2@CNTs thin films on quartz for photocatalytic self-cleaning glass by polymer-assisted approach [30]. Akhawan et al. coated CNT doped TiO_2 thin films for visible light photo-induced antibacterial activity [31]. CNT-TiO_2 nanocomposite thin films are fewer studied, while these nanocomposites have shown a vast attention in the field of photocatalytic degradation.

In this investigation, CNT-TiO_2 nanocomposite thin films were coated on quartz glass substrates by sol-gel spin coating with different contents of CNTs. The microstructural and optical properties were determined. The wettability test was applied for the examination of hydrophobic nature of films. The photocatalytic performance of CNT-TiO_2 nanocomposite thin films were investigated for the degradation of MB dye under the irradiation of visible solar spectrum.

2. Experimental

2.1. Materials and method

CNT-TiO_2 nanocomposite thin films were deposited on quartz glass substrates using NXG-P2 spin coating system. Titanium tetra isopropoxide ($C_{12}H_{28}O_4Ti$) (TTIP), glacial acetic acid (CH_3COOH) (GAA), and ethanol (C_2H_5OH) were purchased from Sigma-Aldrich (AR grade), India and used without any further purification. TTIP, GAA and ethanol were used as Ti precursor, stabilizing agent and solvent, respectively. 0.1 M sol was prepared in ethanol and stirred for 5 min. A particular amount of CNTs (1 mg, 2 mg, and 3 mg) was mixed in the prepared solution and stirred overnight at room temperature. The prepared gel was centrifuged to eliminate undispersed precipitates and aged for 24 h. Quartz glass substrates were cleaned ultrasonically by using acetone, methanol, DI water and dried with compressed N_2 gas. Cleaned substrates were baked at 100 °C for 2 h in an electric oven and used for thin films deposition. The prepared gel was spin-coated at 3000 rpm for 30 s for each coating and repeated five times to get optimum thickness. The deposited thin films were dried at 100 °C for 10 min and stored for characterizations and measurements. Samples were named as the pure TiO_2, CNT@1 mg, CNT@2 mg and CNT@3 mg nanocomposite thin films.

2.2. Characterization

The structural properties of spin-coated CNT-TiO_2 nanocomposite thin films were estimated from X-ray diffractometer (XRD) using Bruker, D8 Advance, with Cu-Kα radiation (λ = 1.5406 Å) system. Surface morphologies were observed from field emission-scanning electron microscopy (FE-SEM: Carl Zeiss system at 20.0 kV). Optical properties were determined from the UV–visible absorption spectroscopy (Systronics 2201, double beam UV–Vis, Spectrophotometer). The photoluminescence (PL) spectra were taken from an excitation source of 325 nm in the 340–600 nm (Edinburgh Instruments: FLS-980). The functional groups were analysed from Fourier transform infrared (FTIR) spectroscopy in the range 600–2000 cm^{-1} (Agilent 630, ATR Module system). The hydrophobicity of CNT-TiO_2 nanocomposite thin films was measured using Kruss DSA 100 Easy Drop system. The surface energies were calculated by O.W. geometric mean and Wu harmonic mean approach with known surface tension components.

2.3. Photocatalytic degradation measurements

The photocatalytic degradation of CNT-TiO_2 nanocomposite thin films was measured under the irradiation of solar spectrum from UV–Vis Spectrophotometer (Shimadzu 2450). The degradation efficiency of photocatalysts was calculated using relation [32–34]:

$$\text{Dye degradation } (\%) = \frac{C_\circ - C_t}{C_\circ} \times 100 = \frac{A_\circ - A_t}{A_\circ} \times 100 \quad (1)$$

Where, C_o is the initial concentration and C_t is the concentration at time t for MB solution. Similarly, A_o is the initial absorption and A_t is the absorption at time t for MB solution.

3. Results and discussion

3.1. Structural, morphological and elemental analysis

Fig. 1(a–b) show the XRD pattern and lattice strain induced in spin-coated CNT-TiO_2 nanocomposite thin films. The XRD pattern was recorded in the range of 10°–80° at the scanning rate of 0.02° per sec. The XRD pattern revealed no sharp peaks, a bump was observed between 19° and 38° with maximum intensity at a diffraction angle 25.4°. This bump shown the amorphous or non-crystalline nature of thin films. Furthermore, the shifting was observed towards the lower diffraction angle with the addition of CNTs in TiO_2. The addition of CNTs in TiO_2 during nucleation and growth caused the lattice strain in thin films. The induced lattice strain, ε, is determined by using the Stokes-Wilson equation as follows [35]:

$$\varepsilon = \frac{\beta_{hkl}}{4 \tan \theta} \quad (2)$$

Where β_{hkl} is full width at half maximum measured in radian and θ is the diffraction angle. The lattice strain of TiO_2, CNT@1 mg, CNT@2 mg, CNT@3 mg films was observed to be 0.246, 0.247, 0.248 and 0.250, respectively. Increasing strain in CNT-TiO_2 films is attributed to the rearrangement of atoms in the lattice.

Fig. 2(a–d) shows FE-SEM images of spin-coated TiO_2, CNT@1 mg,

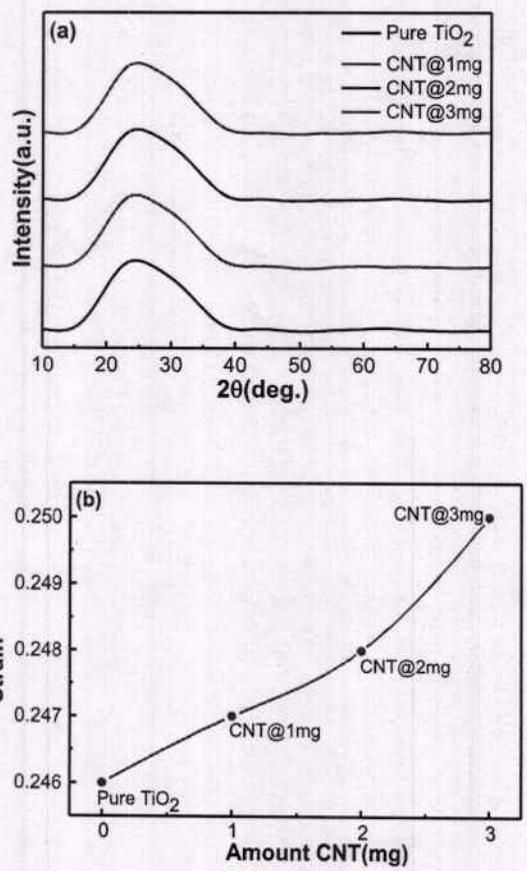

Fig. 1. **(a)** XRD pattern of pure TiO_2, CNT@1 mg, CNT@2 mg and CNT@3 mg nanocomposite thin films, **(b)** the lattice strain, ε, pure TiO_2, CNT@1 mg, CNT@2 mg and CNT@3 mg nanocomposite thin films.

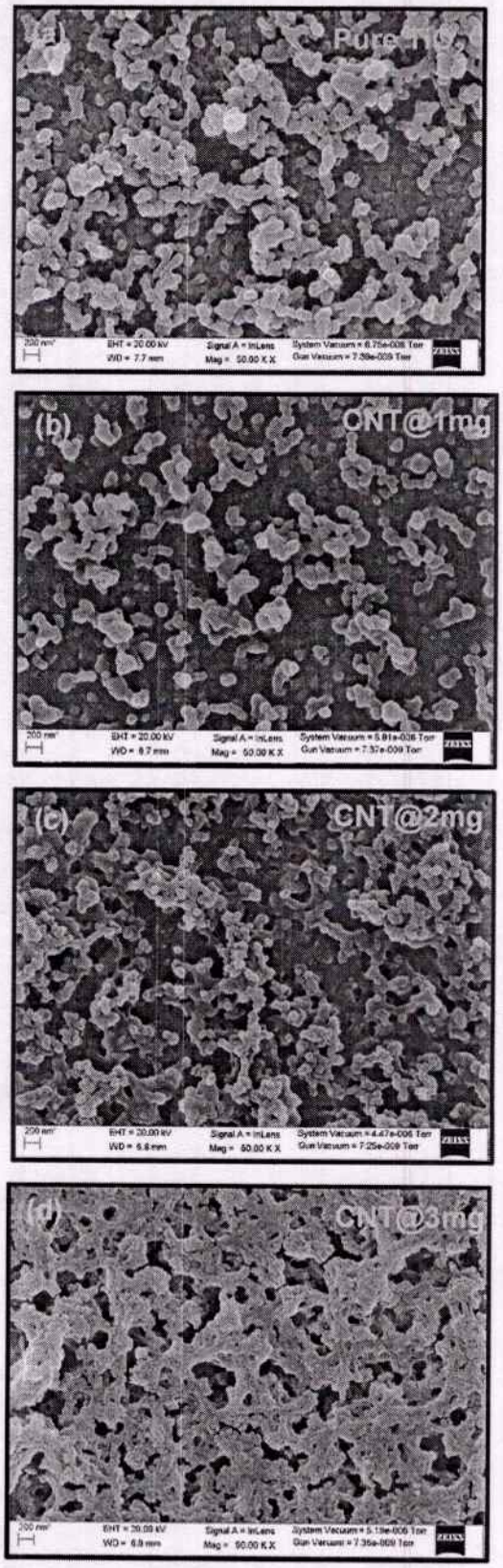

Fig. 2. FE-SEM images of CNT-TiO_2 nanocomposite thin films, **(a)** pure TiO_2, **(b)** CNT@1 mg, **(c)** CNT@2 mg, **(d)** CNT@3 mg.

CNT@2 mg, and CNT@3 mg thin films with a magnification of 50 K. The morphologies of CNT-TiO_2 nanocomposite thin films showed non-uniform porous thin films. The pure TiO_2 thin films was observed less porous due the presence of the scattered grains. The porosity was observed to be increased as the scattered grains agglomerate to each other with the concentration of CNT. The maximum porosity was observed for the thin film of CNT@3 mg. The agglomeration of grains increased by adding CNTs (1–3 mg) in TiO_2 during the nucleation and growth. As a result, the porosity was observed to be increased due to the hydrophobic behaviour of CNTs. The qualitative analysis was taken from FE-SEM images using ImageJ software. The average pore diameter of films was measured to be 47 nm, 140 nm, 150 nm and 274 nm as the concentration of CNTs increased from 1 to 3 mg. The thickness of CNT-TiO_2 thin films was determined from the cross-sections of all samples. The thickness of pure TiO_2 thin film was observed to be 95 nm. Meanwhile, the thickness of CNT-TiO_2 hybrid nanocomposites thin films increased due to increasing the concentration of CNTs in the solution. The thicknesses of CNT@1/2/3 mg nanocomposite thin films were observed to be 105, 150 and 200 nm, respectively.

Fig. 3(a-d) shows EDAX spectra of the pure TiO_2, CNT@1 mg, CNT@2 mg, and CNT@3 mg nanocomposite thin films respectively. The EDAX spectra of all samples confirmed the presence of O, Ti, and C elements in the nanocomposites. The presence of oxygen (O) and titanium (Ti) elements confirms the synthesis of pure TiO_2 thin films. At the same time, the presence of carbon (C) confirmed the synthesis and deposition of CNT-TiO_2 nanocomposite thin films. The detailed analysis of the elements O, Ti, and C is summarised in Table 1.

3.2. Optical properties and contact angle measurement

Fig. 4(a–b) shows the absorption spectra and Tauc's plot of spin-coated CNT-TiO_2 nanocomposite thin films. The maximum absorbance was observed for pure TiO_2 thin film (Fig. 4(a)). The addition of CNT concentration in TiO_2 nanocomposites, the absorption decreased continuously for samples CNT@1 mg, CNT@2 mg, and CNT@3 mg along with the movement of maxima towards higher wavelength. The direct optical bandgap of spin-coated thin films for samples pure TiO_2, CNT@1 mg, CNT@2 mg, and CNT@3 mg was determined from Tauc's plot method as follows [36,37]:

$$(\alpha h\nu)^2 = B(h\nu - E_g) \tag{3}$$

Where α is the absorption coefficient, hν is the energy of incident photons, Eg is the optical bandgap and B is the proportionality constant. The optical bandgap was determined by the extrapolation of the linear portion of the $(\alpha h\nu)^2$ versus the photon energy ($h\nu$) (Fig. 4b). The bandgap of pure TiO_2, CNT@1 mg, CNT@2 mg and CNT@3 mg nanocomposite thin films were determined to be 3.94 eV, 3.76 eV, 3.75 eV and 3.70 eV. The optical bandgap of pure TiO_2 thin films was higher, while CNT-TiO_2 nanocomposite thin films decreased significantly by adding different amounts of CNTs. The CNT as dopant materials interact with TiO_2 and creates a new carbonaceous chemical bond Ti–O–C, which generates the new electronic energy states between the conduction band (CB) and valence band (VB) of TiO_2 [31,37]. These new electronic energy states facilitate the absorption of the light spectrum towards the higher wavelength, and the optical bandgap of CNT-TiO_2 nanocomposite thin films was decreased.

Fig. 5(a–d) shows the PL spectra with deconvoluted graphs (Gaussian fitting) of pure TiO_2 thin films, CNT@1 mg, CNT@2 mg, and CNT@3 mg nanocomposite thin films measured in the range 340 nm–600 nm wavelength under an excitation wavelength 325 nm. From the deconvoluted graphs, in the low wavelength region, the emission peak shows the band-to-band recombination across the bandgap (red lines). The PL spectra of high wavelength region correspond to excitons (green lines), resulting from the oxygen vacancies or defects at the surface (blue lines). The CNT-TiO_2 nanocomposite thin film with CNT@3 mg shows the

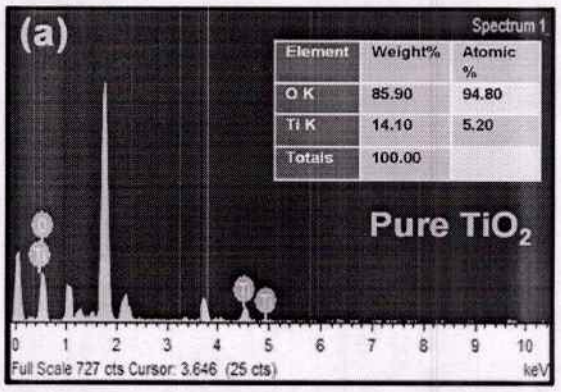

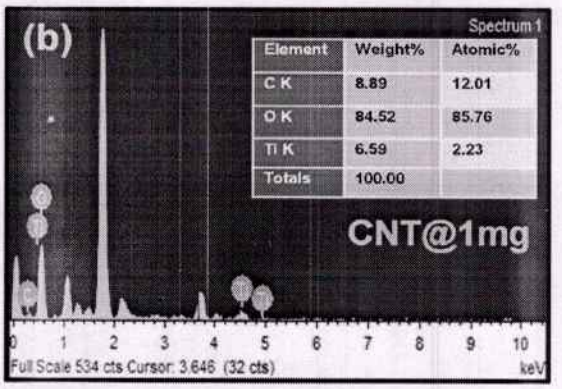

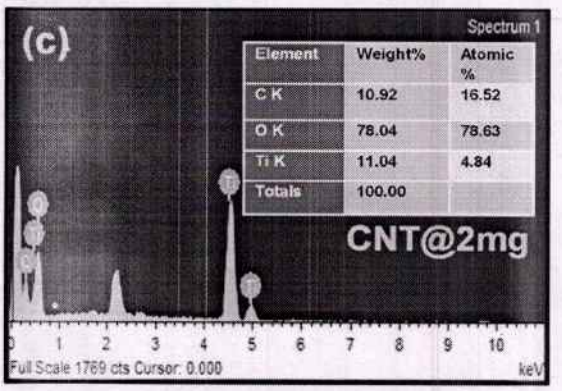

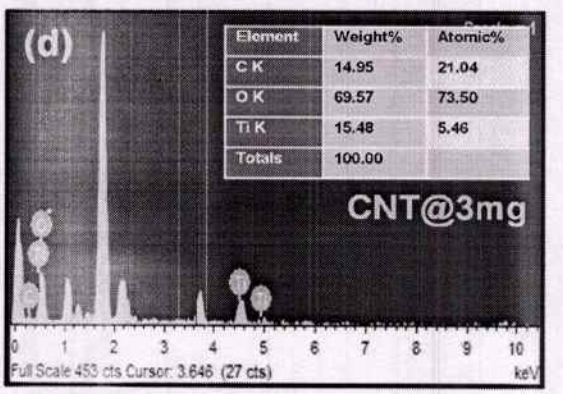

Fig. 3. EDAX spectrum of CNT-TiO_2 nanocomposite thin films, **(a)** pure TiO_2, **(b)** CNT@1 mg, (c) CNT@2 mg, **(d)** CNT@3 mg.

Table 1
Analysis of EDAX Spectrum: pure TiO_2, CNT@1 mg, CNT@2 mg and CNT@3 mg nanocomposite thin films.

Sample Name	Wt./At. (%)	Carbon C K	Oxygen O K	Titanium Ti K	Total
Pure TiO_2	Wt.%	–	85.9	14.1	100
	At.%	–	94.8	5.2	
CNT@1 mg	Wt.%	8.89	84.52	6.59	
	At.%	12.01	85.76	2.23	
CNT@2 mg	Wt.%	10.92	78.04	11.04	
	At.%	16.52	78.63	4.84	
CNT@3 mg	Wt.%	14.95	69.57	15.48	
	At.%	21.04	73.5	5.46	

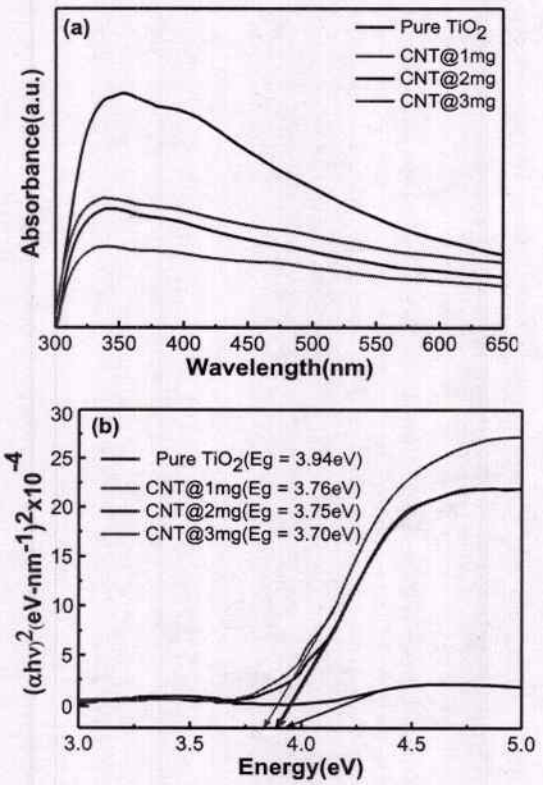

Fig. 4. **(a)** The absorbance spectra of pure TiO_2, CNT@1 mg, CNT@2 mg and CNT@3 mg nanocomposite thin films, **(b)** Tauc's plot for determining optical bandgap.

emission at 521 nm (cyan line) allocated to the recombination of electrons with holes trapped in states above the VB. This peak is more noticeable in CNT-TiO_2 nanocomposite thin films CNT@3 mg with the appropriate amount of 3 mg of CNTs, the hybridization that makes new electronic energy states, facilitating more charge separation across the CNT-TiO_2 interface.

Moreover, compared to pure TiO_2, the PL intensity of samples CNT@1 mg, CNT@2 mg, and CNT@3 mg decreased continuously. This indicates the migration of photogenerated electrons from TiO_2 to carbon atoms of CNTs. The migration or transfer of photogenerated electrons increases the separation of electron-hole pairs and delays the recombination of these pairs. The decreased PL intensity also the signature of defects in the lattice which results in the trapping of charge carriers [38, 39]. Owing to the migration/transfer of electrons, the creation of defects and trapping of charge carriers improve the materials optical and electronic properties, which further assist the material in activities such as photocatalytic activity, antibacterial activity and so on.

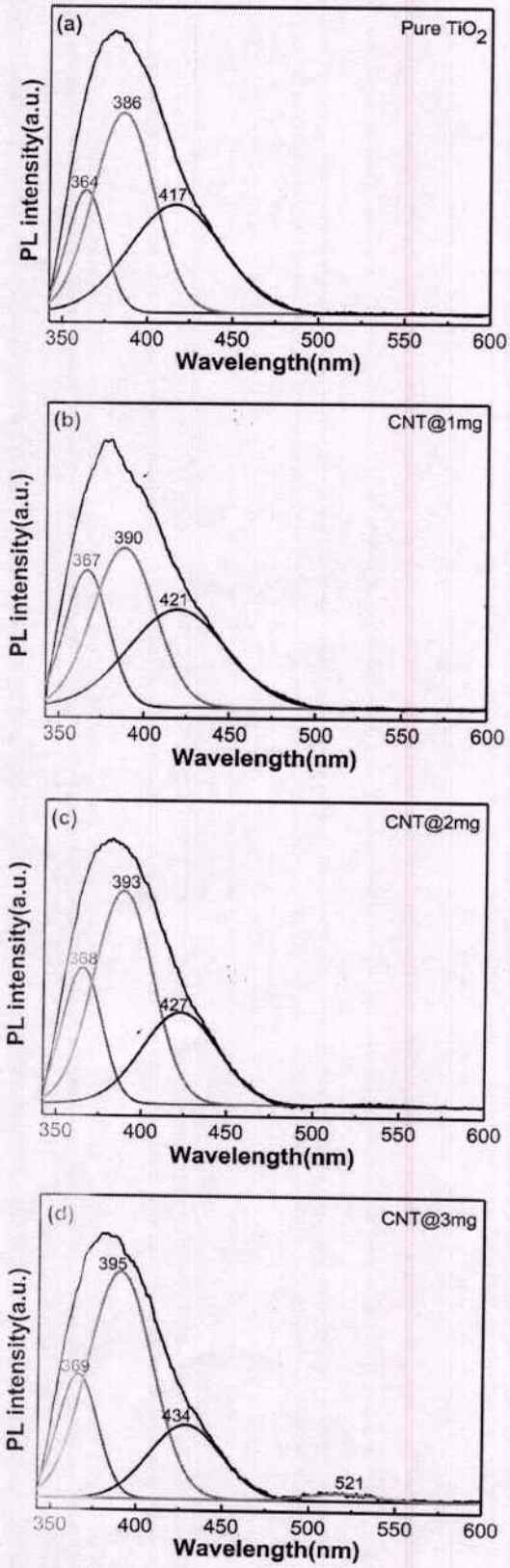

Fig. 5. The photoluminescence (PL) spectra of all samples under an excitation source of wavelength 325 nm and the deconvoluted graphs (Gaussian fitting), **(a)** pure TiO_2, (b) CNT@1 mg, **(c)** CNT@2 mg, **(d)** CNT@3 mg.

Fig. 6 shows the FTIR spectra of pure TiO_2, CNT@1 mg, CNT@2 mg, and CNT@3 mg nanocomposite thin films. The fundamental vibrations of TiO_2 ascribed at 650-670 cm^{-1} for the Ti–O bond and at nearly 750 cm^{-1} deliberated to be another IR active fundamental vibration of the Ti–O–Ti bond. The peak at 866 cm^{-1} shows strong C–H bending. More importantly, in CNT-TiO_2 nanocomposite thin films, the signals between 1040 and 1160 cm^{-1} confirm the presence of carbon atoms of CNT in the Ti–O lattice with the stretching vibrations of the Ti–O–C bond [40].

Fig. 7 shows the wettability test of pure TiO_2, CNT@1 mg, CNT@2 mg, and CNT@3 mg nanocomposite thin films. The surface wettability has tremendous attention for self-cleaning effects exhibited by Lotus leaves in nature. Young studied wettability by proposing a minimization model of three-phase interfacial energies solid-vapour (γ_{sv}), solid-liquid (γ_{sl}), and liquid-vapour (γ_{lv}) through the following equation [41]:

$$Cos\,\theta_w = \frac{\gamma_{sv} - \gamma_{sl}}{\gamma_{lv}} \tag{4}$$

where, θ_w is the water contact angle known as the Young water contact angle. If $\theta_w < 90°$, the surface is hydrophilic. For $\theta_w > 90°$, the surface is hydrophobic and if $\theta_w \geq 145°$ the surface is superhydrophobic [42]. The distilled deionised water droplets were dropped on the deposited surfaces using a micro syringe. Experimental drop profiles picked the average water contact angle value at five different positions for the same sample. The variation of static water contact angle is the function of the amount of CNT used. All the deposited pure and CNT-TiO_2 nanocomposite thin films were found to be hydrophobic and the contact angle lies in the range 136.5°–138.7°. The surface energy, defined as the excess energy at the surface of a material, is related to the contact angle by Young's equation. It has two components, namely polar and dispersive components. Wu, through the mean harmonic approach, presented the following additional equation to calculate the surface energy of a solid [43].

$$\gamma_{sl} = \gamma_{lv} + \gamma_{sv} - 4\left[\frac{\gamma_{lv}^{D} \times \gamma_{sv}^{D}}{\gamma_{lv}^{D} + \gamma_{sv}^{D}} + \frac{\gamma_{lv}^{P} \times \gamma_{sv}^{P}}{\gamma_{lv}^{P} + \gamma_{sv}^{P}}\right] \tag{5}$$

An additional equation is required to measure these two components. Owens-Wendt presented the following equation to calculate the two components of surface energy [44].

$$\gamma_{sl} = \gamma_{sv} + \gamma_{lv} - 2\left[\sqrt{\gamma_{sv}^{D}\gamma_{lv}^{D}} + \sqrt{\gamma_{sv}^{P}\gamma_{lv}^{P}}\right] \tag{6}$$

where, γ_{sv}^{D}, γ_{sv}^{D} and γ_{lv}^{P}, γ_{lv}^{P} are the dispersive and polar components of solid–vapour (γ_{sv}) energy and liquid–vapour (γ_{lv}) energy, respectively. Table 2 lists the surface energy of pure TiO_2, CNT@1 mg, CNT@2 mg, and CNT@3 mg nanocomposite thin films. The surface energy calculated

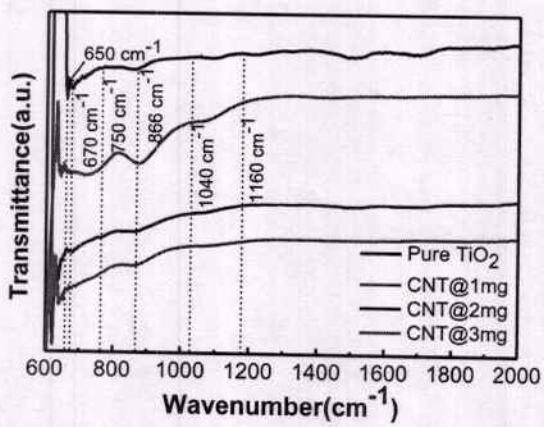

Fig. 6. The FTIR spectra of pure TiO_2, CNT@1 mg, CNT@2 mg and CNT@3 mg nanocomposite thin films.

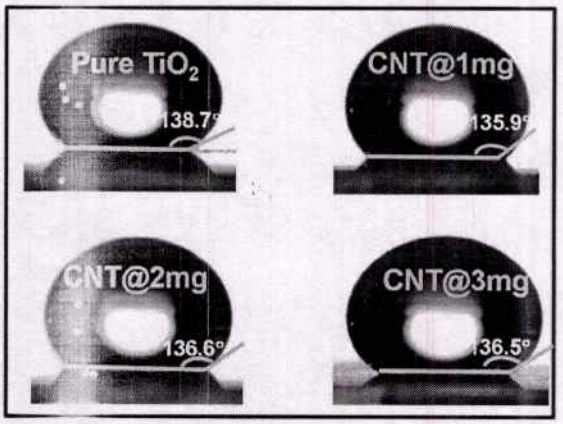

Fig. 7. The contact angle measurement of pure TiO_2, CNT@1 mg, CNT@2 mg and CNT@3 mg nanocomposite thin films.

by Wu and Owens-Wendt methods is in agreement with each other. The surface energy for the film CNT@2 mg was observed to be minimum and hence detected the higher hydrophobicity.

3.3. Photocatalytic performances and degradation mechanism

Fig. 8(a-d) shows the photocatalytic degradation of organic dye MB using pure TiO_2, CNT@1 mg, CNT@2 mg, and CNT@3 mg nanocomposite thin film under the irradiation of visible light for 3 h. The maxima of absorption peak for MB has occurred at ~662 nm for all the samples. The highest degradation of MB was observed for nanocomposite thin films CNT@2 mg. The photocatalytic performance of nanocomposite thin films CNT@2 mg was increased due to forming a new carbonaceous chemical bond Ti–O–C defended in FTIR spectroscopy.

Fig. 8(e) shows the changes in the normalized concentration of MB solution in the presence of deposited thin films as a photocatalyst with the irradiation of visible light. The normalized concentration (C_t/C_o) of MB, with the irradiation time t, was assumed to be proportional to normalized the maximum absorbance (A_t/A_o).

Fig. 8(f) shows the degradation percentage (%) of MB solution concerning pure TiO_2, CNT@1 mg, CNT@2 mg, and CNT@3 mg nanocomposite thin films with the irradiation of visible light for 3 h. The highest degradation of MB was achieved for a particular CNT@2 mg sample. It is indicated that the irradiation of visible light for 3 h degraded the MB of ~83% by CNT@2 mg thin films.

Fig. 8(g) shows the chemical kinetics of the photo-degradation of MB dye with pure TiO_2, CNT@1 mg, CNT@2 mg, and CNT@3 mg nanocomposite thin films using the first-order equation as [45,46]:

$$\ln\left(\frac{C_o}{C_t}\right) = k\,t \tag{7}$$

Where, C_o is the initial concentration, C_t is the concentration after time t, and k is the rate constant (min^{-1}) of MB, respectively. The first-order degradation rate constant k, of MB concentration was calculated from the linear relationship of $\ln(C_o/C_t)$ versus irradiation time t. The reaction rate constant for the degradation of MB solution was 0.00852 min^{-1} for pure TiO_2, 0.00601 min^{-1} for CNT@1 mg, 0.00973 min^{-1} for CNT@2 mg and 0.00551 for CNT@3 mg films. The degradation rate constant was observed to be highest for nanocomposite thin films of CNT@2 mg.

Fig. 8(h) shows the stability of TiO_2 nanocomposite thin films CNT@2 mg up to five cycles under the irradiation of visible light with a time of 3 h for each process. The remaining sample was subjected to the next cycle. The least significant deviations were observed after each process and the photocatalytic performance of films was regarded because of less availability of functional sites by the repetition of cycles.

Fig. 9 shows the schematic illustration of the charge transfer mechanism from TiO_2 to CNT. Most photocatalysts show lower photocatalytic performances because of the high recombination rate (10^{-9} s) of intrinsic electron-hole pairs. The increased work function of CNT (4.9–5.05 eV) plays the role of electron sink so that the transferred electron from a high energy level can reside in the sink for more than its usual recombination time [47]. Therefore, the introduction of CNT in TiO_2 can modify the electronic properties by forming new intermediate electronic energy states between VB and CB, increasing the separation time between electrons and holes. The increased separation time improves photocatalytic performances.

During visible light illumination, the photogenerated electrons excited from the VB to CB and transferred to the carbon nanotube (Eq^n. 8 & 9). The generated holes reside in the VB of TiO_2. The photogenerated electrons transferred from TiO_2 to CNT react with adsorbed oxygen, O_2, and reduced it into superoxide free radical as ($^{\bullet}O_2^-$) (Eq^n. 10). The VB of TiO_2 required one electron to return to the stable state, which was captured from water molecule or the holes (h^+) in the VB of TiO_2 reacted with OH^- ions generating hydroxyl free radical ($^{\bullet}OH$) under oxidation process (Eq^n. 11). Therefore, generated free radical species superoxide and hydroxyl with following chemical reactions continuously strike to MB molecules to degrade it into some small intermediate molecules/ions and some harmless products like carbon dioxide (CO_2) and water (H_2O) (Eq^n. 12) [48].

$$TiO_2 + hv \rightarrow TiO_2\left(h_{VB}^+ - e_{CB}^-\right) \tag{8}$$

$$TiO_2\left(e_{CB}^-\right) + CNT \rightarrow TiO_2 + CNT\left(e_{CB}^-\right) \tag{9}$$

$$CNT\left(e_{CB}^-\right) + O_2 \rightarrow CNT + {}^{\bullet}O_2^- \tag{10}$$

$$TiO_2\left(h_{VB}^+\right) + OH^- \rightarrow {}^{\bullet}O\,H \tag{11}$$

$$MB + O_2^-\bullet / O_{\bullet}H \rightarrow degradation(H_2O + CO_2\uparrow) \tag{12}$$

The photocatalytic degradation of CNT-TiO_2 nanocomposite thin films is discussed for the organic pollutants, particularly MB, that is comparable to TiO_2-based nanocomposite powders and summarised in Table 3.

Tan et al. developed the TiO_2-based flat membrane and estimated the photocatalytic degradation of MB to be 98% under UV light exposure for 8 h [33]. Ataabadi et al. prepared TiO_2/glass thin films and tested photocatalytic degradation of MB (77%) under UV irradiation for 5 h

Table 2
Calculated surface energy: pure TiO_2, CNT@1 mg, CNT@2 mg and CNT@3 mg nanocomposite thin films.

Samples Name	Contact angle (θ_w)	Method					
		Wu			Owens & Wendt		
		γ_{sv} (mN/m)	γ_{sv}^D (mN/m)	γ_{sv}^p (mN/m)	γ_{sv} (mN/m)	γ_{sv}^D (mN/m)	γ_{sv}^p (mN/m)
Pure TiO_2	138.7°	4.79 (±0.01)	1.78 (±0.00)	3.02 (±0.01)	1.15 (±0.00)	0.51 (±0.00)	0.64 (±0.00)
CNT@1 mg	135.9°	5.49 (±0.01)	2.16 (±0.00)	3.34 (±0.00)	1.48 (±0.00)	0.66 (±0.00)	0.82 (±0.00)
CNT@2 mg	136.6°	5.31 (±0.11)	2.06 (±0.04)	3.25 (±0.07)	1.39 (±0.01)	0.62 (±0.01)	0.77 (±0.01)
CNT@3 mg	136.5°	5.34 (±0.01)	2.07 (±0.00)	3.27 (±0.01)	1.40 (±0.00)	0.63 (±0.00)	0.78 (±0.00)

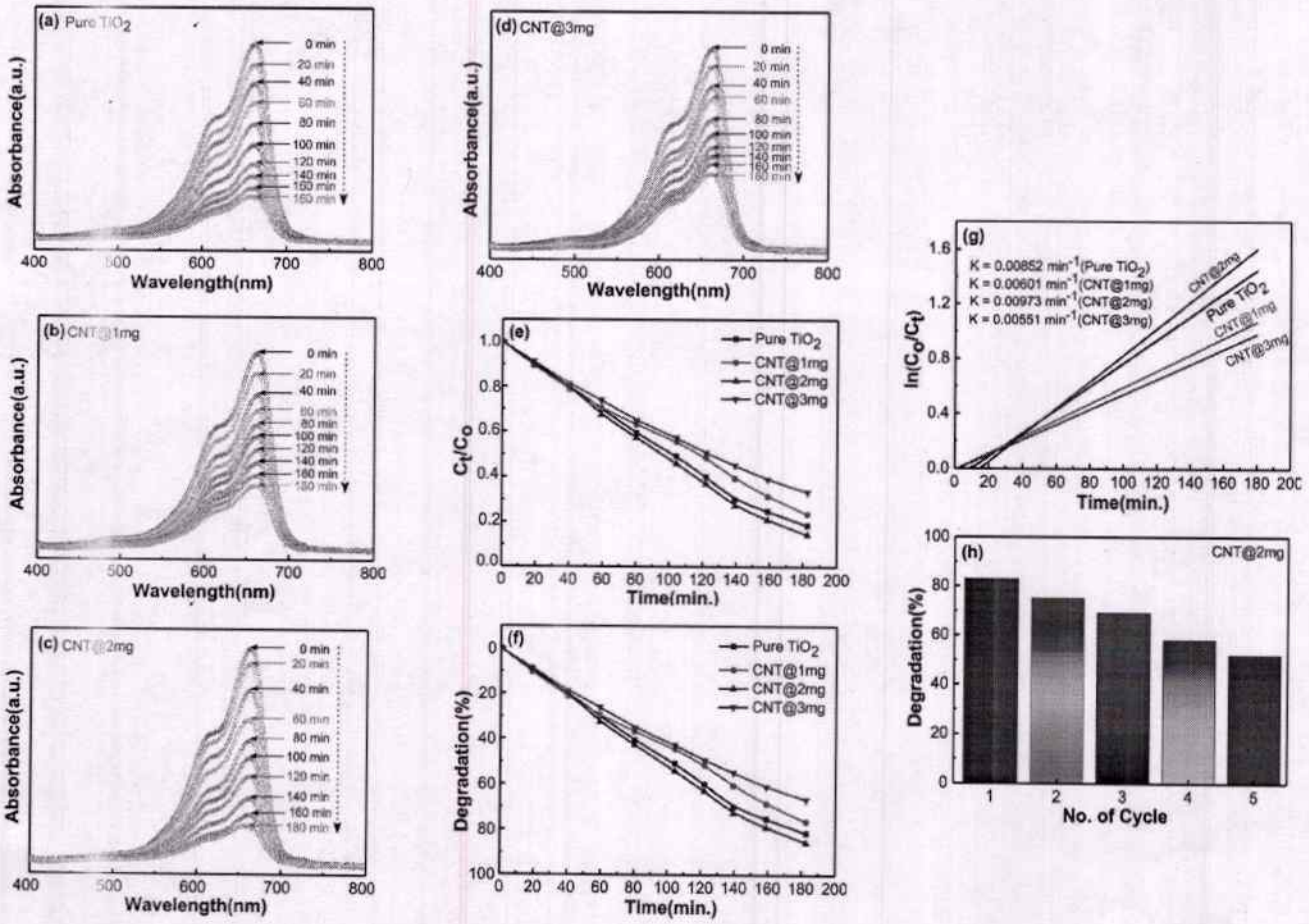

Fig. 8. Time-dependent visible light absorbance spectra for MB solution in the presence of nanocomposite thin films, **(a)** pure TiO_2, **(b)** CNT@1 mg, **(c)** CNT@2 mg, **(d)** CNT@3 mg. **(e)** The measurement of relative concentration (C_t/C_0) of MB at different times for pure TiO_2, CNT@1 mg, CNT@2 mg and CNT@3 mg films. **(f)** The photocatalytic degradation of MB using pure TiO_2, CNT@1 mg, CNT@2 mg and CNT@3 mg. **(g)** The rate constant estimated for all samples inset the value. **(h)** The stability of CNT-TiO_2 nanocomposite thin films of CNT@2 mg over five successive cycles for MB degradation process under visible light irradiation.

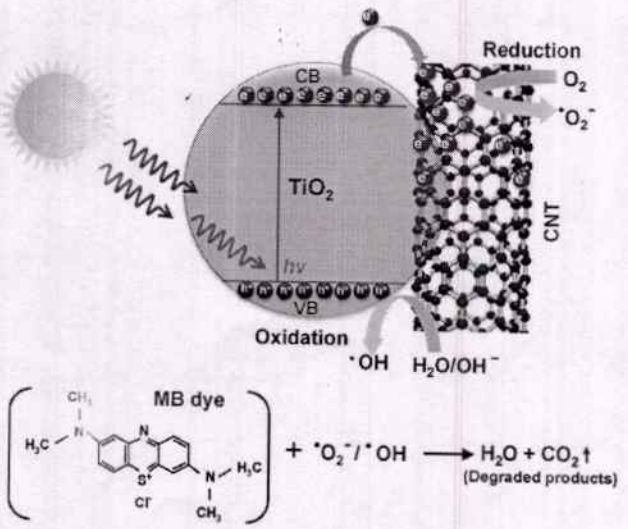

Fig. 9. The schematic illustration showed the photocatalytic degradation mechanism for MB using CNT-TiO_2 nanocomposite thin films.

[11]. Akhter et al. developed CNTs/TiO_2 nanocomposite using the hydrothermal method and observed the photocatalytic degradation of MB (85%) under visible light irradiation for 3 h [28]. Shaban et al. synthesised TiO_2 nanoribbons (NRs)/CNTs nanocomposite through a novel method followed by chemical vapour deposition. They tested the photocatalytic degradation of MB (92%) under the irradiation of visible spectrum for 5 h [50]. Among the photoctalytic degradation of nanocomposites, the reported material, CNT-TiO_2 is comparable and better in terms of used materials and recovery (Table 3). Therefore, it is suggested that the prepared nanocomposites will be useful for the fabrication of membrane for the photocatalytic degradation of organics dyes or other pharmaceutical discharged water.

4. Conclusions

CNT-TiO_2 nanocomposite thin films were deposited successfully on the quartz glass substrates by the sol-gel spin coating method. All samples showed the non-crystalline or amorphous TiO_2 thin films with increased lattice strain. FE-SEM images of CNT-TiO_2 nanocomposite thin films showed highly porous. The porous networking was increased by adding CNTs concentration in TiO_2. The optical bandgap of CNT-TiO_2 nanocomposite thin films decreased significantly from 3.94 to 3.70 eV. The PL spectra of CNT-TiO_2 nanocomposite thin films confirmed the formation of defects in the lattice. CNT being as an electron sink, the transferred electrons from TiO_2 to CNT were trapped in defects which facilitate the delay in the recombination of electron-hole pairs. The FTIR spectra confirmed the presence of Ti–O, Ti–O–Ti, and Ti–O–C chemical

Table 3
Summarises the comparative data concerning the photocatalysts, light source, pollutants, irradiation time, and degradation (%).

S. No.	Photocatalyst	Light source	Organic pollutant	Irradiation time (min.)	Degradation (%)	Ref.
1.	TiO_2	UV	MB	480	98	[33]
2.	TiO_2	UV	MB	300	77	[11]
3.	CNTs/TiO_2	Visible light	MB	180	85	[28]
4.	CNTs/TiO_2	Visible light	Acetaldehyde	180	70	[49]
5.	CNTs/TiO_2	Visible light	MB	300	92	[50]
6.	CNTs/TiO_2	UV	MB	180	65	[51]
7.	CNTs/TiO_2	UV	Phenol	60	60	[52]
8.	CNTs/TiO_2	UV	MB	60	70	[53]
9.	CNTs/TiO_2	Visible light	MO	120	60	[54]
10.	CNTs/TiO_2	Visible light	MB	180	83	Reported

bonds at particular vibrational frequencies. The surface energy of CNT@2 mg thin films was observed at a minimum and, hence, highly hydrophobic. Finally, spin-coated CNT-TiO_2 nanocomposite thin films exhibited high porosity with significant photoluminescence (PL) properties for various photocatalytic applications.

CRediT authorship contribution statement

Hitesh Kumar Sharma: Methodology, Formal analysis, Data curation, Conceptualization. **Beer Pal Singh:** Writing – review & editing, Supervision, Resources, Project administration. **Sanjeev K. Sharma:** Writing – review & editing, Writing – original draft, Visualization, Supervision, Resources, Methodology, Investigation, Formal analysis, Data curation, Conceptualization.

Declaration of competing interest

The authors declare that they have no known competing financial interests or personal relationships that could have appeared to influence the work reported in this paper.

Acknowledgements

All the authors would like to express their gratitude to the Department of Science and Technology (DST) for granting DST-FIST project, SR/FST/PSI-177/2012, Department of Physics, CCS University, Meerut, UP, India as this research work partially completed under this grant.

References

[1] K. Preeti, A. Kumar, N. Jain, A. Kaushik, Y.K. Mishra, S.K. Sharma, Tailored ZnO nanostructures for efficient sensing of toxic metallic ions of drainage systems, Mater. Today Sustain. 24 (2023) 100515.
[2] N. Tyagi, G. Sharma, D. Kumar, P. Pratap Neelratan, D. Sharma, M. Khanuja, M. K. Singh, V. Singh, A. Kaushik, S.K. Sharma, 2D-MXenes to tackle wastewater: from purification to SERS-based sensing, Coord. Chem. Rev. 496 (2023) 215394.
[3] Z. Long, Q. Li, T. Wei, G. Zhang, Z. Ren, Historical development and prospects of photocatalysts for pollutant removal in water, J. Hazard Mater. 395 (2020) 122599.
[4] M.M. Khan, S.A. Ansari, D. Pradhan, M.O. Ansari, D.H. Han, J. Lee, M.H. Cho, Band gap engineered TiO2 nanoparticles for visible light induced photoelectrochemical and photocatalytic studies, J. Mater. Chem. A 2 (2014) 637–644.
[5] H.K. Sharma, S.K. Sharma, S. Kumar, B.P. Singh, Effect of CNT on the growth and agglomeration of TiO2 nanoparticles, Ind. J. Pure Appl. Phys. 58 (2020) 825–831.
[6] M. Basante-Romo, J.O. Gutierrez-M, R. Camargo-Amado, Non-toxic doses of modified titanium dioxide nanoparticles (m-TiO2NPs) in albino CFW mice, Heliyon 7 (2021) e06514.
[7] L. Krivoshapkina, M. Ilkaeva, V. Avdin, Z. Amghouz, S.A. Khainakov, J.R. García, E. Díaz, S. Ordóñez, Exceptional thermal stability of undoped anatase TiO2 photocatalysts prepared by a solvent-exchange method, RSC Adv. 5 (2015) 36634–36641.
[8] M.A. Al-Nuaim, A.A. Alwasiti, Z.Y. Shnain, The photocatalytic process in the treatment of polluted water, Chem. Pap. 77 (2023) 677–701.
[9] K. Indira, S. Shanmugam, A. Hari, S. Vasantharaj, S. Sathiyavimal, K. Brindhadevi, A. El Askary, A. Elfasakhany, A. Pugazhendhi, Photocatalytic degradation of Congo red dye using nickel–titanium dioxide nanoflakes synthesized by Mukia madraspatna leaf extract, Environ. Res. 202 (2021) 111647.
[10] R. Zhu, R. Nadimicherla, X. Guo, Ultraviolet photocatalytic degradation of methyl orange by nanostructured TiO2/ZnO heterojunctions, J. Mater. Chem. A 3 (2015) 6565–6574.
[11] M.R. Ataabadi, M. Jamshidi, Improved photocatalytic degradation of methylene blue under visible light using acrylic nanocomposite contained silane grafted nano TiO2, J. Photochem. Photobiol. Chem. 443 (2023) 114832.
[12] Y. Yu, W. Wen, X.-Y. Qian, J.-B. Liu, J.-M. Wu, UV and visible light photocatalytic activity of Au/TiO2 nanoforests with Anatase/Rutile phase junctions and controlled Au locations, Sci. Rep. 7 (2017) 41253.
[13] M.-Y. Xie, K.-Y. Su, X.-Y. Peng, R.-J. Wu, M. Chavali, W.-C. Chang, Hydrogen production by photocatalytic water-splitting on Pt-doped TiO2–ZnO under visible light, J. Taiwan Inst. Chem. Eng. 70 (2017) 161–167.
[14] N. Seifvand, E. Kowsari, Synthesis of mesoporous Pd-doped TiO2 templated by a magnetic recyclable ionic liquid for efficient photocatalytic air treatment, Ind. Eng. Chem. Res. 55 (2016) 10533–10543.
[15] R.J. Delgado-Macuil, M. Rojas-López, V.L. Gayou, A. Orduña-Díaz, J. Díaz-Reyes, V. Camacho-Pernas, Synthesis of Au/TiO2 thin films for photocatalytic degradation of methylene blue, MRS Online Proc. Libr. 1242 (2010) 146.
[16] J. Yu, L. Qi, M. Jaroniec, Hydrogen production by photocatalytic water splitting over Pt/TiO2 nanosheets with exposed (001) facets, J. Phys. Chem. C 114 (2010) 13118–13125.
[17] D. Madan, K.P. Misra, S. Chattopadhyay, N. Halder, Rare Earth-Doped TiO2 Nanoparticles for Photocatalytic Dye Remediation, 2022, pp. 215–234.
[18] S.M. Al-Shomar, Synthesis and characterization of Eu3+ doped TiO2 thin films deposited by spray pyrolysis technique for photocatalytic application, Mater. Res. Express 8 (2021) 026402.
[19] Y. Chen, L. Cai, J. Gong, H. Lai, Synthesis of GR/TiO2 photocatalyst for degradation of methylene Blue—A laboratory experiment for preservice teachers, J. Chem. Educ. 100 (2023) 1597–1602.
[20] P.N.O. Gillespie, N. Martsinovich, Origin of charge trapping in TiO2/reduced graphene oxide photocatalytic composites: insights from theory, ACS Appl. Mater. Interfaces 11 (2019) 31909–31922.
[21] H.K. Sharma, S.K. Sharma, K. Vemula, A.R. Koirala, H.M. Yadav, B.P. Singh, CNT facilitated interfacial charge transfer of TiO2 nanocomposite for controlling the electron-hole recombination, Solid State Sci. 112 (2021) 106492.
[22] S.K. Sharma, G. Sharma, A. Sharma, K. Bhardwaj, K. Preeti, K. Singh, A. Kumar, V. K. Pal, E.H. Choi, S.P. Singh, N.K. Kaushik, Synthesis of silica and carbon-based nanomaterials from rice husk ash by ambient fiery and furnace sweltering using a chemical method, Appl. Surf. Sci. Adv. 8 (2022) 100225.
[23] S. Iijima, T. Ichihashi, Single-shell carbon nanotubes of 1-nm diameter, Nature 363 (1993) 603–605.
[24] A. Peigney, C. Laurent, E. Flahaut, R. Bacsa, A. Rousset, Specific surface area of carbon nanotubes and bundles of carbon nanotubes, Carbon 39 (2001) 507–514.
[25] A. Takakura, K. Beppu, T. Nishihara, A. Fukui, T. Kozeki, T. Namazu, Y. Miyauchi, K. Itami, Strength of carbon nanotubes depends on their chemical structures, Nat. Commun. 10 (2019) 3040.
[26] M. Shiraishi, M. Ata, Work function of carbon nanotubes, Carbon 39 (2001) 1913–1917.
[27] L. Wan, C. Deng, Z.-Y. Zhao, H.-B. Zhao, Y.-Z. Wang, A titanium dioxide–carbon nanotube hybrid to simultaneously achieve the mechanical enhancement of natural rubber and its stability under extreme frictional conditions, Mater. Adv. 2 (2021) 2408–2418.
[28] P. Akhter, F. Ali, A. Ali, M. Hussain, TiO2 decorated CNTs nanocomposite for efficient photocatalytic degradation of methylene blue, Diam. Relat. Mater. 141 (2024) 110702.
[29] E.R. Morales, N.R. Mathews, D. Reyes-Coronado, C.R. Magaña, D.R. Acosta, G. Alonso-Nunez, O.S. Martinez, X. Mathew, Physical properties of the CNT:TiO2 thin films prepared by sol–gel dip coating, Sol. Energy 86 (2012) 1037–1044.
[30] Q. Yi, H. Wang, S. Cong, Y. Cao, Y. Wang, Y. Sun, Y. Lou, J. Zhao, J. Wu, G. Zou, Self-cleaning glass of photocatalytic anatase TiO2@Carbon nanotubes thin film by polymer-assisted approach, Nanoscale Res. Lett. 11 (2016) 457.
[31] O. Akhavan, R. Azimirad, S. Safa, M.M. Larijani, Visible light photo-induced antibacterial activity of CNT-doped TiO2 thin films with various CNT contents, J. Mater. Chem. 20 (2010) 7386–7392.
[32] S.K. Sharma, R. Gupta, G. Sharma, K. Vemula, A.R. Koirala, N.K. Kaushik, E. H. Choi, D.Y. Kim, L.P. Purohit, B.P. Singh, Photocatalytic performance of yttrium-doped CNT-ZnO nanoflowers synthesized from hydrothermal method, Mater. Today Chem. 20 (2021) 100452.
[33] S.K. Sharma, K.-N.P. Kumar, K.J. Kang, R.M. Mehra, Effect of illumination on hydrogenated amorphous silicon thin films doped with chalcogens, J. Non-Cryst. Solids 355 (2009) 1638–1643.

[34] A. Banerra, V. Singh, S. Khan, U. Parihar, A. Singh, S. Gautam, S.K. Sharma, H. Furukawa, A. Khosla, Impact of rGO concentration on the physical characteristics of CuO/rGO nanocomposite for sensing and optoelectronic applications, ECS J. Solid State Sci. Technol. 12 (2023) 067001.
[35] H.K. Sharma, R. Archana, R. Sankar ganesh, B.P. Singh, S. Ponnusamy, Y. Hayakawa, C. Muthamizhchelvan, P. Raji, D.Y. Kim, S.K. Sharma, Substitution of Al3+ to Zn2+ sites of ZnO enhanced the photocatalytic degradation of methylene blue under irradiation of visible light, Solid State Sci. 94 (2019) 45–53.
[36] N. Kaur, S.K. Sharma, D.Y. Kim, H. Sharma, N. Singh, Synthesis of imine-bearing ZnO nanoparticle thin films and characterization of their structural, morphological and optical properties, J. Nanosci. Nanotechnol. 15 (2015) 8114–8119.
[37] V.S. Rana, L.P. Purohit, G. Sharma, S.P. Singh, S.K. Sharma, Effect of RF power on physical and electrical properties of Al-doped ZnO thin films, Indian J. Pure Appl. Phys. 60 (2022) 246–253.
[38] F.H. Abdulrazzak, F.H. Hussein, A.F. Alkaim, I. Ivanova, A.V. Emeline, D. W. Bahnemannd, Sonochemical/hydration—dehydration synthesis of Pt—TiO2 NPs/decorated carbon nanotubes with enhanced photocatalytic hydrogen production activity, Photochem. Photobiol. Sci. 15 (2016) 1347–1357.
[39] S.K. Sharma, K. Preeti, G. Sharma, R. Gupta, G.S. Ghodake, A. Singh, Defect emission photoluminescence peak tuning by encapsulation of Au-NPs on ZnO mesoporous nanosponges, J. Lumin. 244 (2022) 118695.
[40] K. Hemalatha, A.S. Prakash, G.K.M. Jayakumar, TiO2 coated carbon nanotubes for electrochemical energy storage, J. Mater. Chem. A 2 (2014) 1757–1766.
[41] T. Young III., An essay on the cohesion of fluids. Phil. Trans. Roy. Soc. Lond. 95 (1805) 65–87.
[42] K.-Y. Law, Definitions for hydrophilicity, hydrophobicity, and superhydrophobicity: getting the basics right, J. Phys. Chem. Lett. 5 (2014) 686–688.
[43] S. Wu, Calculation of interfacial tension in polymer systems, J. Polym. Sci. Part C: Polymer Symposia 34 (1971) 19–30.
[44] D.K. Owens, R.C. Wendt, Estimation of the surface free energy of polymers, J. Appl. Polym. Sci. 13 (1969) 1741–1747.
[45] T. Sakthivel, K. Krishnamoorthy, K. Velmurugan, N. Raju, S. Kim, G. Venugopal, Graphdiyne-ZnO nanohybrids as an advanced photocatalytic material, J. Phys. Chem. C 119 (2015) 150828160025007.
[46] J. Akter, M.A. Hanif, M.A. Islam, K.P. Sapkota, J.R. Hahn, Selective growth of Ti3+/TiO2/CNT and Ti3+/TiO2/C nanocomposite for enhanced visible-light utilization to degrade organic pollutants by lowering TiO2-bandgap, Sci. Rep. 11 (2021) 9490.
[47] P. Liu, Q. Sun, F. Zhu, K. Liu, K. Jiang, L. Liu, Q. Li, S. Fan, Measuring the work function of carbon nanotubes with thermionic method, Nano Lett. 8 (2008) 647–651.
[48] D. Chaudhary, V.D. Vankar, N. Khare, Noble metal-free g-C3N4/TiO2/CNT ternary nanocomposite with enhanced photocatalytic performance under visible-light irradiation via multi-step charge transfer process, Sol. Energy 158 (2017) 132–139.
[49] B.K. Vijayan, N.M. Dimitrijević, D. Finkelstein-Shapiro, J. Wu, K.A. Gray, Coupling titania nanotubes and carbon nanotubes to create photocatalytic nanocomposites, ACS Catal. 2 (2012) 223–229.
[50] M. Shaban, A.M. Ashraf, M.R. Abukhadra, TiO2 nanoribbons/carbon nanotubes composite with enhanced photocatalytic activity; fabrication, characterization, and application, Sci. Rep. 8 (2018) 781.
[51] B. Gao, G.Z. Chen, G. Li Puma, Carbon nanotubes/titanium dioxide (CNTs/TiO2) nanocomposites prepared by conventional and novel surfactant wrapping sol–gel methods exhibiting enhanced photocatalytic activity, Appl. Catal. B Environ. 89 (2009) 503–509.
[52] Y. Yao, G. Li, S. Ciston, R.M. Lueptow, K.A. Gray, Photoreactive TiO2/carbon nanotube composites: synthesis and reactivity, Environ. Sci. Technol. 42 (2008) 4952–4957.
[53] W.C. Oh, F.J. Zhang, M.L. Chen, Preparation of MWCNT/TiO2 composites by using MWCNTs and titanium(IV) alkoxide precursors in benzene and their photocatalytic effect and bactericidal activity, Bull. Kor. Chem. Soc. 30 (2009) 2637–2642.
[54] K. Zhang, F.J. Zhang, M.L. Chen, W.C. Oh, Comparison of catalytic activities for photocatalytic and sonocatalytic degradation of methylene blue in present of anatase TiO2–CNT catalysts, Ultrason. Sonochem. 18 (2011) 765–772.